AD-A032 011 TECHNION RESEARCH AND DEVELOPMENT FOUNDATION LTD HAI--ETC F/G 11/1
MECHANICAL BEHAVIOR OF MULTIMATERIAL COMPOSITE SYSTEMS. INTERLA--ETC(U)
APR 76 O ISHAI, D PERETZ, S GALI DAJA37-75-C-1890

UNCLASSIFIED NL

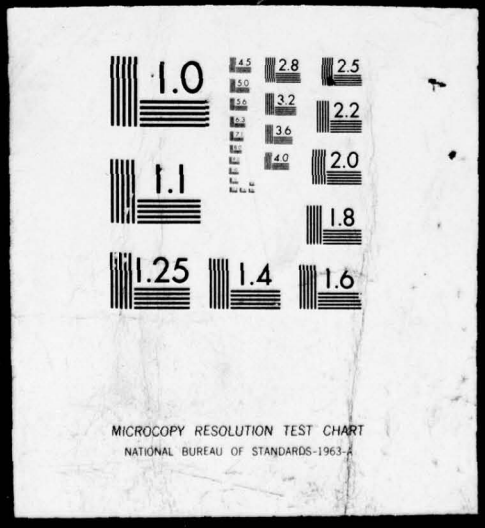
1 OF 2
AD A032011



SIFIED

1 OF 2

AD
A032011



AD A032011

MECHANICAL BEHAVIOR OF MULTIMATERIAL COMPOSITE SYSTEMS

INTERLAMINAR BEHAVIOR

Final Technical Report

(Second Research Year)

by

Ori Ishai, Dan Peretz and Shlomit Gali

DDC
RECEIVED
NOV 15 1976
B

April 1976

EUROPEAN RESEARCH OFFICE
United States Army
London W. 1, England

Contract Number DAJA 37-75-C-1890

Copy available to DDC does not permit fully legible reproduction

Technion Research and Development Foundation Ltd.
Technion — Israel Institute of Technology, Haifa, Israel

APPROVED FOR PUBLIC RELEASE; DISTRIBUTION UNLIMITED

UNCLASSIFIED

SECURITY CLASSIFICATION OF THIS PAGE (When Data Entered)

REPORT DOCUMENTATION PAGE

READ INSTRUCTIONS BEFORE COMPLETING FORM

1. REPORT NUMBER	2. GOVT ACCESSION NO. / 3. RECIPIENT'S CATALOG NUMBER (9)
4. TITLE (and Subtitle) (6) MECHANICAL BEHAVIOR OF MULTIMATERIAL COMPOSITE SYSTEMS. Interlaminar Behavior.	5. TYPE OF REPORT & PERIOD COVERED FINAL TECHNICAL REPORT. Oct 75 - Mar 76.
	6. PERFORMING ORG. REPORT NUMBER
7. AUTHOR(s) PROFESSOR O. ISHAI, D. PERETZ, S. GALI (15)	8. CONTRACT OR GRANT NUMBER(s) DAJA37-75-C-1890 new
9. PERFORMING ORGANIZATION NAME AND ADDRESS TECHNION RESEARCH & DEVELOPMENT FOUNDATION HAIFA, ISRAEL.	10. PROGRAM ELEMENT, PROJECT, TASK AREA & WORK UNIT NUMBERS 6.11.02A-1T161102B35E--00-516
11. CONTROLLING OFFICE NAME AND ADDRESS U.S. ARMY RESEARCH & STANDARDIZATION GROUP (EUR) BOX 65, FPO NEW YORK 09510 (11)	12. REPORT DATE Apr[illegible]976 (12)
	13. NUMBER OF PAGES 102 (103 P.)
14. MONITORING AGENCY NAME & ADDRESS (if different from Controlling Office) (10) Orit/IShai; Dan/Peretz Shlomit/Gali	15. SECURITY CLASS. (of this report) UNCLASSIFIED
	15a. DECLASSIFICATION/DOWNGRADING SCHEDULE

16. DISTRIBUTION STATEMENT (of this Report)

APPROVED FOR PUBLIC RELEASE
DISTRIBUTION UNLIMITED

(16) 1T161102B35E / (17) 00

17. DISTRIBUTION STATEMENT (of the abstract entered in Block 20, if different from Report)

18. SUPPLEMENTARY NOTES

19. KEY WORDS (Continue on reverse side if necessary and identify by block number)

COMPOSITE SYSTEMS, INTERLAYER STRENGTH, HYBRID COMPOSITES

20. ABSTRACT (Continue on reverse side if necessary and identify by block number)

SEE NEXT PAGE.

DD FORM 1 JAN 73 1473 EDITION OF 1 NOV 65 IS OBSOLETE

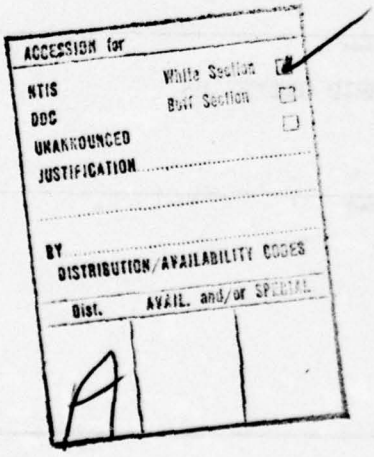
UNCLASSIFIED

SECURITY CLASSIFICATION OF THIS PAGE (When Data Entered)

388338

1/B

20. Stress analysis of interlaminar adhesive layer (IAL) within a multimaterial doubler model which was evaluated in the previous years work is further investigated. Two dimensional IAL stress distribution were derived by means of the finite element method, with emphasis on the behavior close to the edges. Thermoelastic behavior of symmetrical and nonsymmetrical models was investigated analytically and experimentally. A direct method for measuring IAL stress and strain distribution was developed and compared successfully with the analytical predictions. These studies provide a wider basis for current and future research into the non-linearity and ultimate behavior of the IAL.



MECHANICAL BEHAVIOR OF MULTIMATERIAL COMPOSITE SYSTEMS

Interlaminar Behavior

O. Ishai*, D. Peretz** and S. Gali***

ABSTRACT

Stress analysis of interlaminar adhesive layer (IAL) within a multimaterial doubler model which was evaluated in the previous report, is further investigated. Two dimensional IAL stress distributions were derived by means of the finite element method, with emphasis on the behavior close to the edges. ThermoElastic behavior of symmetrical and nonsymmetrical models was investigated analytically and experimentally. A direct method for measuring IAL stress and strain distribution was developed and compared successfully with the analytical predictions. These studies provide a wider basis for current and future research into the non-linearity and ultimate behavior of the IAL.

*) Associate Professor, Faculty of Mechanical Engineering, Technion - Israel Institute of Technology, Haifa, Israel

**) Lecturer, Faculty of Mechanical Engineering, Technion - Israel Institute of Technology, Haifa, Israel

***) Instructor, D.Sc. Candidate, Faculty of Mechanical Engineering, Technion - Israel Institute of Technology, Haifa, Israel

MECHANICAL BEHAVIOR OF MULTIMATERIAL COMPOSITE SYSTEMS

Interlaminar Behavior

TABLE OF CONTENTS

1. Introduction. 1

2. Literature Survey 2

3. Two-Dimensional Interlaminar Stress Distribution in the Adhesive Layer of a Symmetrical Doubler Model 6

   3.1 Introduction 6

   3.2 Model Representation 6

   3.3 FEM vs Analytical Solution 7

   3.4 Two-dimensional Stress Distribution. 8

   3.5 Discussion 9

   3.6 Conclusions. 11

4. Direct Determination of Average Interlaminar Stress Distribution in a Polymeric Adhesive Layer. 12

   4.1 Introduction 12

   4.2 Analytical Background. 12

   4.3 Experimental Procedure 13

   4.4 Test Results and Discussion. 14

   4.5 Conclusions. 15

5. Thermoelastic Behavior of Multimaterial Doubler Models. . 16

   5.1 Thermoelastic Behavior of a Symmetrical Doubler Model (SMD). 16

   5.2 Thermoelastic Behavior of a Nonsymmetrical Doubler (NMD). 18

6. Shear Stress-Strain Characteristics of Adhesive Layer *in situ*. 22

6.1 Introduction 22

6.2 Testing Procedure. 22

6.3 Results and Discussion 23

6.4 Future Program 23

7. Summary and General Conclusions 25

8. Recommendations for Future Research 26

Bibliography. 27

Glossary. 33

Figures 35

Tables. 71

Appendices. . . . . .

Appendix 1. 73

Appendix 2. 82

LIST OF FIGURES

Fig. 1: Symmetrical doubler model.

Fig. 2: Illustration of the finite element networks for SMD.

Fig. 3: Axial distribution of IAL lateral normal stresses (analytical vs FEM solutions).

Fig. 4: Axial distribution of IAL shear stresses (analytical vs FEM solutions).

Fig. 5: Axial distribution of axial normal stresses through the central adherend.

Fig. 6: Axial distribution of axial normal stresses through the external adherends.

Fig. 7: Axial distribution of shear stresses through the central adherend

Fig. 8: Axial distribution of shear stresses through the external adherends.

Fig. 9: Axial distribution of lateral normal stresses through the central adherend.

Fig. 10: Axial distribution of lateral normal stresses through the external adherends.

Fig. 11: Axial distribution of axial normal stresses through the IAL.

Fig. 12: Axial distribution of shear stresses through the IAL.

Fig. 13: Axial distribution of lateral normal stresses through the IAL.

Fig. 14: Distribution of axial normal stresses close to the IAL edges.

Fig. 15: Distribution of shear stresses close to the IAL edges.

Fig. 16: Distribution of lateral normal stresses close to the IAL edges.

Fig. 17: Distribution of principal stresses close to the IAL edges.

Fig. 18: Variation of principal stress orientation through the IAL (layer 1, Fig. 2C).

Fig. 19: Schema of shear displacement pattern through the IAL.

Fig. 20: Electromechanical extensometer for measuring shear displacement.

Fig. 21: Electromechanical extensometer for measuring lateral normal displacement.

Fig. 22: Applied load vs. shear and lateral normal displacement at the adhesive layer edge.

Fig. 23: Interlaminar shear stress distribution. Experimental vs. analytical solution Model A21).

Fig. 24: Interlaminar lateral normal stress distribution. Experimental vs. analytical solution (Model A21).

Fig. 25: Strain measuring system for the SMD.

Fig. 26: Effect of temperature on axial strains at the EAL surface (Model A02).

Fig. 27: Normalized strain distribution resulting from thermal changes along the EAL external surface (Model A02).

Fig. 28: Stress analysis schema of a nonsymmetrical doubler *model (NMD).*

Fig. 29: Interlaminar normal stress distribution for different adhesive rigidities.

Fig. 30: Interlaminar shear stress distribution for different adhesive rigidities.

Fig. 31: Schema for measuring system of NMD deflections.

Fig. 32: Thermoelastic deflection curve of NMD.

Fig. 33: Schema of modified torsion.testing device for direct measurement of the shear stress-strain behavior of the adhesive layer *in situ.*

Fig. 34: Typical shear stress-strain curves for the adhesive layer *in situ.*

Fig. 35: The effect of adhesive layer on its initial shear modulus

Fig. 36: Flow chart for a future program on non-linear behavior of the interlaminar adhesive layer within a multi-material doubler model.

Fig. 37: Flow chart for a future program on three dimensional behavior of the interlaminar adhesive layer within a multimaterial doubler model.

LIST OF TABLES

Table 1: Dimensions and elastic parameters of the SMD test model.

Table 2: Elastic and thermoelastic parameters of the SMD test model (A02).

Table 3: Dimensions and elastic parameters of the NMD test model.

LIST OF APPENDICES

Appendix 1: Analysis of information on the mechanical behavior of adhesive bonded joints.

Appendix 2: Finite element computer program for stress analysis in orthotropic bonded structural systems.

1. INTRODUCTION

Most of the work conducted during the second research year concentrated on extending and refining the results found during the first year.

Based on up-dating of the literature survey on mechanics of bonded joints, our data and analytical solutions were compared to the results of others, which then raised certain questions necessitating additional study. The main objectives were to clarify some dubious points and to check the controversial information on this subject.

Accordingly, the work was conducted as follows:

- The finite element method (FEM) was used to solve the problem of stress distribution through the adhesive layer thickness and closer to its edges.

- The thermoelastic behavior of symmetrical and non-symmetrical doubler configurations was studied with the use of approximate models, and analytical results were verified experimentally.

- A direct method for measuring stress distribution along the interlaminar adhesive layer (IAL) was developed and the analytical results of the first year were confirmed at a region very close to the IAL edges.

- Improved techniques for the evaluation of strength characteristics and deformational behavior of bonded adhesives were developed to provide a data base for nonlinear and ultimate stress analysis.

- The effect of adhesive layer thickness on the above characteristics was studied.

At present, most of the efforts focus on two major topics: an analytical study of the effect of the nonlinear (inelastic) IAL stress-strain relation on stress distribution, and an investigation of failure mechanism and strength characteristics of doublers composed of aluminum and different composite adherends. It is planned to continue these subjects during the next research year.

The current program and future goals are illustrated schematically in Figs. 36 and 37.

2. LITERATURE SURVEY

An up-to-date bibliography on the subjects of bonded joints and interlaminar behavior is provided in chronological order at the end of this report in Appendix 1 which classifies this literature according to several categories.

Most of the literature reviewed here deals with joints composed of rigid adherends and flexible polymeric adhesives. The adherends were metal-to-metal (aluminum and titanium), composite-to-composite, and, less frequently, metal-to-composite.

The mechanical, analytical representation consisted of main thin beams or plates on elastic substrate in bending. The common structural models were single and double lap joints and, mainly in the case of composite material bonding, scarfed and stepped joints.

Linear elastic behavior of both adherends and adhesives and a state of plane strain in the adhesive and of plane stress in the adherends were assumed in most cases. The common, approximate assumptions were uniform stress distributions through the adhesive thickness, negligible transverse shear deformations, and axial normal interlaminar stresses. Consequently, two main variables were assumed to have a predominant role in adhesive layer behavior, namely, axial shear and lateral normal interlaminar stresses.

Boundary conditions were zero forces and moments at the adherend ends and zero shear stress at the adhesive free edges in the case of square geometry. In several closed form solutions, the last condition was not satisfied because the analytical model did not have enough degrees of freedom.

Earlier works neglected the presence of lateral normal stresses and dealt only with axial shear along the IAL. Volkersen (1938), in his first study of the problem [2], obtained a simple expression for the shear distribution of a single lap joint (SLJ) composed of uniform adherends of different materials and thicknesses. According to Volkersen, maximum shear stress is attained at the adhesive free edge; the IAL stress level is mainly dependent on a parameter consisting of the rigidities and thicknesses of adherends and adhesive layers.

DeBruyen (1944) [3] demonstrated the improvement achieved in stress distribution by varying the thickness of adherends down to zero at the edge. Basing his analytical prediction on Volkersen's solution, he found the dependence of joint strength on the IAL thickness/length ratio to be the governing relationship for an assessment of the performance of bonded joints.

Damarkless (1955) [8] extended Volkersen's solution to cover the effects of shear deformation in the adherend. An earlier publication by Inglis (1923) [1] indicated the existence of pronounced transverse stresses and stress concentration at the joint edges. This problem was studied much later by Adams and Peppiatt (1973) [40], who revealed the presence of high transverse shear stresses on the IAL which were due to the Poisson effect of the adherend.

The breakthrough in this field was achieved by the classical contribution of Goland and Reissner (1944) [4], who provided a closed form analytical solution for single lap joints with expressions of shear and lateral normal stress distributions through the IAL. They presented a model of thin adherend plates of equal thickness and rigidity under cylindrical bending. Here again, though, the boundary conditions of zero shear stress at the IAL edges was unsatisfied. An approximate solution based on their work was given by Plantema (1949) [5]; it included the effect of external moment on IAL shear stresses, but neglected this effect on the respective normal stresses.

Sherrer (1957) [10] extended the work of [4] to cover adherends of different materials by assuming a plane stress for the adherends and a plane strain for the adhesive.

Cornell (1953) [7] presented a model of beams representing the adherends not affected by the adhesive layer, which was represented by a series of tensile and torsional springs.

Iyengar and Alwar (1961) [13] attempted to solve the model of [4] by fulfilling boundary conditions for the free IAL edges. Kunzi and Stevens (1963) [15] corrected the solution of [4] and extended it to cover adherends of different characteristics.

Volkersen (1965) [18], in a later work, suggested a solution which included both shear and normal stresses and satisfied the IAL free edge conditions.

The above-mentioned solutions following [4] were based on many approximate assumptions and over-simplified models. This was due to the complexity of an exact model. It was later found that a few assumptions led to an incorrect solution at the critical region near the edges. Numerical solutions were suggested in order to obtain a more exact solution, and the major effort was devoted to applying the finite element method (FEM) to solve the problem. At first, this method was applied for checking experimental tests to determine joint strength and, especially, the effect of edge geometry. Later, the whole IAL stress distribution was derived by the FEM.

In recent years, several works were published which used FEM to solve the problems of SLJ and DLJ models. Among the first was the report by Kutscha *et al.* (1969) [25], which is based on available FEM programs. The solution derived is for states of plane stress and plane strain. The model used was the same as those of [2] and [4], and the results provided a measure for the accuracy of the closed form analytical solution.

Wooley and Carver (1971) [33] developed a general solution for SLJ, based on FEM, which agreed well with [4] but did not account for the free edge boundary conditions.

Dickson *et al.* (1972) [36] derived analytical solution for joints with orthotropic adherends; they also developed a computer program based on FEM which enables one to deal with different joint geometries and non-linear IAL stress-strain behavior.

A similar attempt to deal with non-linear behavior was carried out by Grimes *et al.* (1972) [39], who suggested a numerical solution to the problem of joints composed of orthotropic FRP adherends.

Contributions by Barker and Hatt (1973) [47], and Adams and Peppiatt (1974) [51], dealt with the problem of singularity at the IAL edges by means of the finite element method. At the same time, works by Hart-Smith (1973) [42-46] and Renton and Vinson (1974) (41,58] suggested analytical solutions to the problem of structural bonded joint including anisotropic composite adherends.

An attempt to tackle the problem of stress distribution through the IAL thickness was undertaken by Pirvics (1974) [5] using finite difference methods. His solution may violate the common assumption of uniform shear and tension through the IAL that was postulated by many authors.

In recent years, much more attention has been given to the present subject; the scope was expanded, and efforts were more oriented towards the applied aspects of analysis and the design of structural bonding.

To sum up, the numerous contributions on the subject during the past decade may be classified into the following topics:

I. Mechanics of joints composed of orthotropic composite adherends [reference numbers: 20, 23, 25, 29, 36, 37, 39, 41, 42, 43, 55, 56, 58, 59, 63].

II. Fracture mechanics approach and testing methods [reference numbers: 49, 53, 60, 64].

III. Environmental effects on bonded joint performance (including thermoelastic behavior), [reference numbers: 21, 35, 49, 50, 54, 64].

IV. Dynamic behavior (fatigue) of structural joints [reference numbers: 21, 32, 36, 41, 54, 55, 56, 63].

V. Effect of non-elastic adhesive characteristics on bonded joint performance [reference numbers: 29, 37, 38, 39, 42, 46, 63].

VI. Effect of varying geometry and adhesive composition at the IAL boundaries on structural performance of the joint, (this may provide guidelines for optimization of structural bonding) [reference numbers: 17, 3 , 40, 47, 51, 61].

VII. Analysis of joints (stepped and scarfed) with complex configurations to fit design requirements [reference numbers: 34, 45, 46, 47, 55, 59, 61].

VIII. Design considerations and evaluation of design allowables for structural bonded joints [reference numbers: 19, 23, 24, 29, 31, 37, 46, 54, 58].

The last topic, VIII, is based on the work by Hughes and Rutherford (1968) [24], who developed a testing methodology for direct measurement of stress-strain behavior, modulus and strength of the adhesive layer *in situ*. In the course of their investigation, they evaluated the mechanical characteristics in shear and tension of different structural adhesives of varying thicknesses.

Numerous articles are available on the chemical and physical aspects of the problem, as well as on the more technological aspects involved in the fabrication and inspection of adhesive joints. These contributions are beyond the scope of the present survey, which is limited to the subject of the mechanical behavior of structural bonded systems.

3. TWO DIMENSIONAL INTERLAMINAR STRESS DISTRIBUTION IN THE ADHESIVE LAYER OF A SYMMETRICAL DOUBLER MODEL.

3.1 Introduction

In order to derive a closed form analytical solution for stress distribution of the IAL, the previous report [65] postulated certain simplified assumptions, which were shared by other authors [4, 7,15,18,41]: uniform shear and normal stress distribution through the thickness direction (z).

The neglect of axial normal stress (σ_x) in the adhesive is also common to many publications on bonded lap joints. These simplified assumptions and the fact that the analytical model does not have sufficient degree of freedom lead to several inconsistencies in equilibrium relationships and violate the boundary condition of zero shear stress at the free IAL square edges.

Because of the mathematical complexity required of a more rigorous solution, and the fact that a realistic bond-line is very thin relative to adherend thickness, only a few studies have been made on IAL lateral stress distribution. Pirvics [52 obtained a solution by finite difference minimization of the internal energy distribution for typical simple lap and butt joint models. His solution, though suffering from inconsistencies, clearly indicates the pronounced non-uniformity in the distribution of both shear and normal stresses through the adhesive thickness.

The present study is intended to deal with the problem by means of the finite element method. The main purposes were to check analytical solutions and to provide basic data for an investigation of strength and failure, for which the local principal stress components, rather than their average values, are required.

3.2 Model Representation

The model for the finite element solution of the SMD is based on orthogonal and triangular elements with a uniform strain field. The elements satisfy the compatability conditions at each of the material points, as well as equilibrium conditions in each element. The mechanical behavior is limited to the elastic-linear range and to the two-dimensional case. A state of plane strain was assumed for the IAL (x-z plane) because of its high width to thickness ratio and its low adhesive-to-adherend stiffness ratio. Although this assumption is less accurate when relating to the adherend layers, it is justified for the present study, which focuses on the IAL. The results of preliminary comparative studies between plane stress and plane strain conditions for the adherends exhibited only small differences.

IAL behavior is best represented by the SMD structural model shown in Fig. 1. This model was also selected for the FEM program because of the following advantages:

- Double symmetry in geometry, materials, boundary, and loading conditions, which allows treatment of one quarter of the model only (in contrast with the SLJ model).

- Wide separation between external loading region and the critical IAL zones where maximum stresses and strains are located. This allows the isolation of the IAL boundary zone which is of main interest for both experimental and analytical study.

- Continuity of stress and strain fields over all the IAL region, which reduces the number of boundary conditions (in contrast to the case of the SLJ model).

The model for the present specific case is composed of aluminum adherends and epoxy adhesive, the characteristics of which are given in Table 1 (test model A21).

The FEM program consisted of three steps. In the first step, uniform stress distributions through IAL thickness was assumed and the IAL was divided into rectangular elements having the IAL lateral dimensions (Fig. 2a).

In the second step, the IAL thickness was divided into two longitudinal strips (Fig. 2b). In the final step, which aimed at deriving the stress distribution through the IAL thickness, it was divided into 4 longitudinal strips as shown in Fig. 2c.

3.3 FEM vs. Analytical Solution

The FEM was first examined by comparing its results (based on the model of Fig. 2A) to the analytical closed-form solution of ref. [65]. Good agreement was found between numerical and analytical results both for the normal stress distribution (Fig. 3) and for the shear stress distribution, except at the region close to the IAL edges (Fig. 4).*) A preliminary study of the effect of a finer network in the axial direction showed only slight differences in results.

The second step revealed different stress patterns close to the edges. Shear stress distribution was found to reverse its slope at the boundary zone ($\chi>0.98$) and to drop to zero towards the IAL edges (Fig. 3). Normal stress, on the other hand, increased steeply towards the edge of the IAL layer close to the

---

*) In all stress distributions (Figs. 3-17) the stresses are normalized with respect to average applied stress acting at the central adherend $p_c=F/2h$. Accordingly: $\bar{\tau}_{xzi}=\tau_{xzi}/p_c$; $\bar{\sigma}_{xi}=\sigma_{xi}/p_c$ $\bar{\sigma}_{xzi}=\sigma_{xzi}/p_c$.

central adherend but reversed their slope and dropped to zero towards the free edges of the IAL layers close the external adherends (Fig. 4).

3.4 Two-Dimensional Stress Distribution

The third step of the FEM solution, in which the IAL was divided into 4 sub-layers, yielded a two-dimensional stress distribution for both adhesive and adherend.*)

3.4.1 Stress Distribution in Adherends

The predominant stress component obtained at the adherends is the axial normal one - σ_{xi} (Figs. 5-6), which was higher by an order of magnitude than the other adherend stresses, σ_{zi} and τ_{xzi} (Figs. 7-10); σ_{xi} was almost uniform through the adherend thickness.

In the case of metallic adherends, in which other stresses besides σ_{xi} are negligible, the assumption of uniform stress distribution through the adherend thickness was justified. However, with adherends composed of multilayer, composite laminates, in which interlaminar stiffness and strength characteristics are significantly lower than axial ones, adherend lateral stresses τ_{xzi} and σ_{zi} have a major role and cannot be neglected. These stresses exhibited pronounced variations through the thickness. In this case, a finer mesh for the FEM solution is essential, especially if strength characteristics are required.

The axial distribution of axial normal stresses through the external layer of adherend 2 exhibited the pattern which was found both analytically and experimentally in ref. [65] (Fig. 30), namely a change from tension to compression close to the adherend edge (Fig. 5).

3.4.2 Stress Distributions Through Adhesive

In the IAL, all stress components are of the same order of magnitude and exhibited a pronounced variation through the thickness (along the z axis); (Figs. 11-13, 14-16). The axial distribution of shear stress (τ_{xzo}) showed a trend similar to that in Step 2, i.e., slope reversal at the 'boundary zone' (from each edge up to a distance of 1% of the IAL length), and a drop towards zero at the free IAL edges. This finding is consistent with boundary conditions but contradicts the closed-form analytical solution (Figs. 12,15).

Axial distribution of lateral normal stresses (σ_{zo}) along the 'boundary zone' showed a pronounced divergence from their

---

*) The results obtained in the present report were related to a model of isotropic adherends. The FEM program, which is given in Appendix 2, is, however, adequate for orthotropic adherend cases as well.

average reference distribution, whereas the normal stress through the external IAL layer rose steeply towards the edge far beyond its slope and dropped towards zero at the free edge (Figs. 13,16).

Axial distribution of axial normal stresses (σ_{xo}) was uniform throughout the "middle zone" (98% of the IAL length) but dropped steeply at the "boundary zone" towards zero at the free edges (Fig.s 11, 14).

It may be concluded that axial interlaminar stress distributions (σ_{zo}, τ_{xzo}) derived by FEM are in close agreement with the closed-form solutions along the "middle zone". The major divergence between the numerical and closed-form solutions resulted from the assumption of uniform lateral stress distributions. As shown in Figs. 15,16, such an assumption did not hold up at the "boundary zone" in cases of shear and normal lateral stresses. The neglect of axial normal stresses through the IAL is also unjustified as these stresses attained a level having the same order of magnitude as other stress components (Fig. 14).

Lateral normal stress distribution at the boundary zone shows the maximum deviation from uniformity (Figs. 13,16), being almost zero close to the external adherend and increasing steeply and linearily to its maximum level towards the central adherend. Similarly, both IAL shear and axial normal stresses attained their maximum value close to the intersection of the free IAL edge and the upper surface of the central adherend (point m of Fig. 1).

3.5 Discussion

Given the values of the three stress components at the IAL boundary zone, their principal value can be derived. Fig. 17 shows the axial and lateral distributions of the principal stresses emphasizing the major trends found for the stress components. The expected finding of the location of maximum stress being close to point m is also demonstrated.

In the case of brittle IAL characteristics, the data given by the principal stress distribution may provide the basic clue for failure mechanism, the delamination process, and strength evaluation for the overall bonded structure as represented by the SMD model. The finite element method seems to provide an accurate solution which conforms well to basic mechanical and boundary conditions. The interrelation among the different functions found for the different stresses can be examined by satisfying the classical equilibrium conditions.

According to the first equilibrium equation

$$\frac{d\sigma_x}{dx} = - \frac{d\tau_{xz}}{dz} \qquad (1)$$

which means that τ_{xz} is uniformly distributed along the z axis in the region where σ_x is uniformly distributed along x. This interrelation prevails at the "middle zone" of the IAL, as is shown when Fig. 15 is compared with Fig. 14.

According to the second equilibrium equation,

$$\frac{d\sigma_z}{dz} = - \frac{d\tau_{xz}}{dx} \qquad (2)$$

which means that where the τ_{xz} distribution along x reverses its slope, the σ_z function along z will also reverse but in the opposite direction. This change occurs simultaneously for the two functions at about χ=0.99 within the "boundary zone", as demonstrated by a comparison of Fig. 15 with Fig. 16.

At the middle zone, the $\tau_{xz}(x)$ functions coincided (Fig. 15), thus σ_z functions are supposed to be linear functions of z, as is clearly shown in Fig. 16.

The above findings referred to an idealized case of thick adhesive relative to its adherends. It is expected that similar distribution patterns will be found, though to a lesser degree, for the more practical cases of thinner and stiffer adhesives. The most important finding of the locations of the maximum principal stresses is also expected to be generally valid.

A more detailed solution for interlaminar adherend stresses is essential for the strength analysis of orthotropic composite bonded systems.

In order to obtain more realistic solutions which provide quantitative data for design allowables, the effects of nonlinearity in an adhesive stress-strain relationship and the effect of edge geometry have to be studied.

Some of the above topics are currently being treated by the finite element method and will be presented in the future.

3.6 Conclusions

The following conclusions emanate from the solutions obtained by applying the finite element method to the symmetrical doubler model, composed of aluminum adherends bonded by thick adhesive layers (IAL). Most of the conclusions concern the stress distributions through the IAL, which is the main subject of the present investigation.

1. The distribution of shear and lateral normal stress through the IAL thickness was approximately uniform within the "middle zone" ($-0.98<\chi<0.98$).

2. Axial normal stress distribution [$\sigma_x(x)$] was uniform within the"middle zone" but varied linearly through the IAL thickness.

3. For all interlaminar stress functions, drastic variations occurred at the "boundary zone".

4. The distribution of IAL axial shear stress attained its maxima within the "boundary zone", reversed its slope and dropped towards zero at the free edge. A similar trend was found for σ_z distributions close to the external adherends.

5. The normal lateral stress function $\sigma_z(z)$ exhibited an approximately linear distribution, which reversed its slope abruptly within the "boundary zone".

6. Maximum values of all stresses and their principal counterparts were attained at the "boundary zone", close to the central adherend interface.

7. The different patterns which characterized stress functions along the z and x axes were consistent with basic differential equilibrium equations and boundary conditions of the IAL.

8. The average interlaminar stress levels were significantly lower than their actual individual extreme levels; thus, they could not be used to predict the doubler strength.

9. Because of the narrow dimensions of the boundary zone, its stress behavior will not be reflected in the overly deformational behavior of the bonded structure, nor could this behavior be directly detected experimentally. It is, however, predominantly influential on the ultimate behavior of the IAL and has to be considered when failure mechanism and strength characteristics are discussed.

4. DIRECT DETERMINATION OF AVERAGE INTERLAMINAR STRESS DISTRIBUTIONS IN A POLYMERIC ADHESIVE LAYER.

4.1 Introduction

The real stress distribution through IAL is still undecided because of the controversy over the different solutions of the problem. Unfortunately, there is no satisfactory experimental means of direct characterization of these stresses. Matting [16] and Kreiger [49] measured directly only the shear displacement of SLJ and compared it with solutions of [2] and [4]. Most attempts at such characterization employed indirect measurement of strains at the external adherend surfaces by means of strain gages [65,42], or photoelastic [65,36,9], or Moiré [70] methods. In all cases, the patterns were obscured by the interference of other factors such as stress concentrations, edge effects of the photo-stress coating, etc. Moreover, the interlaminar stress distribution cannot be conclusively established from data on adherend strains. This problem is crucial, considering that the location of the joint, where extreme stresses develop and enhance delamination, is very close to the edges of the adhesive layer. The object of the present investigation is, therefore, twofold:

a. To develop a method for direct determination of the interlaminar strain and stress distribution which will provide a check on the validity of existing analytical solutions;

b. to devise a tool for the direct measurement of the critical stresses which control the ultimate performance of the joint or laminate under different loads and environmental conditions.

4.2 Analytical Background

A simplified expression of IAL shear stress distribution for the SMD model (Fig. 1) is given in eq. (3):

$$\tau^* = \frac{h_2\phi}{c}\,\frac{\sinh\phi\chi}{\cosh\phi} \qquad (\chi = \frac{x}{c}) \tag{3}$$

where $\tau^* = \frac{\tau}{p_0}$ is the normalized shear stress;

$$\phi^2 = \frac{c^2 G_0}{h_0 h_1 E_1}\,(1 + \mu) \tag{4}$$

$$\mu = \frac{E_1 h_1}{E_2 h_2} \tag{5}$$

and

$$p_0 = \frac{F}{2h_2(1+\mu)} \tag{6}$$

is the reference axial normal stress (acting at the external adherend layer -(EAL) midpoint under the action of F). The derivation of eq. (3) and the more exact solution for shear stress distribution is given in ref. [65].

The similarity of the simplified to the more exact solution for a case of multimaterial doubler model is shown in Fig. 9 of ref. [65].

The derivation of the expression for interlaminar lateral normal stresses, $\sigma_z^{(0)}$, is more complex than that for shear stress analysis. It involves the solution of differential equations of the 6th order, as is fully described in ref. [65]. Typical distribution curves of σ^* for different boundary conditions are shown in Fig. 10 of this reference. ($\sigma^*=\sigma_z^{(0)}/p_0$ is the normalized expression for IAL lateral stresses.)

4.3 Experimental Procedure

Shear strain γ and shear stress τ are obtainable from the shear displacement Δu, i.e., the differential displacement of the adherend surfaces (Fig. 19):

$$\gamma_0 = \frac{\Delta u}{h_0} \qquad \tau_0 = \frac{\Delta u}{h_0} G_0 \tag{7}$$

Similarly, by measuring the net lateral displacement, normal lateral stresses are obtainable from eq. (8):

$$\sigma_0 = \frac{w_0}{h_0} E_0 \tag{8}$$

Instron electromechanical extensometers were modified and used for measuring Δu and w_0, respectively.

Measuring Devices. The shear-displacement extensometer shown in Fig. 20 is a modification of the Instron Extensometer Type G51-11. It consisted of two parts, each attached to a point at the mid-thickness of the adherends, all of which were originally located on the same line (along the z-axis), but which were shifted relative to each other under axial loading, thereby creating the shear displacement. The normal displacement distribution was obtained in the same manner, utilizing the normal-displacement extensometer shown in Fig. 21, which is a modification of Instron Extensometer G57-11 (originally used for measuring

the Poisson ratio).

The displacements were measured within an accuracy of 0.2μm. The distributions were obtained by applying the extensometers at different points along the model axis.

Preparation of Test Model. The measuring systems were checked on test models consisting of two aluminum adherends and an epoxy IAL having the characteristics given in Table 1.

The surfaces of the adherends were sand blasted, cleaned with MEK and coated with a thin layer of resin, as described in detail in ref. [65]. Immediately following the coating, the adherend strips were inserted into a special fixture which ensured the exact spacing for the IAL phase. The external adherends were longer than the adhesive bond-line in order to enable measurement of displacements at IAL edges (see Fig. 1).

The epoxy-versamid mix (2:1) was prepared under vacuum and poured into the gap; its temperature was kept at 40°C to reduce viscosity and ensure good wetting. The model was unmolded after 24 hours and exposed for 8 hours at 40°C to post-cure the resin.

Loading Procedure. The model was loaded uniaxially on an Instron Tester at the rate of about 10^{-3} (min^{-1}), up to failure. Shear displacement values were recorded continuously. The specimen was unloaded at different loading levels as a check on the reversibility of the response.

4.4 Test Results and Discussion

The relationship between the shear displacement and the reference axial stress, as shown in Fig. 22, is characterized by linear behavior up to approximately 80% of the loading range. Beyond this level, nonlinearity prevailed to the delamination stage.

The shear stresses at the various points along the IAL were calculated from the measured shear-displacement data with the aid of eq. (7). The experimental interlaminar shear stress distribution, shown in Fig. 22, was compared with the approximate analytical solution of eq. (3). Considering the approximations involved, agreement between the experimental data and the analytical prediction is good, especially with regard to the shape of the distribution curve close to the boundary.

The tendency of the shear stresses to increase to their maximum value at the IAL edge was in agreement with the analytical solutions of ref. [4] for bonded joints and of ref. [65] for doubler models. It conflicted, however, with the boundary condition of zero shear stress at the free IAL edge and with solutions based on the finite-element method (Fig. 15).

In order to obtain the exact value of lateral displacement resulting from interlaminar normal stress $\sigma_z^{(0)}$, the contribution of Poisson's effect to the overall displacement must be determined. The Poisson displacement data hardly vary along the model axis and may be calculated or measured separately.

The relationship between lateral normal displacement and the reference axial stress is shown in Fig. 22, where similar trends to those of the shear-displacement data are apparent, i.e., linearity within 80% of the loading range.

The lateral normal stresses at the various points along the IAL were calculated from the net lateral displacement data with the aid of eq. (8).

The experimental interlaminar normal stress distribution (Fig. 24) was compared to the analytical solution given in eq. (33) of ref. [65]. The agreement between the experimental data and the analytical prediction was good, especially with regard to the shape of the distribution curves close to the IAL edges.

4.5 Conclusions

A method of direct measurement of shear and normal displacements and a simple way of determining strain and stress distributions along an interlaminar adhesive layer were examined successfully on a symmetrical doubler model.

The experimental interlaminar stress data were in agreement with available analytical solutions for this model. The advantages of the direct method compared with others are as follows:

a. It is based on direct, local measurement of the deformations of the adhesive layer (as against indirect measurements of adherend strains).

b. It is a simple method utilizing the standard accessories of an Instron extensometer with only slight modifications.

c. The accuracy in measuring displacements to within 0.2μ permits detection of stress variations of about 0.2 kg/mm^2, which is less than 5% of the ultimate shear and stress delamination level.

d. The continuous recording of interlaminar adhesive strains against axial load permits monitoring of IAL behavior from the linear elastic range to the nonlinear inelastic range up to initiation of the failure process.

This study may reveal the actual mechanism of adhesive and cohesive failure modes which are eventually responsible for the delamination of laminates, joints, and other bonded systems that are subjected to mechanical and thermal loading.

5. THERMOELASTIC BEHAVIOR OF MULTIMATERIAL DOUBLER MODELS

The analytical expressions in Ref [65], (eqs. 63, 68, 43), covered the effect of thermal changes on mechanical behavior with respect to elastic and thermoelastic parameters.

The solution was based on the assumption that the coefficient of thermal expansion, and of other material parameters, were not affected by thermal changes. The solution also neglected transverse behavior and its interrelation with axial behavior. Within these limitations, which apply for an isothermal regime, there is a wide range of materials, geometries, and thermoelastic parameters for which the solution is valid.

The thermoelastic behavior of symmetrical and nonsymmetrical doubler models (SMD and NMD, respectively) were studied with a view to checking the validity of analytical formulations of the stress distribution by means of strain- and deflection-measurements along the model's external facings.

5.1 Thermoelastic Behavior of a Symmetrical Doubler Model (SMD)

5.1.1 Analytical Background.

The normalized approximate expression for the external strain distribution of the EAL is given by eq. 9 (eq. (73) of ref. 65):

$$\varepsilon^* = 1 - \frac{\cosh\phi\chi}{\cosh\phi} = \frac{E_2}{p_0}\,\varepsilon_2 \qquad (9)$$

where

$$p_0 = \frac{E_1 h_1 (\alpha_1-\alpha_2) T}{h_2 (1+\mu)} \qquad (10)$$

For non-loaded specimens, eqs. (9) and (10) yield the strain distribution along the EAL external facing:

$$\varepsilon_2 = \frac{\mu}{1+\mu}(\alpha_1-\alpha_2) T \left[1 - \frac{\cosh\phi\chi}{\cosh\phi}\right] \qquad (11)$$

where $\mu = \frac{E_1 h_1}{E_2 h_2}$; α_1, α_2, E_1, E_2, are the thermal coefficients and the elastic moduli in the x-direction, respectively.

Eqs 9-11 are based on the assumption of negligible transverse stresses, i.e.:

$$\sigma_{zy} << \sigma_{zx}$$

In the thermoelastic case, such conditions require near-uniformity of the thermal expansion coefficient in the transverse direction, i.e., $\alpha_{1y} \simeq \alpha_{2y}$.

5.1.2 Experimental Procedure.

Model A02, which had served previously for experimental verification of eq. (9) in the the case of mechanical axial loading, was also used in the thermal tests. Its basic characteristics are given in Table 2.

The axial thermal coefficients α_{x_1} and α_2 were measured by strain gage, whereas α_{y_1} is given by the manufacturer for the GRP 1002 prepregs used. It can be seen from Table 2 that the near-uniformity requirement was satisfied. The test was carried out as follows:

Fourteen gages were glued to the aluminum external EAL surfaces of the test model, as shown in Fig. 25. The specimen was exposed to changes in temperature within a thermal chamber that ranged from 30°C to 60°C. (Higher temperatures were expected to affect the elastic parameters of the polymers.) Strains were recorded simultaneously at the different gage points. The temperature was raised and lowered several times to check reproducibility and reversibility. The results are shown in Figs. 26 and 27, and indicated the following conclusions:

a. The near-linearity of the thermal increase of the elastic strain justified use of the normalized form of eq. (9) for the thermoelastic case (Fig. 26).

b. The measured strain distribution along the external EAL surface was in fair agreement with eq. (9). The near-uniformity of the strain distribution through the major midsection was evident in Fig. 27.

The experimental results provided, however, only an indirect and partial confirmation of the interlaminar shear and normal stress distributions; it did not indicate the actual interlaminar characteristics close to the edge, which is one of the main objectives of the present investigation.

5.2 Thermoelastic Behavior of a Nonsymmetrical Doubler (NMD)

The following experimental and analytical work deals with a nonsymmetrical model composed of two strips, each of a different material, bonded together by a thin layer of polymeric material and subjected to thermal changes (see Fig. 28). These changes and the different coefficients of expansion, bring about thermal stresses causing the strips to deflect. The deflection can be measured and compared with analytical solutions.

5.2.1 Analysis.

Equilibrium conditions of the NMD model give (see Fig. 28):

$$N_1 = N_2 = N \tag{12}$$

$$M_1 + M_2 = N[\frac{h_1}{2} + h_0 + \frac{h_2}{2}] = N[\bar{H}] \tag{13}$$

$$V_1 + V_2 + \tau h_0 = 0 \tag{14}$$

This leads to

$$\frac{dN}{dx} = \tau \tag{15}$$

$$\frac{dV}{dx} = \sigma \tag{16}$$

$$V + \frac{dM}{dx} - \tau \frac{h}{2} = 0 \tag{17}$$

The six equations, together with the compativility conditions yield:

$$\frac{\varepsilon_1 - \varepsilon_2}{h_0} = \frac{1}{G} \frac{d\tau}{dx} \tag{18}$$

$$\frac{1}{\rho + h} = \frac{1}{\rho^2} \tag{19}$$

ρ being the beam curvature.

Introducing elastic stress-strain relations and linear thermal coefficients of expansion results in

$$\varepsilon_1 = \frac{N_1}{E_1 h_1} + \frac{6M_1}{E_1 h_1^2} + \alpha_1 T \tag{20}$$

T being the thermal change

$$\varepsilon_2 = \frac{N_2}{E_2 h_2} - \frac{6M_2}{E_2 h_2^2} + \alpha_2 T \tag{21}$$

This leads to the following governing differential equation

$$[D^2 - C_{21}]M_2 = C_{31} \tag{22}$$

where

$$C_{ij} = \frac{C_i}{C_j} \tag{23}$$

$$C_1 = \frac{2h_0}{c^2 HG}(1+\mu) \tag{24}$$

$$C_2 = \frac{6}{E_2 h_2^2} + \frac{6\mu}{E_1 h_1^2} + \frac{2(1+\mu)}{HE_1 h_1} - \frac{2(1+\mu)}{HE_2 h_2} \tag{25}$$

$$C_3 = (\alpha_2 - \alpha_1) T \tag{26}$$

where $2c = \ell$ - is the NMD length and

$$\mu = \frac{E_1}{E_2}\frac{h_1}{h_2} \tag{27}$$

Solving these governing equations with the boundary condition $M_1 = M_2 = 0$ at $\chi = x/c = \pm 1$ yields:

$$M_2 = \frac{C_3}{C_2}\left[1 - \frac{\cosh\sqrt{C_{21}}\chi}{\cosh\sqrt{C_{21}}}\right] \tag{28}$$

and

$$M_1 = M_2 \mu = M_2 \frac{E_1}{E_2} \tag{29}$$

Eqs. 15-17 lead to the following expressions:

$$\tau = \frac{C_3}{\sqrt{C_1 C_2}} \quad \frac{2(1+\mu)}{cH} \quad \frac{\sinh\sqrt{C_{21}}\chi}{\cosh\sqrt{C_{21}}} \tag{30}$$

$$\sigma = \frac{C_3}{C_1} \quad \frac{(\mu-1)}{2c^2} \quad \frac{\cosh\sqrt{C_{21}}\chi}{\cosh\sqrt{C_{21}}} \tag{31}$$

which are the interlaminar tensile and shear stress distributions through the adhesive layer.

5.2.2 Discussions.

Once the stress distributions of τ and σ_z are known, significant conclusions may be drawn as to the effect of the material and geometrical parameters on the IAL shear and normal stresses while subjected to temperature changes.

For the special case of $h_1 = h_2$, one obtains

$$C_1 = \frac{2h_0}{c^2 HG}(1+\mu) \tag{32}$$

$$C_2 = \frac{4[12\mu + 1-\mu^2]}{E_1 H^2} = \frac{4\bar{\mu}}{E_1 H^2} \tag{33}$$

$$C_3 = \Delta\alpha T \tag{34}$$

Assuming $\frac{h_0/G}{H} = R_0$ to be the rigidity parameter of the IAL leads to the following equations:

$$\bar{\tau} = \frac{\tau}{T} \approx \Delta\alpha \sqrt{\frac{(1+\mu)E}{2\bar{\mu}}} \sqrt{\frac{1}{R}} \quad \frac{\sinh\sqrt{C_{21}}\chi}{\cosh\sqrt{C_{21}}} \tag{35}$$

$$\bar{\sigma} = \frac{\sigma}{T} \approx \Delta\alpha \left(\frac{(\mu-1)}{4(1+\mu)}\right) \frac{1}{R} \frac{\cosh\sqrt{C_{21}}\chi}{\cosh\sqrt{C_{21}}} \tag{36}$$

Both $\bar{\tau}$ and $\bar{\sigma}$ are affected by three main parameters:

a. $\Delta\alpha$, which is the measure of thermal incompatibility;

b. a moduli incompatibility;

c. the rigidity parameter of the adhesive layer.

In Figs. 29 and 30, both $\bar{\tau}$ and $\bar{\sigma}$ were drawn as functions of three different adhesive rigidities for strips composed of aluminum 2024/T-3 and unidirectional (GRP) prepreg 1002 (a 3M product). (See Table 3.)

5.2.3 Experimental Procedure.

The main objective of the experimental phase was to examine the validity of the analytical solution postulated in the previous chapter. For this purpose, the relation between the moments in the different strips and the central deflection w of a simply supported beam was calculated and found to be:

$$w = \frac{1}{EI}\left[\frac{C_3}{C_2}\left(\frac{C_1 c^2 (1-\cosh\sqrt{C_{21}}\chi)}{C_2\cosh\sqrt{C_{21}}}\right) + \frac{\chi^2}{2}\right] \qquad (37)$$

Special grips were designed to enable the measuring of the deflection. The testing device, together with the test specimen, was spaced in an oven, and the temperature was changed by 10 degree intervals. The deflections were measured by a catatometer at several points along the beam (see Fig. 31). The mid-point deflection was drawn as a function of temperature. In Fig. 32, the experimental results are compared with the analytical ones; as shown, there was a good agreement between the two.

5.2.4 Conclusions.

a. The nonsymmetrical multi-material doubler system proved to be a good tool for the analysis of stress distribution through an adhesive layer.

b. The stresses within the IAL were reflected in a measureable deflection of the doubler. This fact may serve as a simple yet effective indirect method for deriving experimentally the distribution and critical values of interlaminar shear and normal stresses caused by thermal changes.

c. As seen from Figs. 29 and 30, adhesive rigidity parameters had a major influence on both stress peak and its gradient. Thick layers of flexible adhesive will result in low stresses at the edges. On the other hand, thin layers of rigid adhesive will cause a very high stress concentration at the doubler edges. These stresses are critical as they cause premature failure.

6. SHEAR STRESS-STRAIN CHARACTERISTICS OF THE ADHESIVE LAYER *IN SITU*

6.1 Introduction

The main problem in characterizing an adhesive as a structural material is whether its behavior in a confined state differs from that of its bulk material reference. To resolve this problem, which is essential for an evaluation of design allowables of bonded joints, it is necessary to carry out elaborate and precise measurements and to develop a special testing device.

A crucial problem in such testing stems from the fact that the thickness of an adhesive has a major effect on its mechanical performance because of the adherend-adhesive boundary constraints and the small measurable displacements obtained in the case of commonly used adhesives, which are relatively very thin. These restrictions limited the available data [23,37,46,54] which originated in the work of Hughes and Rutherford [24]. The available information, which is mainly concerned with adhesive behavior under torsion and uniaxial tension, indicates the following: beyond approximately 0.25 mm, adhesive strength and effective modulus decrease moderately with adhesive thickness and tends to level off at a value close to that of the bulk material. Below this thickness, a steep increase in adhesive strength, and to a lesser degree, of effective tensile modulus, is evident.

During the past research year, shear strength data of adhesives *in situ* were evaluated by a specially constructed torsion device [65]. During the present year, this device was improved and modified by the attachment of a torsional displacement accessory (Fig. 33) which enabled the recording of the shear moment-displacement relationship by means of an Instron extensometer and recorder. The testing procedure is also more efficient because of the separation between the adhesive-adherend unit (which is exchangeable) and the measuring system.

6.2 Testing Procedure

The main objective of this test series was the evaluation of the initial shear characteristics at the linear elastic range far below the ultimate level. Hence, aluminum surfaces were not treated but only cleaned by MEK. The adhesive was composed of Shell resin 828 and General Mills Versamid V-140, in a ratio of 2:1. The adhesive was cast between the adherends' controlled spacing, which varied from 0.1 to 2.0 mm. Curing was for 24 hours at room temperature followed by 48 hours at 50°C.

After curing, the shear specimens were installed in the torsional device which was mounted on the Instron tester. Cross-head speed was 0.5 mm/min. For calibration, shear displacement of specimens composed of tightened adherends of zero adhesive thickness, were recorded to be deducted from the over-all shear displacement of the bonded specimens.

6.3 Results and Discussion.

Shear strains and stresses were computed from the recorded torsional moment-displacement curves by assuming linear shear-strain distribution throughout the adhesive thickness and uniform shear strain distribution at the corss-sectional area. Typical shear stress-strain relationships for different adhesive thicknesses are shown in Fig. 34. Low ultimate values were obtained due to the deliberately weak interfacial bonding. However, a qualitative difference can be distinguished between the behavior of relatively thin and thick adhesives, namely: larger ultimate strains at lower stress levels which may indicate higher ductility and are typical of thin adhesives compared with their thick counterparts.

Initial effective shear modulus values, which were derived from the stress-strain curves with the same assumptions, are shown in Fig. 35 as a function of adhesive thickness.

In spite of the reasonable scatter of the moduli data, the general trend is clear, i.e., an almost linear increase of modulus with an increase in thickness. The higher values of shear modulus, within the range of 90-110 kg/mm^2 found for thick adhesive layers (above h =1.0mm), are compatible with shear data obtained for the bulk epoxy material.

The conflicting evidence of higher effective tensile modulus of thin adhesive layers reported earlier can be settled by two arguments:

a. This trend was found to prevail below 0.1 mm.

b. The case of tensile loading where the lateral restraint of metal adherends reduced longitudinal deformations, is basically different from the relatively free and pure shear situation which prevailed in the torsional shear test.

6.4 Future Program.

The intension is to continue the present investigation along the following lines:

a. Study of the effect of adhesive thickness on tensile modulus, both experimentally and analytically, which will take into account the lateral constraint of adherends and the different characterstics of the interfacial adhesive boundary layers.

b. Taking the same approach, an experimental and analytical study of the effect of adhesive layer thickness on strength in shear and uniaxial tension

c. A device for combined shear-axial loading of adhesive *in situ* had been designed and will be utilized for deriving adhesive strength characteristics under combined states of stress. Resultant data, it is hoped, will provide the basis for evaluating failure envelopes of adhesives which is essential for strength prediction of the SMD model specifically, and for different adhesive bonded joint models in general.

7. SUMMARY AND GENERAL CONCLUSIONS

The present report consists of several topics concerned with stress and strain analysis of the interlaminar adhesive layer within a doubler model. The following conclusions were drawn:

a. Two dimensional stress distribution through IAL derived by the finite element method revealed the following characteristics:

i) Almost uniform shear and lateral normal stress distribution prevailed throughout the IAL thickness along its "middle zone".

ii) Extreme non-uniform distributions exist at the "boundary zone".

iii) Shear stresses attained their peak at the "boundary zone" and dropped steeply towards zero at the IAL edges, which is consistent with boundary and equilibrium conditions.

iv) Axial normal stresses, which were negligible at the IAL "boundary zone", attained the same order of magnitude as other interlaminar stresses along the "middle zone" close to the central adherend.

v) The principal interlaminar stresses reached their extreme value close to the intersection of the IAL edge and the IAL central adherend interface.

b. Stress distributions along the IAL which were determined by a direct measurement of shear and normal relative displacements, show good agreement with both analytical closed form solution and with numerical solution derived by finite element method.

c. Thermoelastic investigation of IAL stresses within symmetrical and nonsymmetrical doubler models showed good agreement between experimental measurements and analytical closed form solutions.

d. The stress-strain relationship of the adhesive layer *in situ*, when measured by a special torsion device, indicated that the adhesive shear modulus increased moderately with the thickness of the adhesive and approached the respective modulus of the bulk epoxy at a thickness of about 1.0 mm.

8. RECOMMENDATIONS FOR FUTURE RESEARCH

It is recommended that the present research be continued along the following lines (see Figs. 36,37):

a. Parametric study of the effects of variations in IAL thickness and its edge geometry, as well as its material characteristics (by FEM).

b. Two dimensional stress analysis of SMD at the nonlinear range of IAL behavior (by FEM).

c. Study of the elastic and thermoelastic three dimensional behavior of SMD.

d. Investigation of strength and failure characteristics of IAL within SMD as related to respective behavior of adhesive *in situ*, under combined loading.

e. Investigation of the environmental effects (temperature and humidity) on IAL mechanical behavior, as reflected by SMD performance.

BIBLIOGRAPHY

ADHESIVE BONDED JOINTS

1. C.E. Inglis, Stress Distribution in a Rectangular Plate Having Two opposing Edges Sheared in Opposite Directions. Proc. Royal Soc. London, Series A., 103, pp. 598-610 (1923).

2. O. Volkersen, Luftfahrtforschung, 15, pp. 41-47 (1938).

3. N.A. DeBruyne, The Strength of Glued Joints, Aircraft Engineering, 16, pp. 115-118 (1944).

4. M. Goland and E. Reissner, The Stresses in Cemented Joints, J. of Applied Mechanics, 11(1), pp. A17-A27 (1944).

5. F.J. Plantema, The Shear Stress in a Glued Joint, National Lucht. Lab., Amsterdam, Report M 1181 (1949).

6. B.J. Aleck, J. of Applied Mechanics, 16, p. 118 (1949).

7. R.W. Cornell, Determination of Stress in Cemented Lap Joints, J. of Applied Mechanics, 20(3), pp. 355-364 (1953).

8. L.R. Demarkles, Investigation of the use of a rubber analog in the study of stress distribution in rivited and cemented joints, Tech. Notes, 3413 (1955).

9. C. Mylonas, Experiments on Composite Models with Applications to Cemented Joints, Proceedings of the Spring Meeting of the Society for Experimental Stress Analysis, 12(2), p. 129 (1955).

10. R.E. Sherrer, Stress in a Lap Joint with Elastic Adhesive, USDA Forest Products Lab. Report No. 1864 (1957).

11. A.S. McLaren and I. Madnnes, British J. of Applied Physics, 9, p.72 (1958).

12. A. Hartman and J.B. DeJange, Nondestructive Tests on Redux Bonded Single and Double Lap Joints with Various Glue Line Thicknesses, NAARI, Amsterdam (1960).

13. K.T.S. Iyengar and R.S. Alwar, Proc. Seventh Congress of Theoretical and Applied Mechanics, Bombay (1961).

14. D.D. Eley (Ed.), Adhesion, Oxford University Press, pp. 207-226 (1961).

15. E.W. Kuenzi and G.H. Stevens, Determinator of the Mechanical Properties of Adhesives for Use in the Design of Bonded Joints, US-FPL Report FPL-011 (1963).

16. A. Matting, Grenzflachen-reaktionen and spannungs-verteilung in metall-klebverbindungen", Kunstoffe,16, Jahrgang Nr 7, 387 (1963).

17. C.H. Lerchenthal, Design of Bonded Lag Joints for Optimum Stress Transfer, Part 1: The Symmetrical (or double) Lap Joint, Israel J. of Technology, 2(1) (1964).

18. O. Volkersen, Construction métalliane, No.4, pp. 3-13 (1965).

19. B.F. Prokhorov, Joints Used in Plastic and Composite Shipboard Super Structures, Deckhouses, Light Bulkheads and Enclosures, Sudostroyeniye, 9, pp. 44-51 (1965).

20. J.I. Gnopp, Measurement of Moments at Edges of Adhesive Lap Joints between Glass-Reinforced Plastic Laminates, Picatinny Arsenal T.M. 1932, (1965).

21. F. Szepe, Strength of Adhesive Bonded Lap Joints with Respect to Change of Temperature and Fatigue, Exper. Mech., 6, pp. 280-286 (1966).

22. A.J. Durelli and V.J. Parks, Experimental Stress Analysis of Loaded Boundaries in Two-Dimensional Second Boundary Value Problems, Report No. 11, Contract No. 2249(06)(1967).

23. G.A. Clark and K.I. Clayton, Structural Techniques for Joining Filamentary Composites, AIAA 5th Annual Meeting, Paper No. 68-1038 (1968).

24. E.J. Hughes, J.L. Rutherford, Study of Micromechanical Properties of Adhesive Bonded Joints, Aerospace Research Center, General Precision Systems, Technical Report 3744 (1968).

25. D. Kutscha et al., Feasibility of Joining Advanced Composite Flight Vehicle Structures, IIT Res. Inst. Technical Report AFML-TR-68-391 (1969).

26. L.J. Hart-Smith, The Strength of Adhesive Bonded Double Lap Joints, IRAD Report, No. MDC - JO367, November 1969.

27. V. Nieorgon, Bonded Joints, A Photoelastic Study, UTIAS Technical Note No. 138 (1970).

28. J.L. Lubkin and L.C. Lewis, Adhesive Shear Flow for an Axially Loaded, Finite Stringer Bonded to an Infinite Sheet, The Quarterly Journal of Mechanics and Applied Math., Vol. XXIII, Part 4, pp. 520-533 (1970).

29. A. Puppo and H. Evenson, Calculation and Design of Joints Made from Composite Materials, USA AV Labs Tech. Report 70-27, U.S. Army Material Laboratories (1970).

30. G.C. Grimes, Stress Distribution in Adhesive Bonded Lap Joints, SAE Transactions, 370-378 (1971)

31. V. Niranjan, Bonded Structures and the Optimum Design of a Joint, Technical Note No. 164, UTIAS (1971).

32. V. Niranjan, D.R. Hamel and C.A. Yang, Static and Fatigue Strength of FM-132-2 Adhesive in Double Strap Joints of Various Lengths of Overlap, UTIAS Technical Note No. 160 (1971).

33. G.R. Wooley and D.R. Carver, Stress Concentration Factors for Bonded Lap Joints, J. Aircr., 8, pp. 817-820 (1971).

34. F. Erdogan and M. Ratwani, Stress Distribution in Bonded Joints, J. Composite Materials, 5, pp. 378-393 (1971).

35. T. Hata, Mechanisms of Adhesive Failure, J. Adhesion, 4, pp. 161-170 (1971).

36. J.N. Dickson, T.M. Hsu and M.J. McKinney, Development of an Understanding of the Fatigue Phenomenal of Bonded and Bolted Joints in Advanced Filamentary Composite Materials, Vol. 1, Analysis Methods. Technical Report AFFDL-TR-72-64 (1972).

37. N. Correlli, Design of Bonded Joints in Composite Materials, NASA Res. Center, Proc. of the Symp. on Welding, Bonding and Fastening, 297-300 (1972).

38. T. Hayashi, Creep Analysis of a Bonded Lap Joint, Composite Materials and Structures, 1(2), pp. 58-63 (1972).

39. G.D. Grimes et al., The Development of Non-Linear Analysis Methods for Bonded Joints in Advanced Filamentary Composite Structures, Technical Report AFFDL-TR-72-97 (1972).

40. R.D. Adams and N.A. Peppiatt, Effect of Poisson's Ratio Strains in Adherends on Stress of an Idealized Lap Joint, J. of Strain Analysis, 8, pp. 134-139 (1973).

41. W.J. Renton and J.R. Vinson, The Analysis and Design of Composite Material Bonded Joints Under Static and Fatigue Loadings, AFOSR-1760-72, Scientific Report AFOSR-TR-73-1627 (1973).

42. L.J. Hart-Smith, Analysis and Design of Advanced Composite Bonded Joints, Final Report NASA CR-2218 (1973).

43. L.J. Hart-Smith, Adhesive-Bonded Double-Lap Joints, NASA Contract Report No. NASA-CR-112235 (1973).

44. L.J. Hart-Smith, Adhesive-Bonded Single-Lap Joints, NASA Contract Report No. NASA-CR-112236 (1973).

45. L.J. Hart-Smith, Adhesive Bonded Scarf and Stepped Lap Joints, NASA Contract Report No. NASA-CR-112237 (1973).

46. L.J. Hart-Smith, Non-Classical Adhesive Bonded Joints in Practical Aerospace Construction, NASA Contract Report No. NASA_CR-112238 (1973).

47. R.M. Barker and F. Hatt, Analysis of Bonded Joints in Vehicular Structures, AIAA Journal, 11(12), pp. 1650-1654 (1973).

48. T. Akasaka and M. Hirano, An Analytical Study on Shear Strength of Lap Joints, Composite Material and Structures, 2(4), pp. 1-4 (1973).

49. R.B. Krieger, Evaluating Structural Adhesives under Sustained Load in Hostile Environment, SAMPE Quart, 5, p.42 (1973).

50. J.E. Lohr, Factors Affecting the Survivability of Stressed Bonds in Adverse Environments, 18th National SAMPE Symposium, 18, pp. 418-426 (1973).

51. R.D. Adams and N.A. Peppiatt, Stress Analysis of Adhesive-Bonded Lap Joints, J. of Strain Analysis, 9(3) (1974).

52. J. Pirvics, Two Dimensional Displacement-Stress Distributions in Adhesive Bonded Composite Structures, J. Adhesion (6), pp. 207-228 (1974).

53. C.K. Lim, M.A. Acitelli and W.C. Haman, Failure Criterion of a Typical Polyamide Cured Epoxy Adhesive, J. Adhesion, 6, pp. 281-288 (1974).

54. E.E. House, Jr. and J.A. White, Adhesive Bonding Increases Fatigue Life of Wing Joint, AIAA Paper No. 74-382 (1974).

55. W.J. Renton and J.R. Vinson, On Fatigue Behavior of Bonded Joints in Composite Materials Structures, AIAA Paper No. 74-484 (1974).

56. W.J. Renton and J.R. Vinson, Fatigue Response of Anisotropic Adherend Bonded Joints, AMMRC MS 74-8, pp. 7-22 (1974).

57. W.N. Sharpe, Jr. and T.J. Muha, Jr., Comparison of Theoretical and Experimental Shear Stress in the Adhesive Layer of a Lap Joint Model, AMMRC MS 74-8, pp. 23044 (1974).

58. W.J. Renton and J.R. Vinson, The Analysis and Design of Anisotropic Bonded Joints, Report No. 2, AFOSR-TR-75-0125 (1974).

59. M.N. Reddy and P.K. Sinha, Stress in Adhesive Bonded Joints for Composites, Fiber Sci. & Tech., 8(1), pp. 33-47 (1975).

60. W.D. Bascom, Adhesive Fracture Behavior of Elastomer-Modified Epoxy Resin, Porc. of 30th Donf. SPI Reinforced Plastics/ Composites Institute, Section 22-D (1975).

61. S. Srinivas, Analysis of Bonded Joints, NASA TN D-7855, 50 pp. (1975).

62. L.M. Keer and K. Chantaramungkorn, Stress Analysis for a Double Lap Joint, J. Applied Mechanics, p.353, June (1975).

63. W.J. Renton and J.R. Vinson, Fatigue Behavior of Bonded Joints in Composite Material Structures, J. Aircraft, 12, pp.442-447 (1975).

64. A.W. Bethune, Durability of Bonded Aluminum Structure, SAMPE J., pp. 4-10 (1975).

65. O. Ishai, D. Peretz and N. Galili, Mechanical Behavior of Multimaterial Composite Systems, Final Technical Report, Contract No. DAJA-37-74-C-2531, January (1975).

INTERLAMINAR BEHAVIOR

66. R.A. Heller, Interlaminar Shear Stress in Sandwich Beams, Technical Report No. 33, Contract No. Nonr 266(78) (1967).

67. A.H. Puppo and H.A. Evensen, Interlaminar Shear in Laminated Composites Under Generalized Plane STress, J. Composite Materials, 4, 204-220 (1970).

68. R.B. Pipes and N.J. Pagano, Interlaminar Stresses in Composite Laminates Under Uniform Axial Extension, J. Composite Materials, Vol. 4, pp. 538-548 (1970).

69. N.J. Pagano and R.B. Pipes, The Influence of Stacking Sequence on Laminate Strength, J. Composite Materials, 5, pp. 50-57 (1971).

70. R.B. Pipes and I.M. Daniel,Moiré Analysis of the Interlaminar Shear Edge Effect in Laminated Composites, J. Composite Materials, 5, pp. 255-259 (1971).

71. A. Levy, H. Armen, Jr. and J. Whiteside, Elastic and Plastic Interlaminar Shear Deformation in Laminated Composites Under Generalized Plane Stress, Airforce Third Conf. on Matrix Methods in Structural Mechanics, W-P AFB, Ohio, pp. 19-21 (1971).

72. R.A. Heller and G.W. Swift, Solutions for the Multilayer Timoshenko Beam, Project THEMIS, Contract No. DAA-F07-70-C-0444 (1971).

73. R.B. Pipes, Interlaminar Stress in Composite Laminates, Technical Report AD-776-053, Air Force (1972).

74. J.M. Whitney, Stress Analysis of Thick Laminated Composite and Sandwich Plates, J. Composite Materials, 6, pp. 426-440 (1972).

75. J.M. Whitney and C.E. Browning, Free-Edge Delamination of Tensile Coupons, J. Composite Materials, 6, pp. 300-303 (1972).

76. J.M. Whitney, Free-Edge Effects in the Characterization of Composite Materials, ASTM STP 521, pp. 167-180 (1973).

77. G.B. McKenna, J.F. Mandell and F.J. McGurry, Interlaminar Strength and Toughness of Fiberglass Laminates, 29th Annual Technical Conf., Section 13-C, pp. 1-8 (1974).

78. C.W. Bert and P.H. Francis, Composite Material Mechanics: Structural Mechanics, AIAA J., 12(9), pp. 1173-1186 (1974).

GLOSSARY

C_{ij} - Structural parameters of NMD

c - length of IAL ($c = \ell/2$)

$E_0, E_1, E_2, (E_i)$ - Young's moduli of IAL, CAL and EAL, respectively

F - axial applied force per unit width

G_0 - shear modulus of IAL

$\bar{H}$ - measure of NMD thickness

h_0, h_1, h_2 - thickness of IAL, CAL and EAL, respectively

K_i - constants

ℓ - IAL length ($\ell=2c$)

$M_2=M$ - moment function along the EAL

$N_1, N_2=N$ - normal force along the CAL and EAL, respectively

p_c - effective applied axial normal stress

p_0 - reference axial stress acting on EAL under uniform axial strain

P - axial applied force

R - structural parameter of NMD

T - temperature difference

u - displacement in x-direction

$V_2=V$ - shear force along EAL

w - displacement in z-direction

x, y, z - axial, transverse and lateral coordinates, respectively

α_i - coefficient of thermal expansion

γ_0 - shear strain at IAL

δ - material and geometrical constant

$\varepsilon_0, \varepsilon_1, \varepsilon_2$ - axial normal strain at IAL, CAL and EAL, respectively

η - material and geometrical constant

λ - material and geometrical constant

μ - material and geometrical constant

ν, ν_0 - Poisson's ratio of adherend and adhesive layers respectively

ρ - curvature of beam

$\tau_{zx_0} = \tau_0$ - axial shear stress (in x-direction) activing at IAL

τ_{zy_0} - transverse shear stress (in y-direction) acting at IAL

$\sigma_{z_0} = \sigma_0$ - lateral normal stress (in z-direction) acting at IAL

$\sigma_{x_0}, \sigma_{x_1}, \sigma_{x_2}$ - longitudinal normal stresses acting at IAL, CAL and EAL respectively

σ_{y_0} σ_{y_1} σ_{y_2} - transverse normal stresses acting at IAL, CAL and EAL respectively

ϕ - material and geometrical constant

χ - non-dimensional axial coordinate

SMD - symmetrical doubler model

NMD - nonsymmetrical doubler model

IAL - interlaminar adhesive layer

CAL - central adherend layer

EAL - external adherend layer

FRP - fiber reinforced plastics

SLJ - single lap joint

DLJ - double lap joint

FEM - finite element method

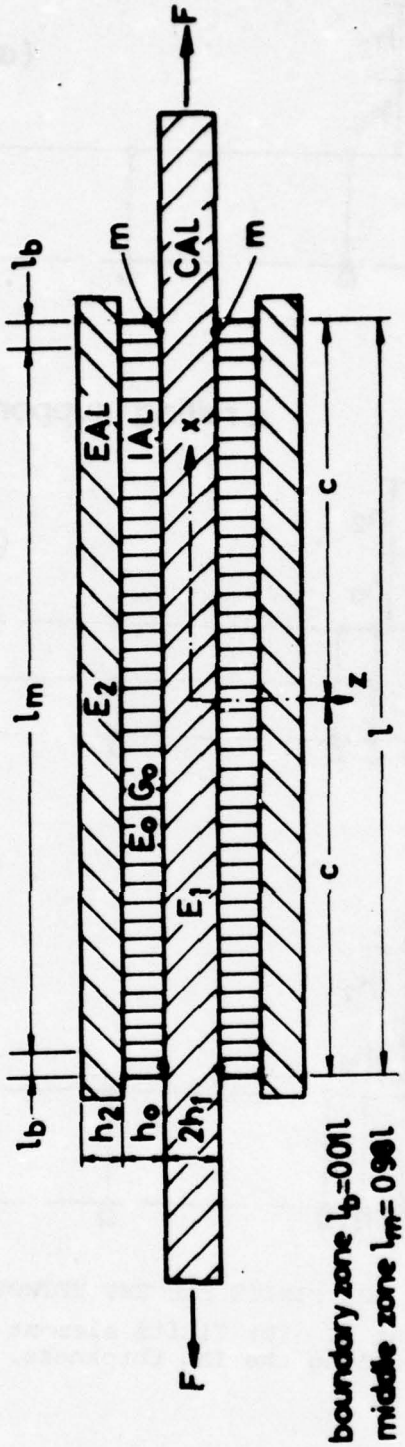


FIG. 1 SYMMETRICAL DOUBLER MODEL.

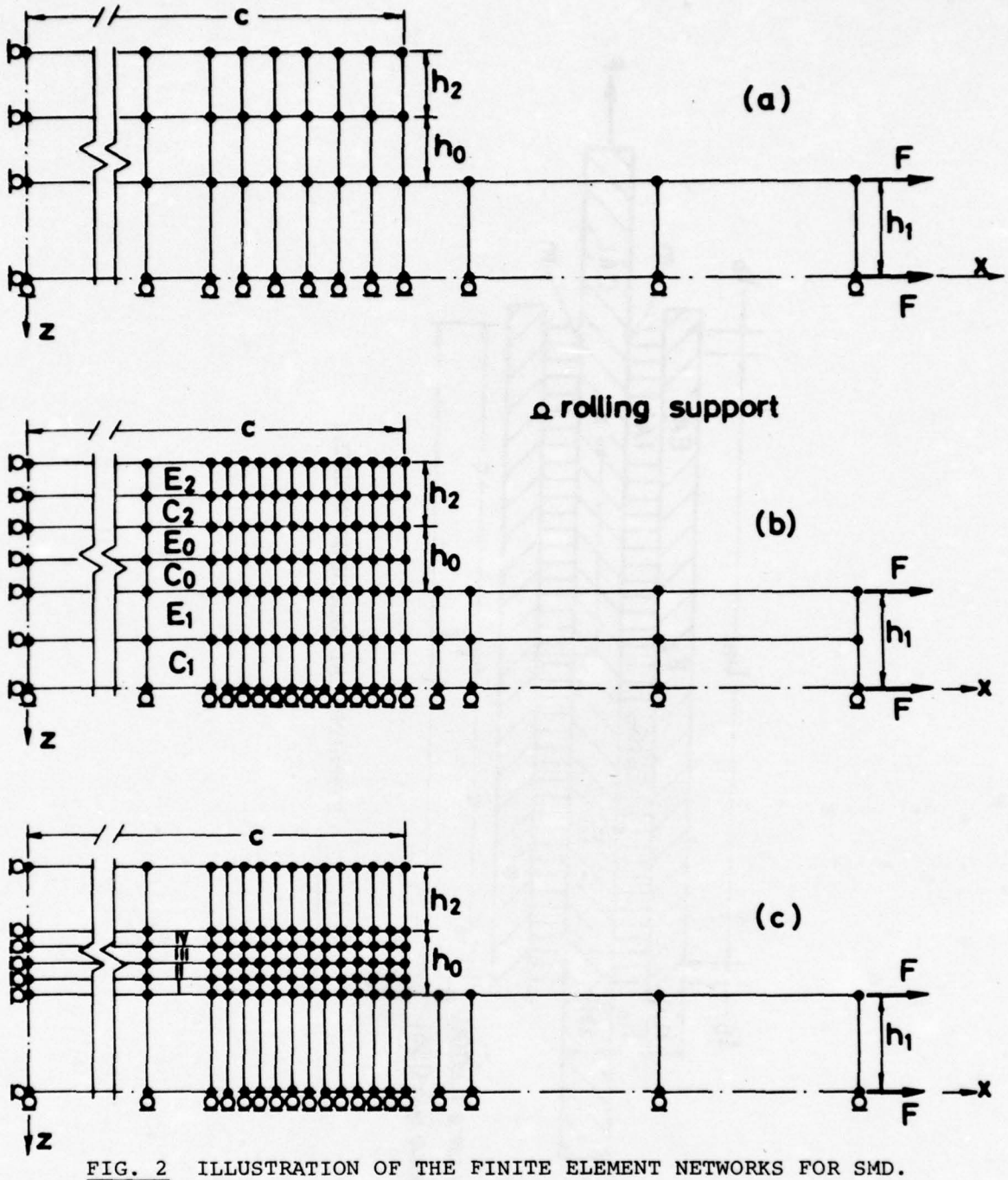


FIG. 2 ILLUSTRATION OF THE FINITE ELEMENT NETWORKS FOR SMD.
(a) finite element 1. (b) finite element 2.
(c) distribution along the IAL thickness.

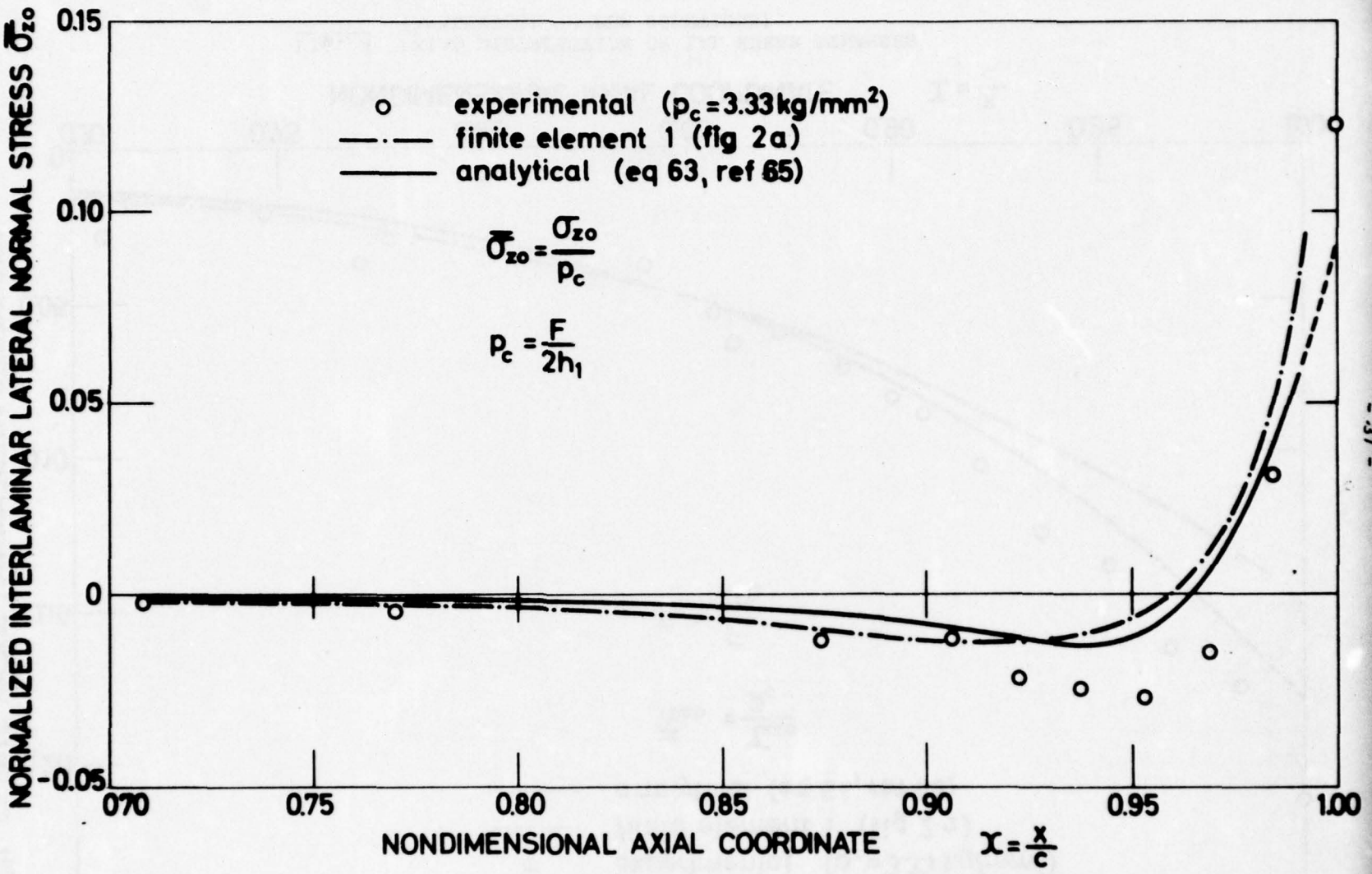


FIG. 3 AXIAL DISTRIBUTION OF IAL LATERAL NORMAL STRESSES (ANALYTICAL VS FEM SOLUTIONS).

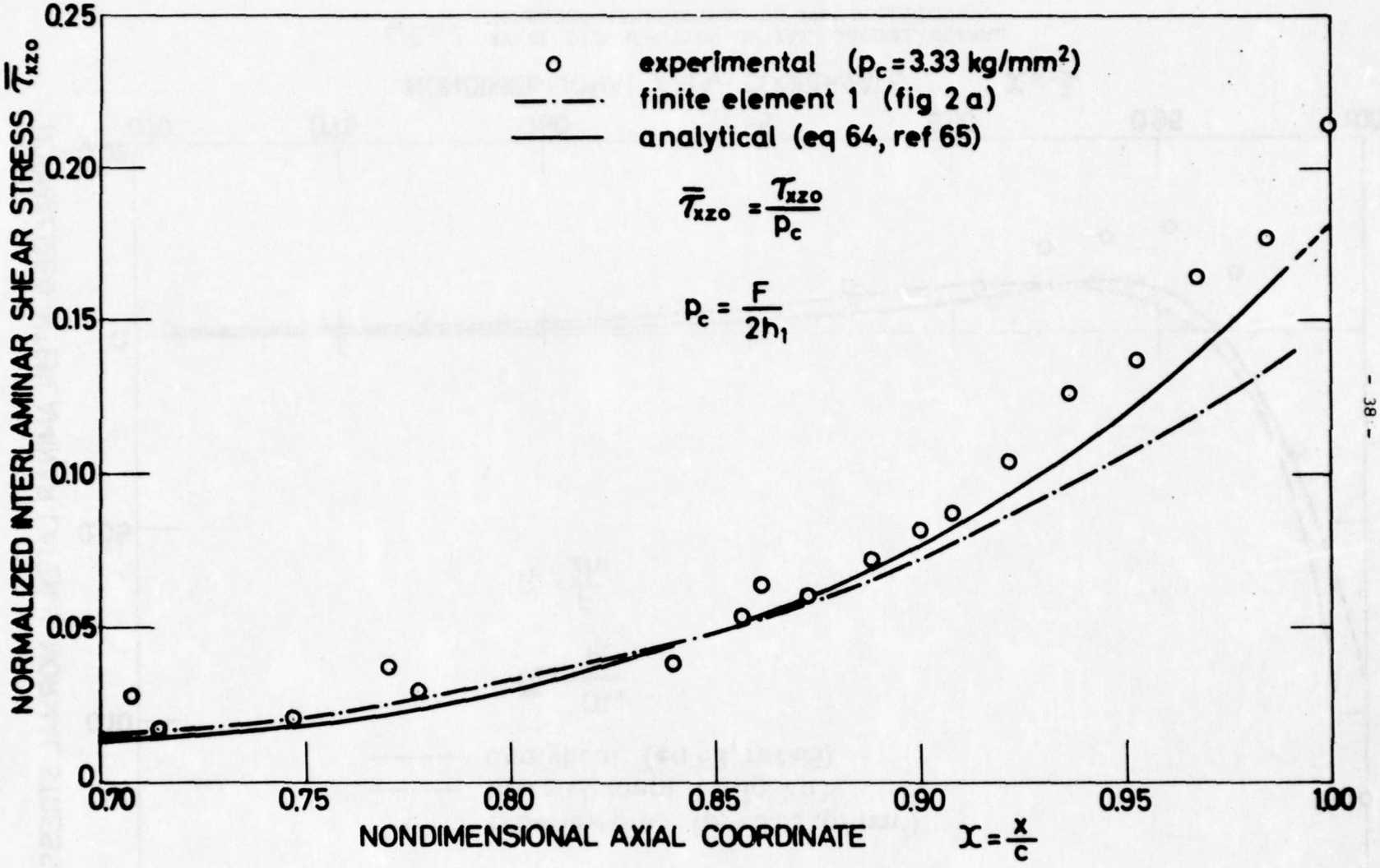


FIG. 4 AXIAL DISTRIBUTION OF IAL SHEAR STRESSES (ANALYTICAL VS FEM SOLUTIONS).

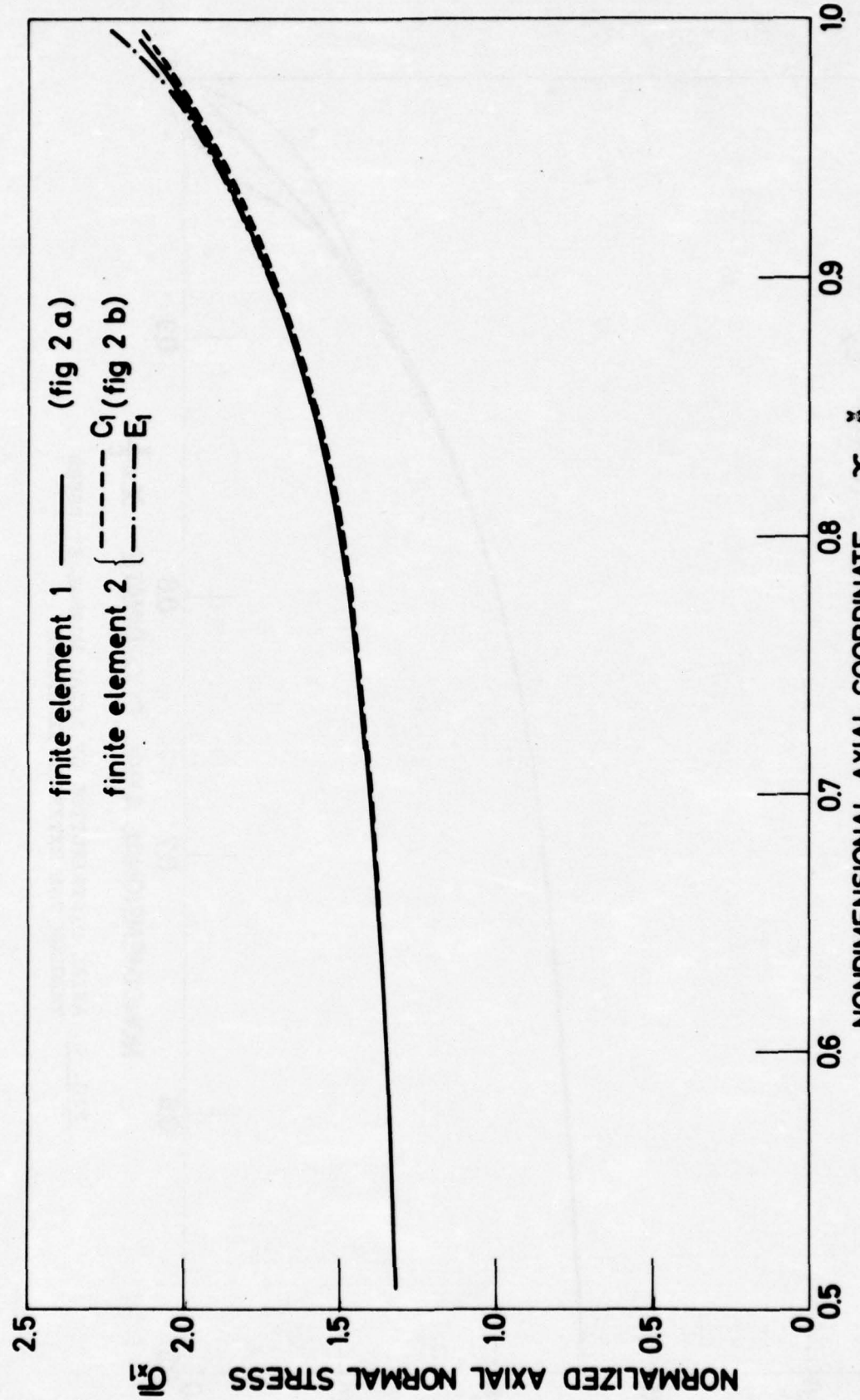


FIG. 5 AXIAL DISTRIBUTION OF AXIAL NORMAL STRESSES THROUGH THE CENTRAL ADHEREND.

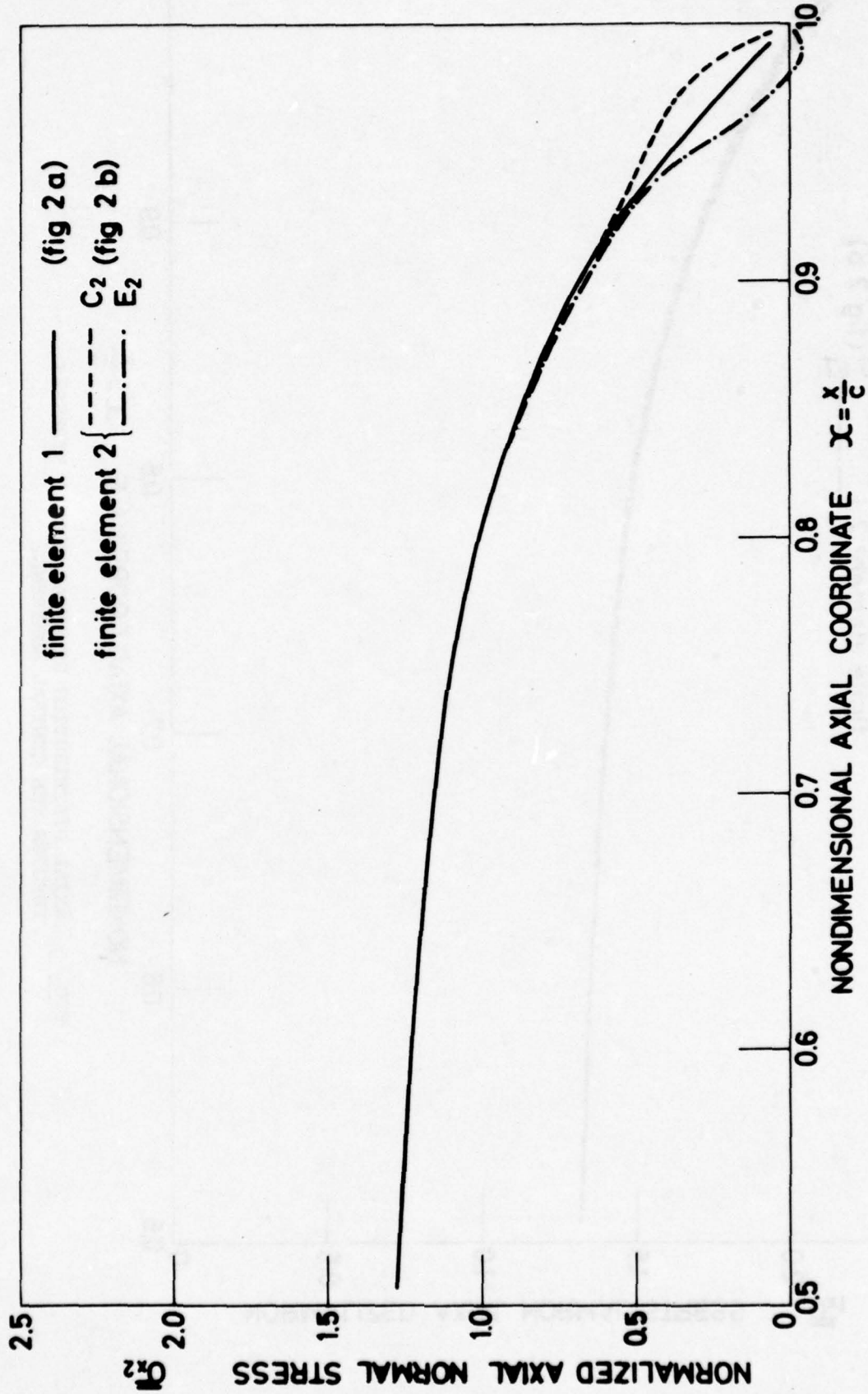


FIG. 6 AXIAL DISTRIBUTION OF AXIAL NORMAL STRESSES THROUGH THE EXTERNAL ADHERENDS.

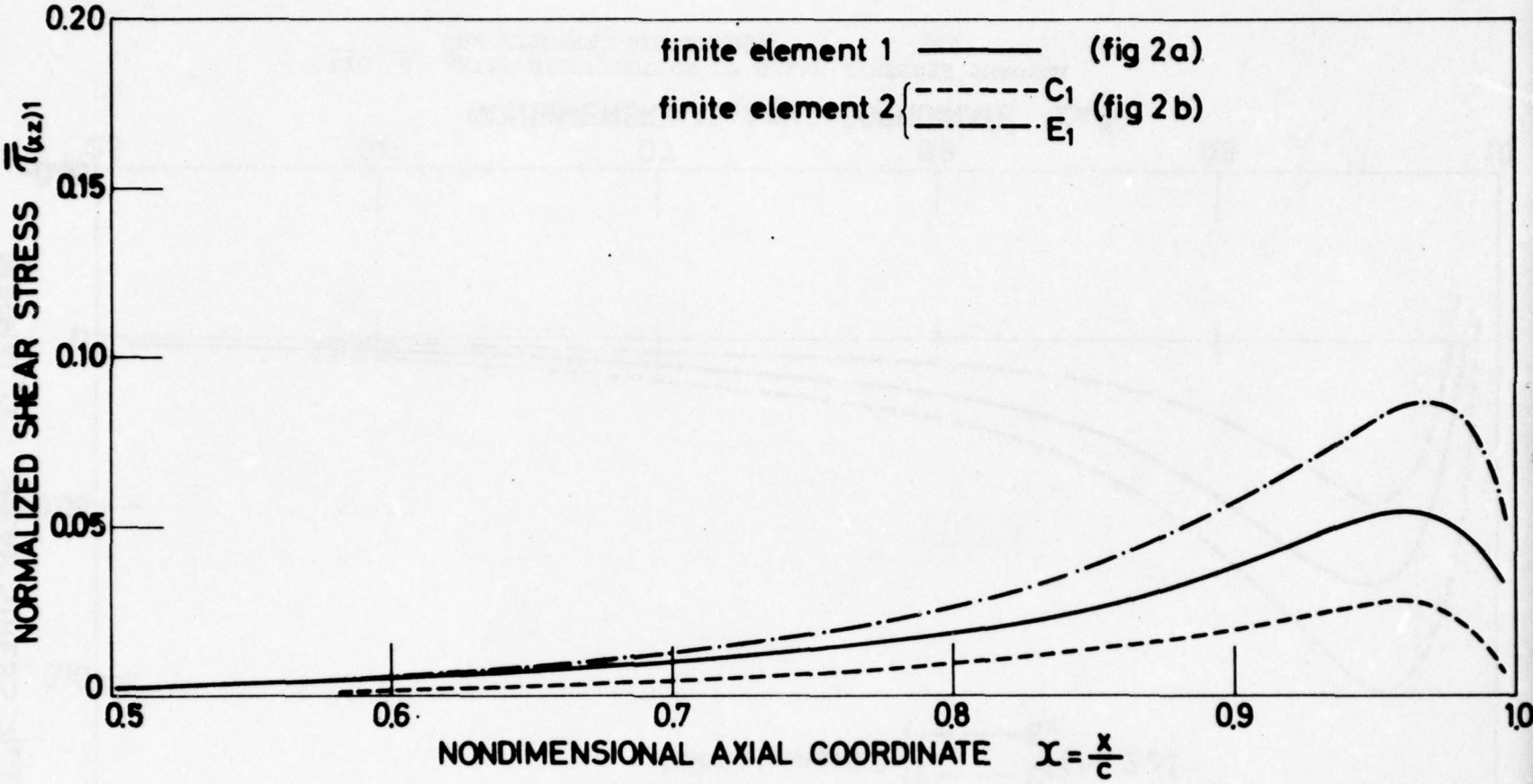


FIG. 7 AXIAL DISTRIBUTION OF SHEAR STRESSES THROUGH THE CENTRAL ADHEREND.

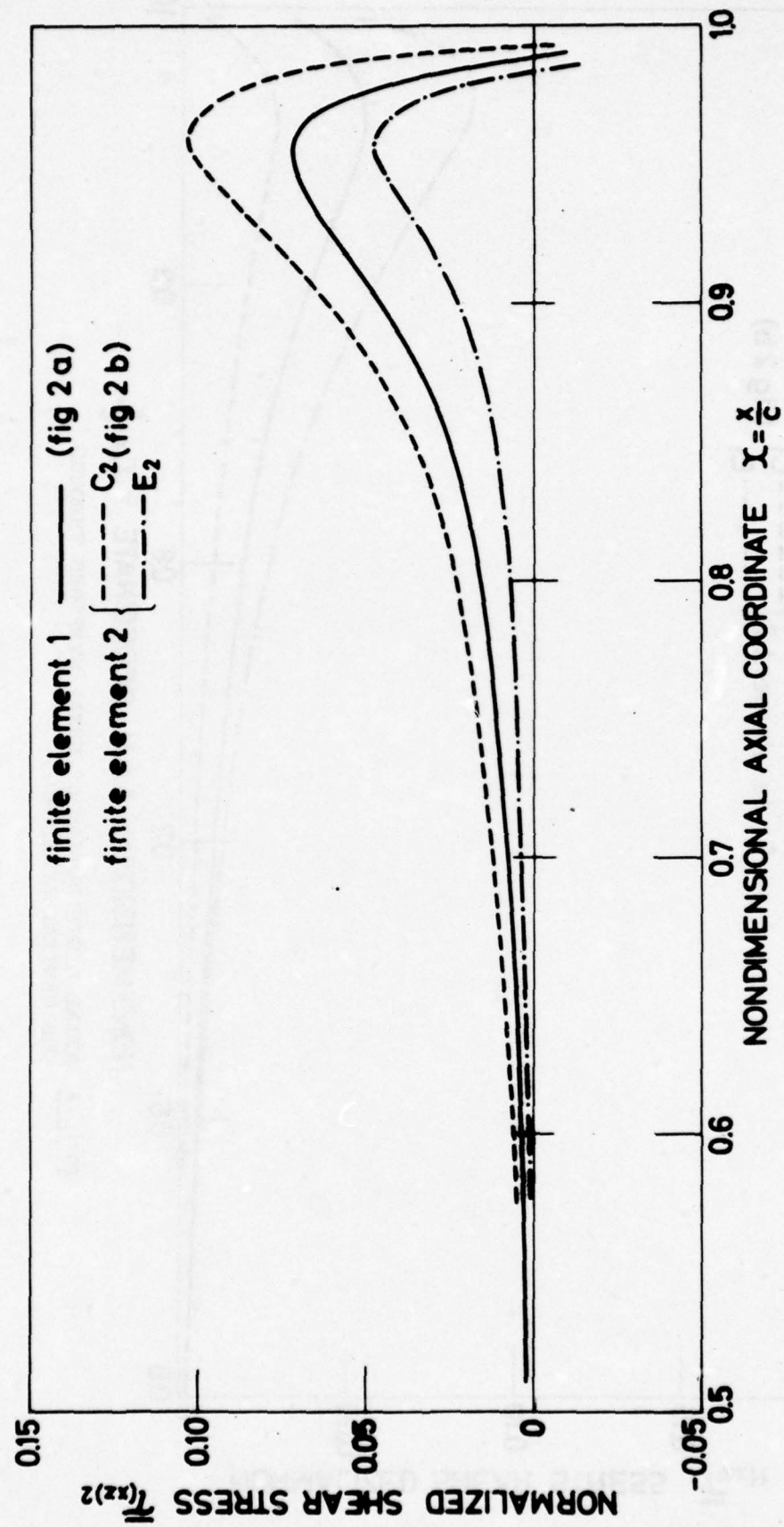


FIG. 8 AXIAL DISTRIBUTION OF SHEAR STRESSES THROUGH THE EXTERNAL ADHERENDS.

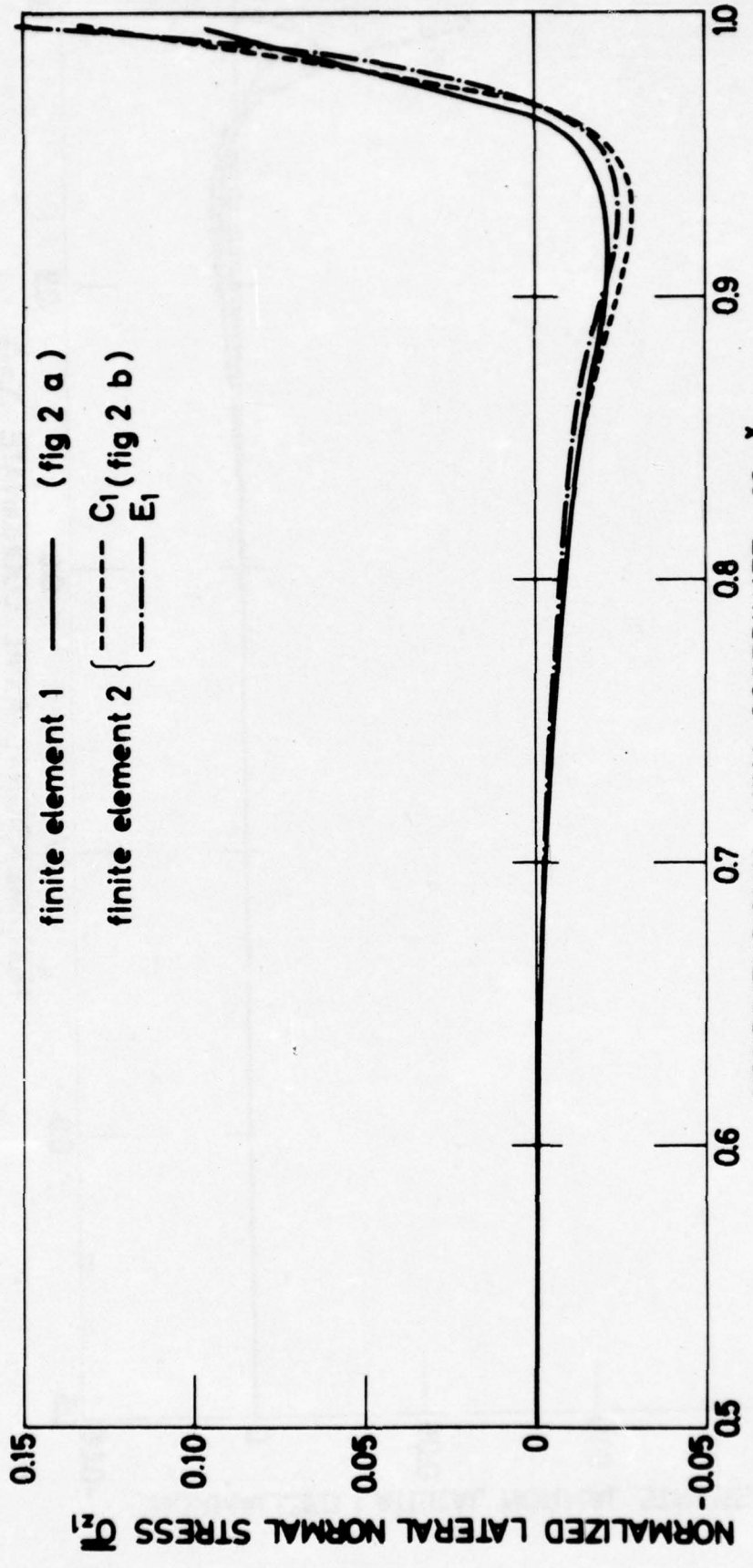


FIG. 9 AXIAL DISTRIBUTION OF LATERAL NORMAL STRESSES THROUGH THE CENTRAL ADHEREND.

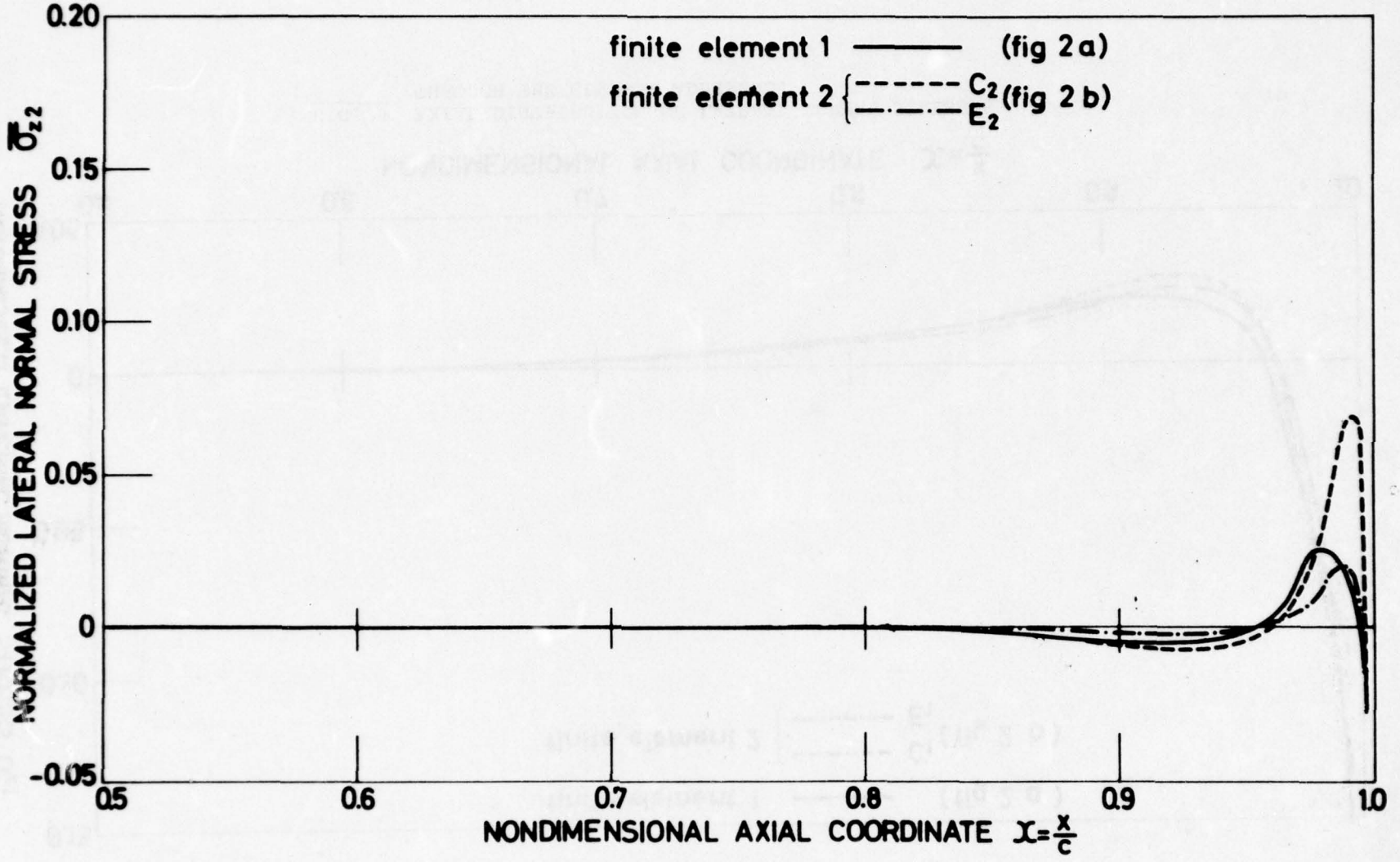


FIG. 10 AXIAL DISTRIBUTION OF LATERAL NORMAL STRESSES THROUGH THE EXTERNAL ADHERENDS.

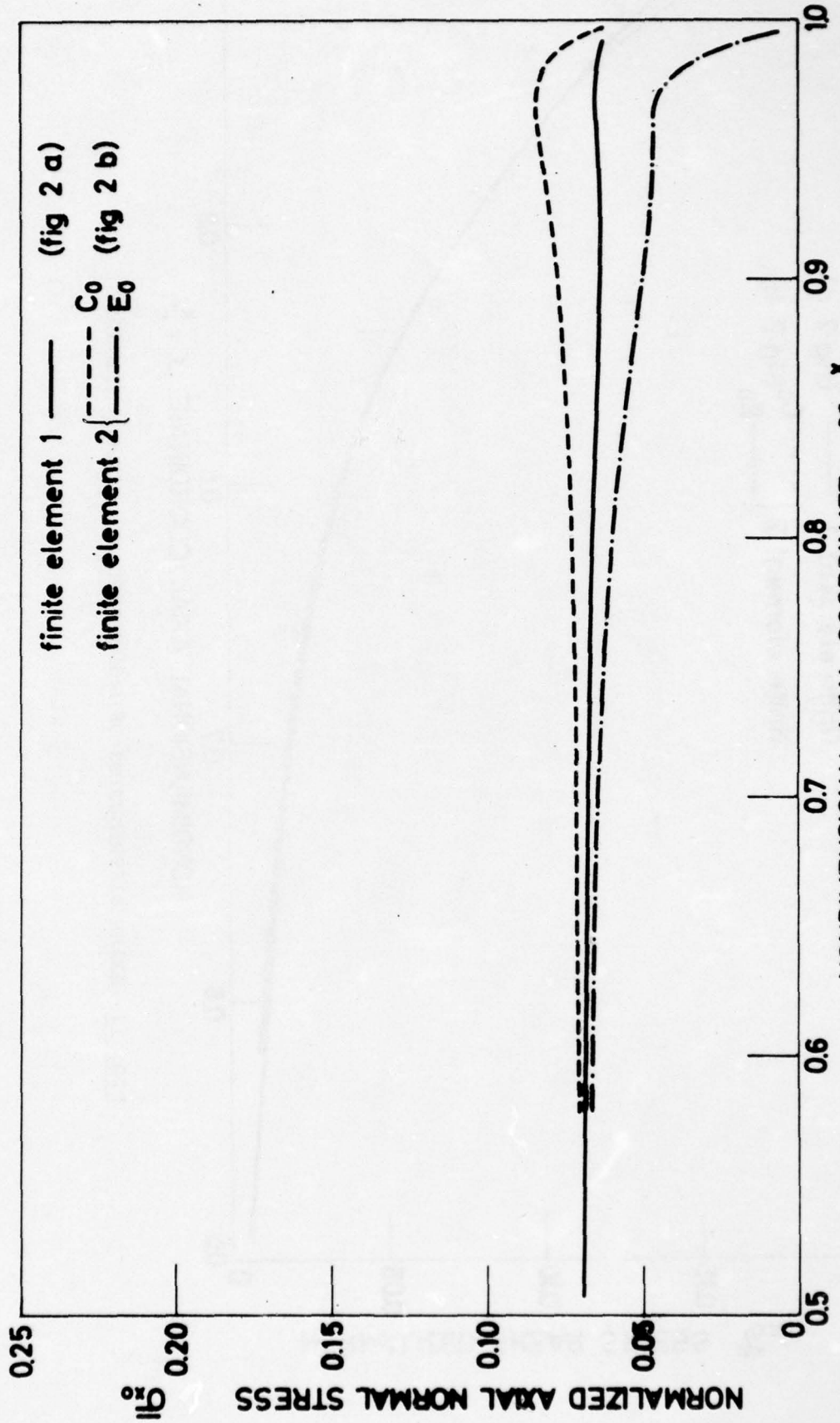


FIG. 11 AXIAL DISTRIBUTION OF AXIAL NORMAL STRESSES THROUGH THE IAL.

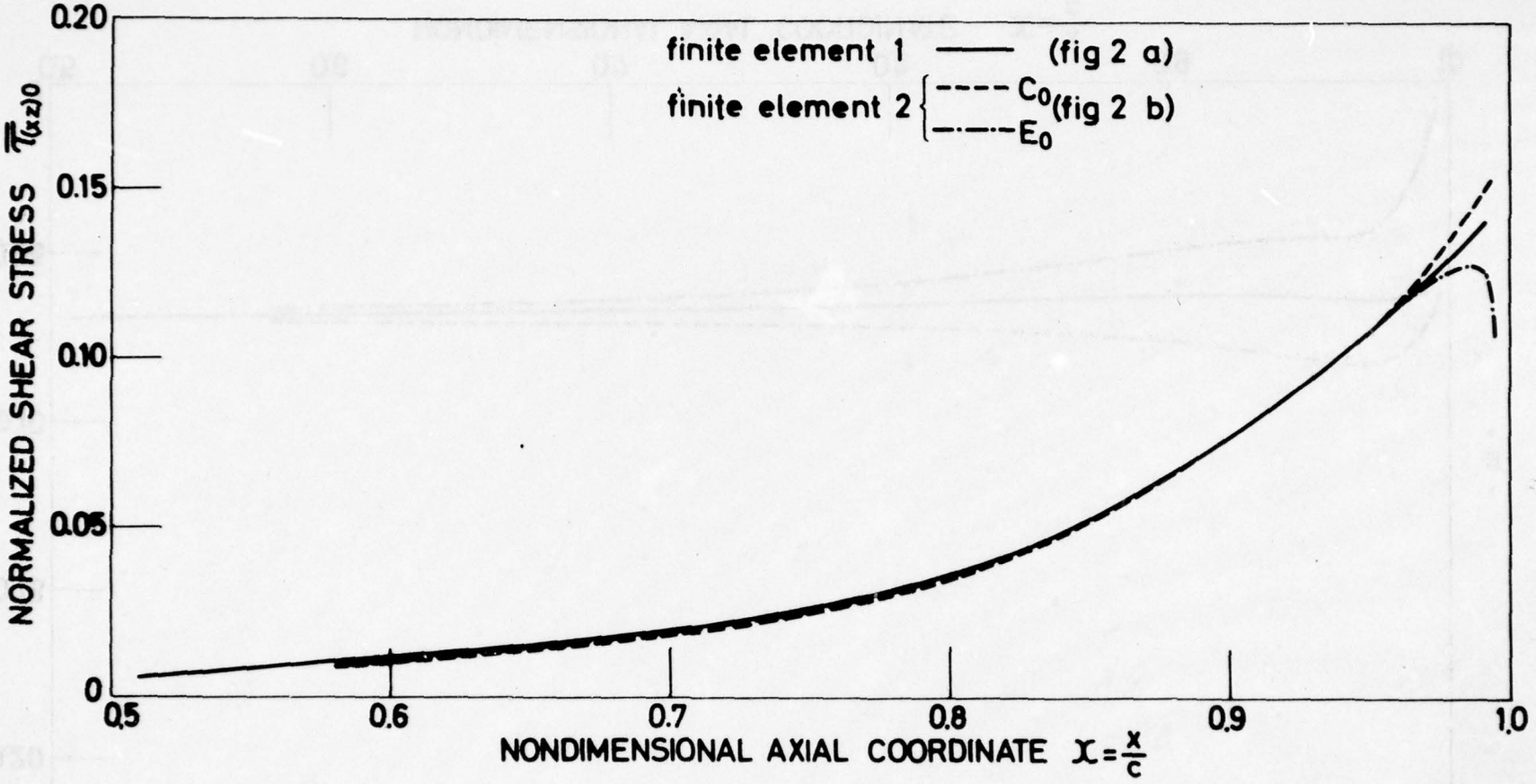


FIG. 12 AXIAL DISTRIBUTION OF SHEAR STRESSES THROUGH THE IAL.

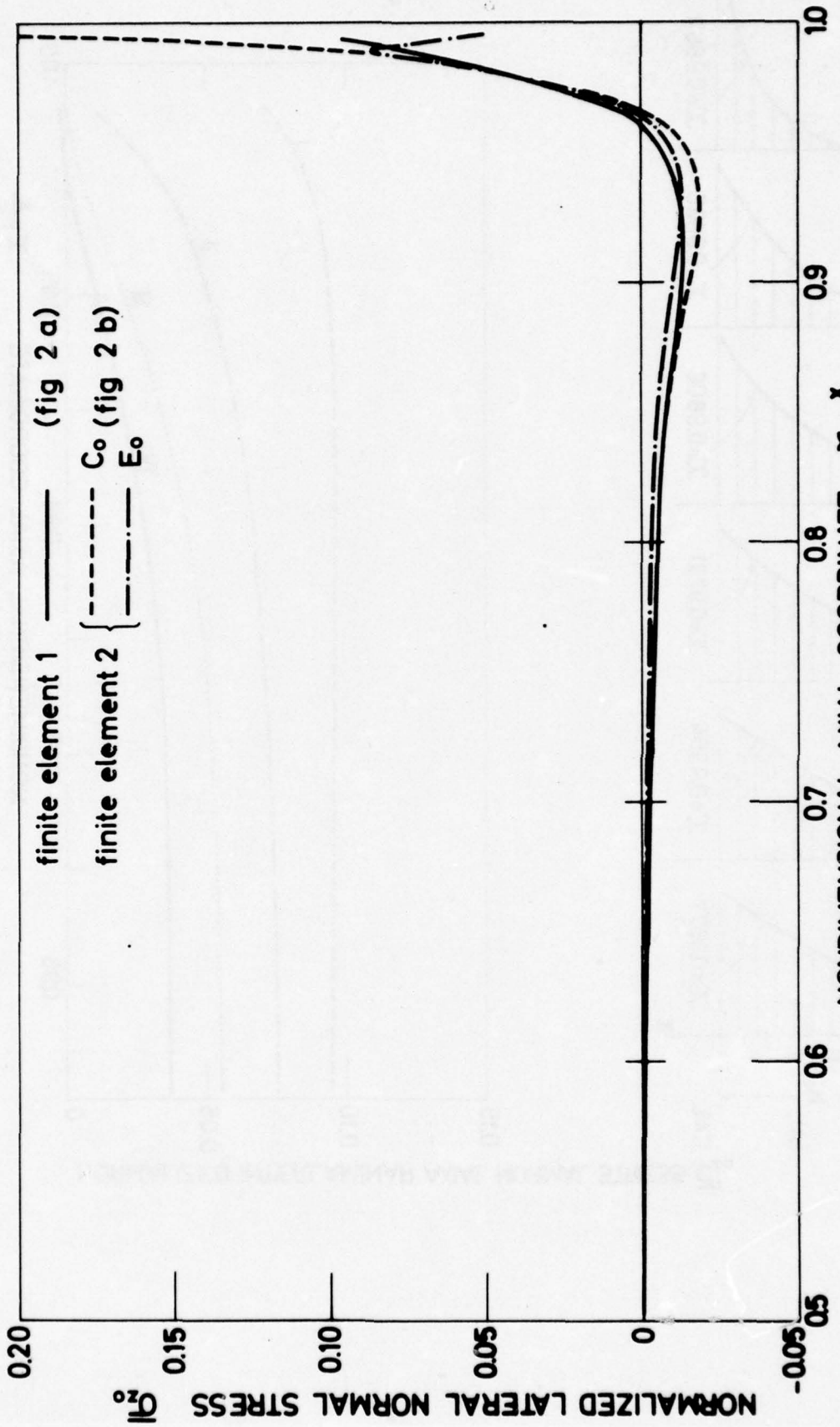


FIG. 13 AXIAL DISTRIBUTION OF LATERAL NORMAL STRESSES THROUGH THE IAL.

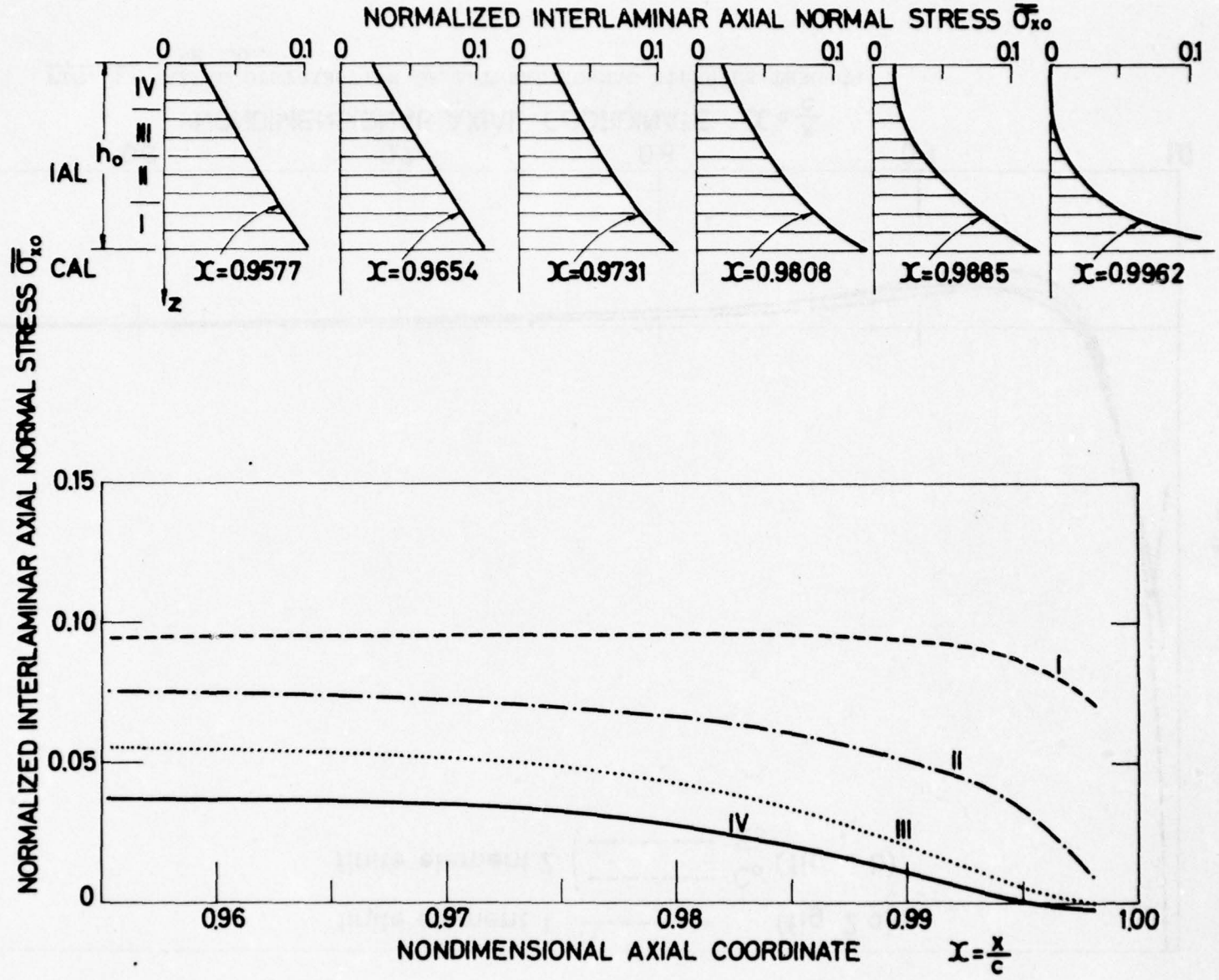


FIG. 14 DISTRIBUTION OF AXIAL NORMAL STRESSES CLOSE TO THE IAL EDGES.

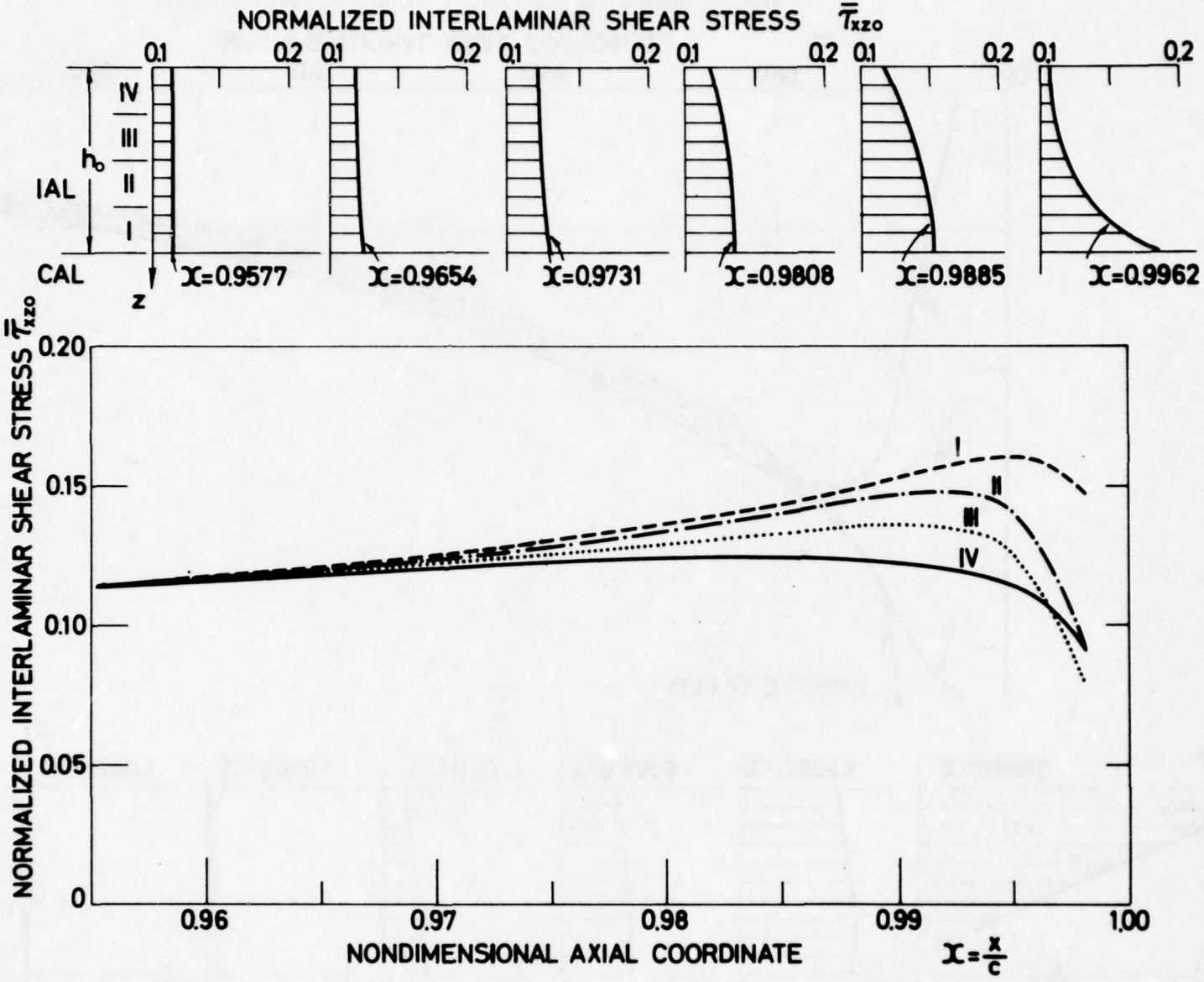


FIG. 15 DISTRIBUTION OF SHEAR STRESSES CLOSE TO THE IAL EDGES.

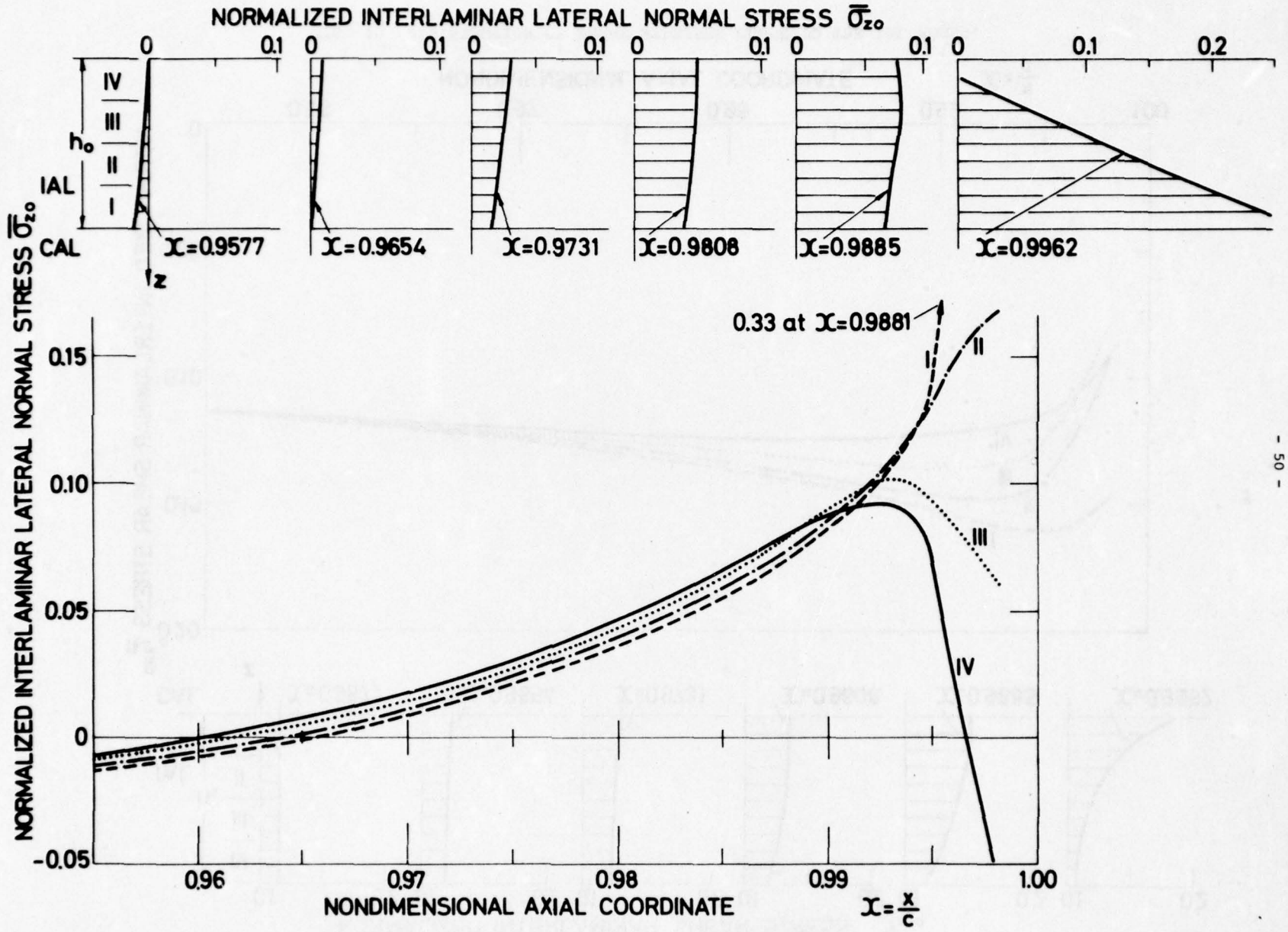


FIG. 16 DISTRIBUTION OF LATERAL NORMAL STRESSES CLOSE TO THE IAL EDGES.

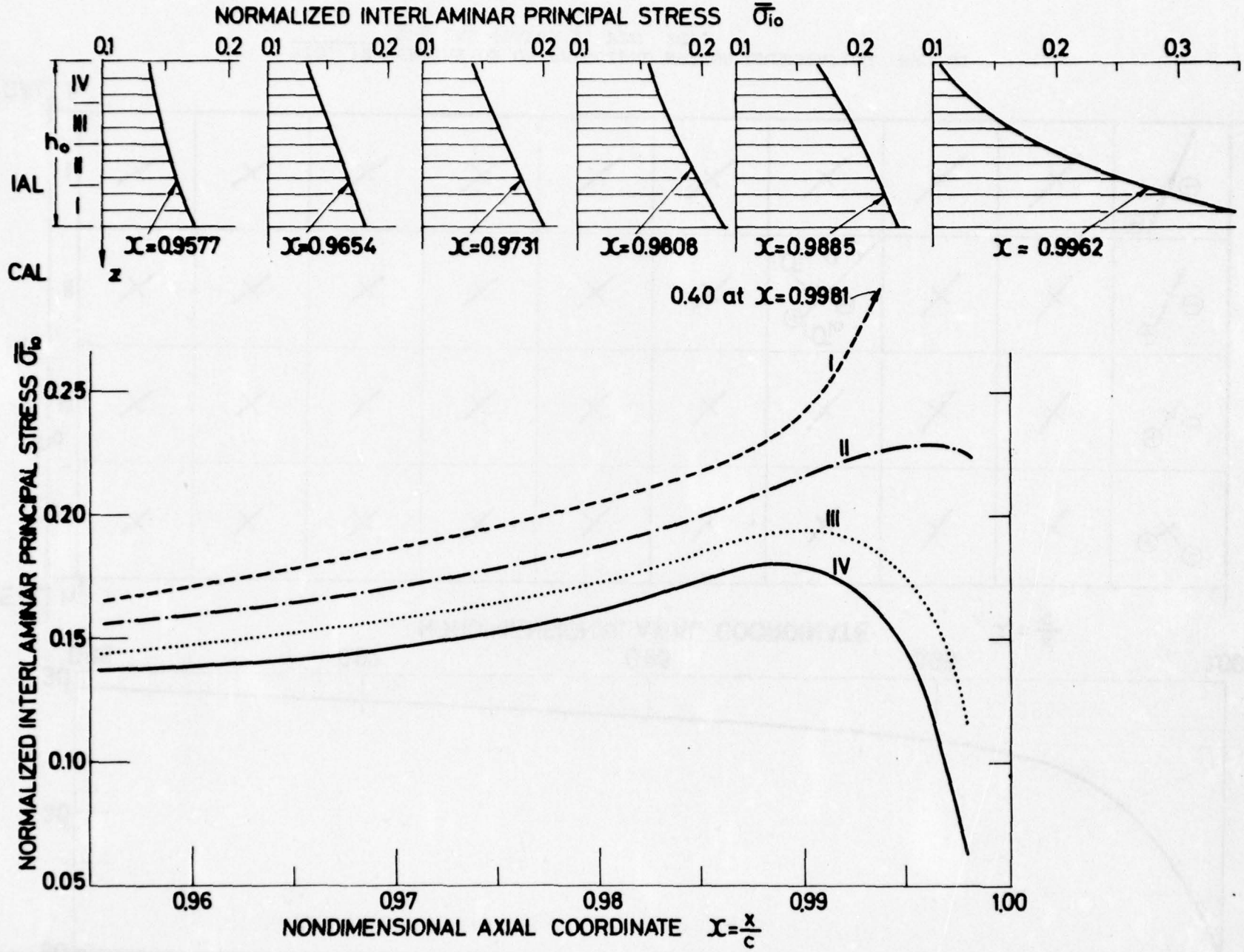


FIG. 17 DISTRIBUTION OF PRINCIPAL STRESSES CLOSE TO THE IAL EDGES.

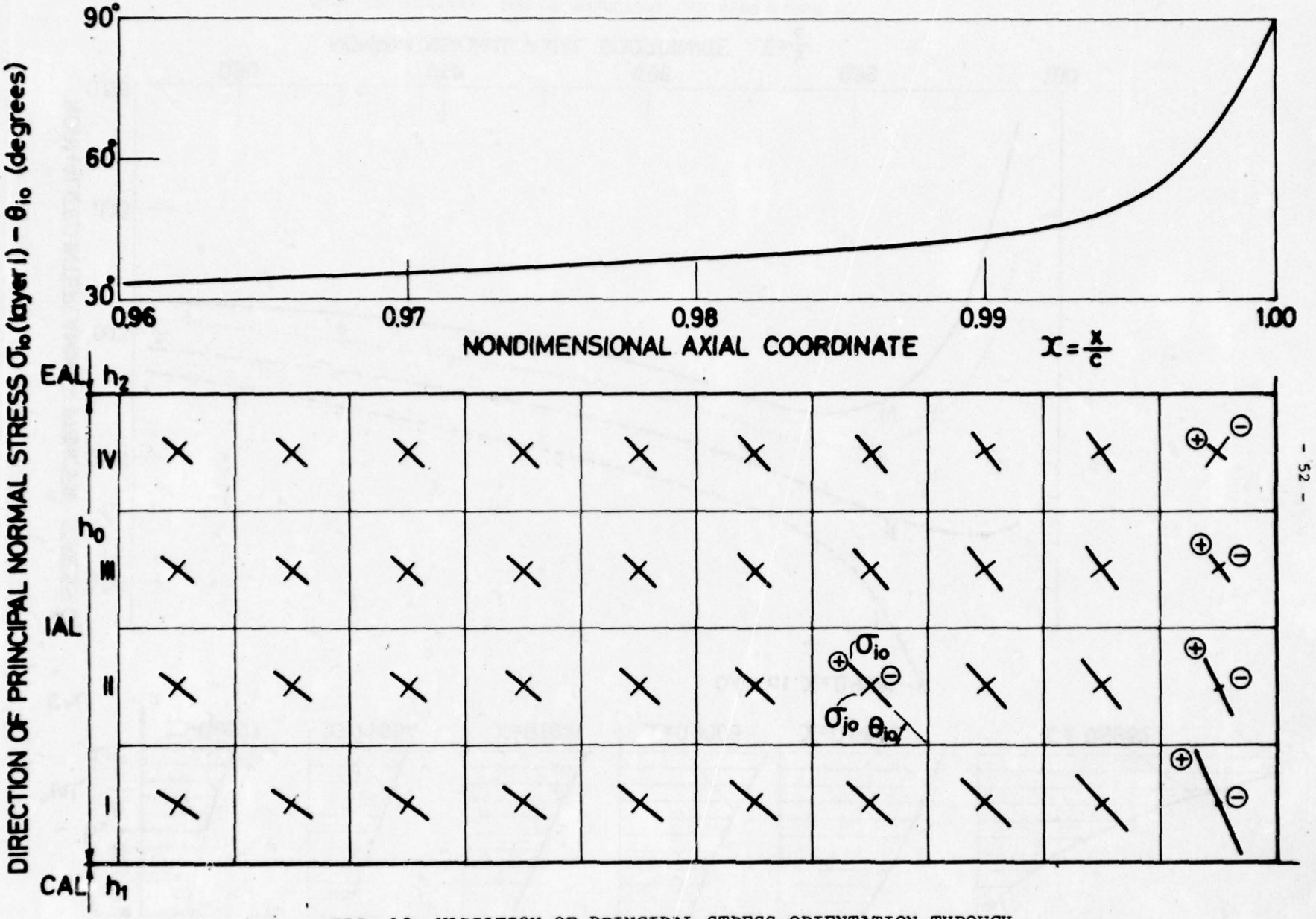


FIG. 18 VARIATION OF PRINCIPAL STRESS ORIENTATION THROUGH THE IAL (LAYER 1, FIG. 2C).

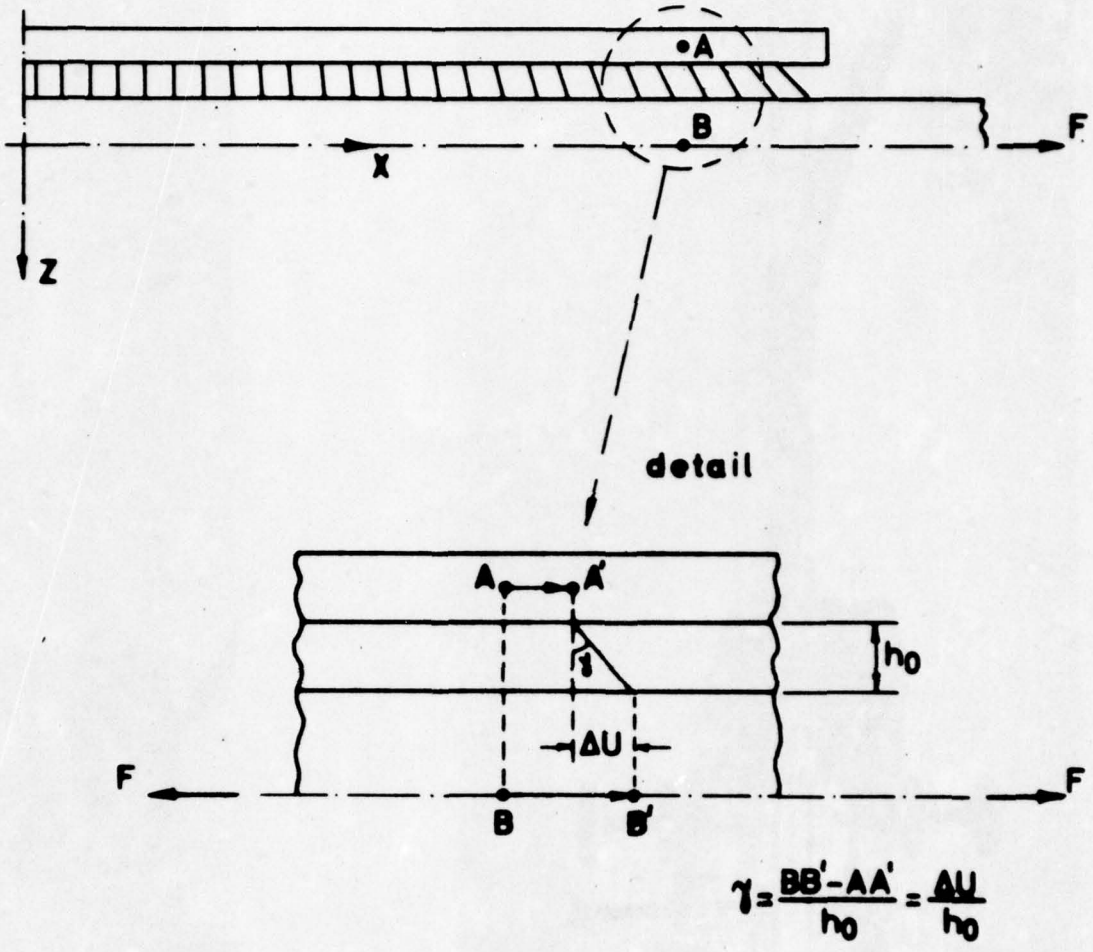


FIG. 19 SCHEME OF SHEAR DISPLACEMENT PATTERN THROUGH THE IAL.

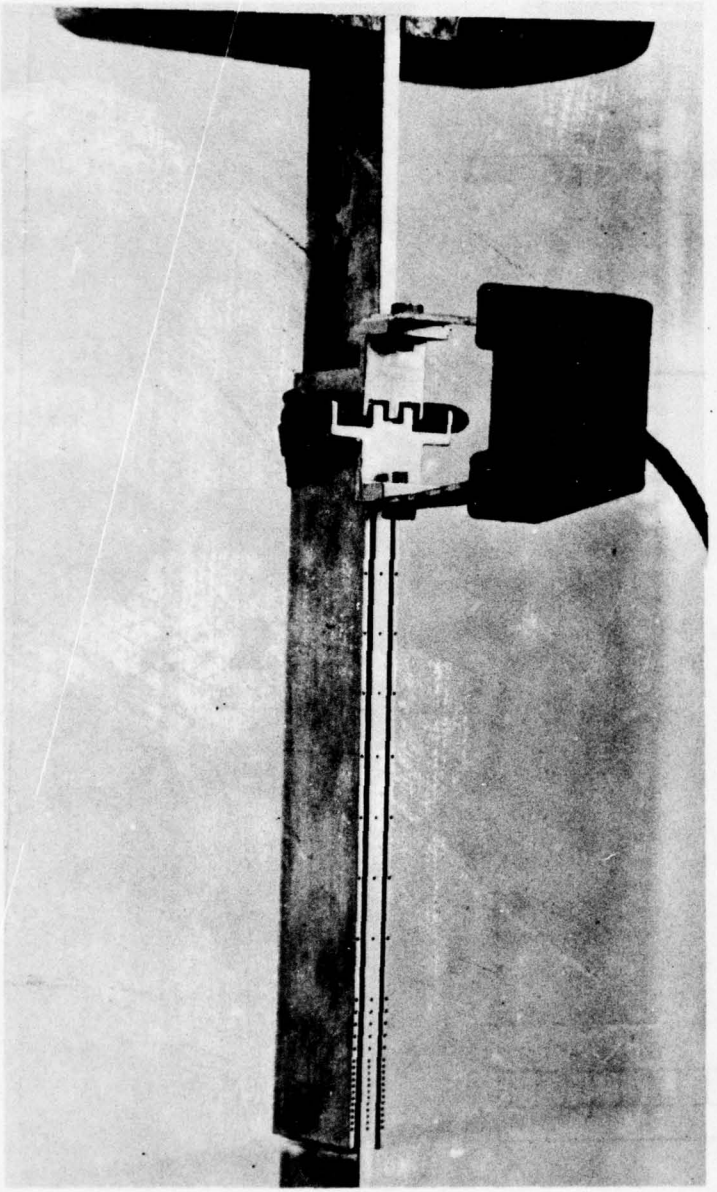


FIG. 20 ELECTROMECHANICAL EXTENSOMETER FOR MEASURING SHEAR DISPLACEMENT.

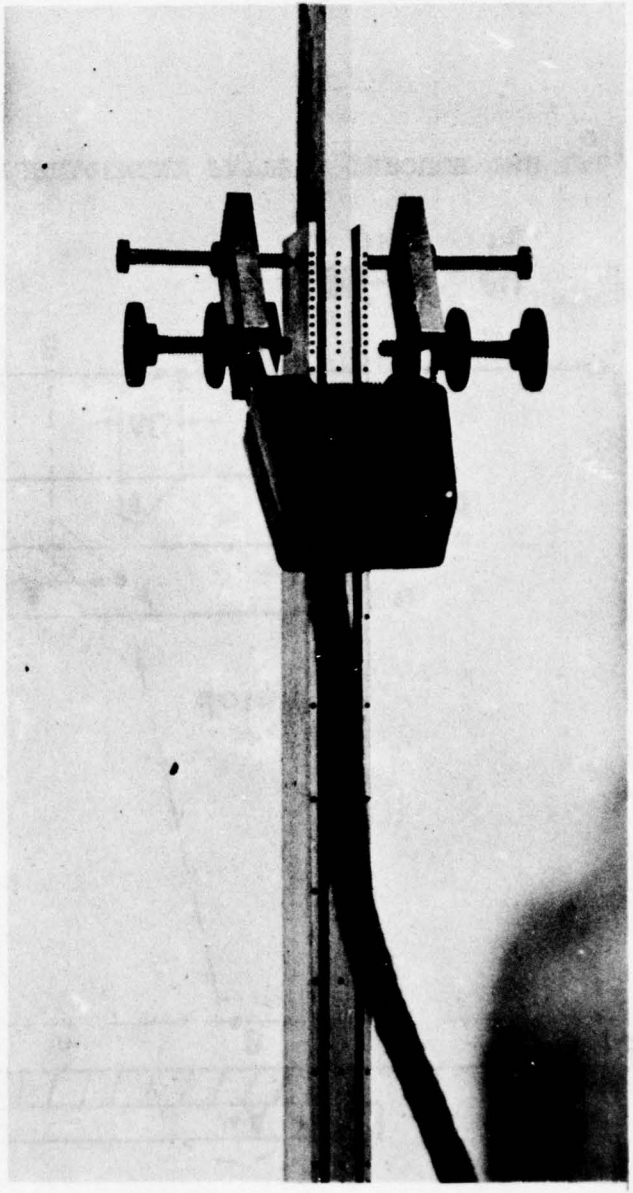


FIG. 21 ELECTROMECHANICAL EXTENSOMETER FOR MEASURING LATERAL NORMAL DISPLACEMENT.

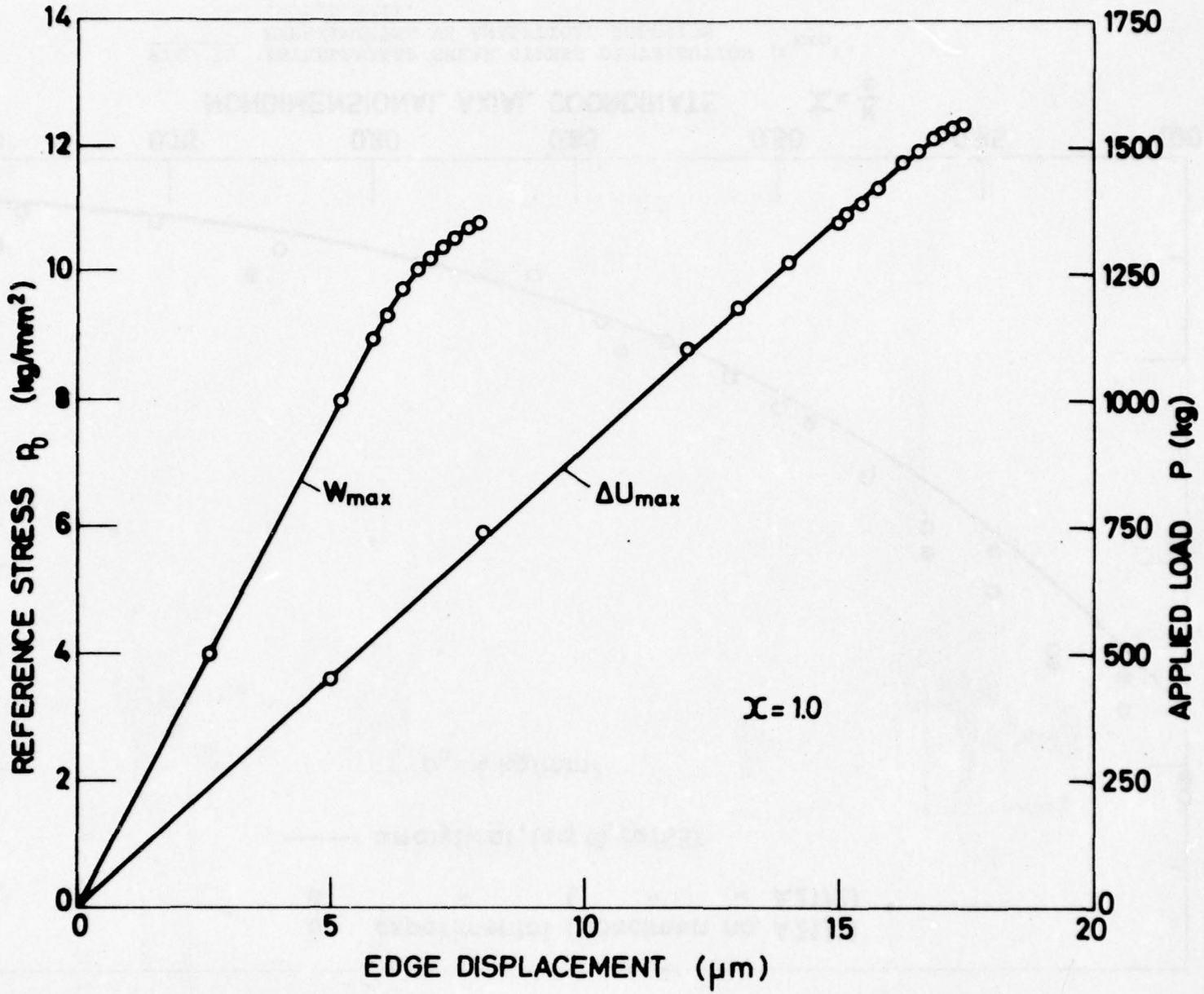


FIG. 22 APPLIED LOAD VS SHEAR AND LATERAL NORMAL DISPLACEMENT AT ADHESIVE LAYER EDGE.

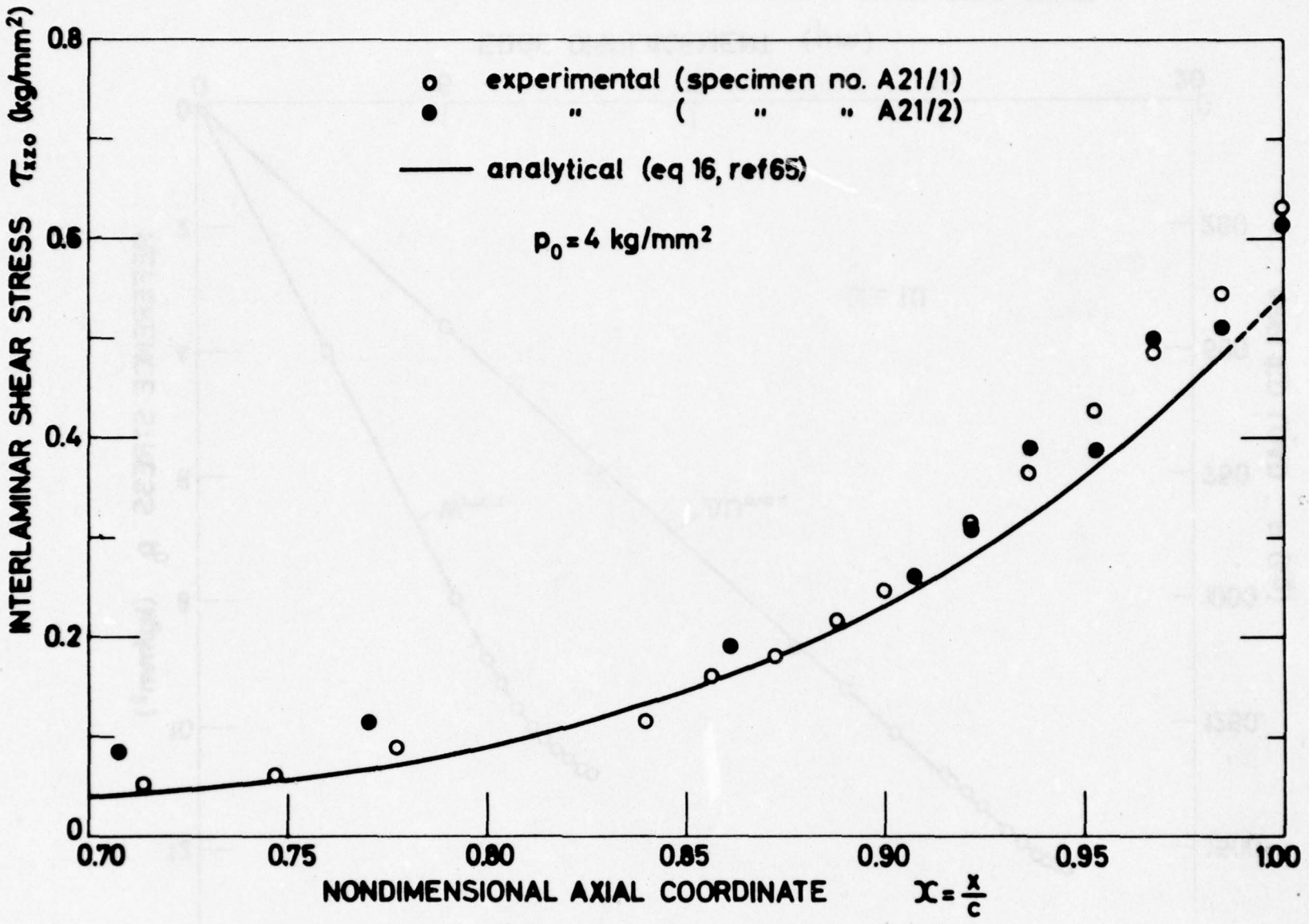


FIG. 23 INTERLAMINAR SHEAR STRESS DISTRIBUTION (τ_{xzo}). EXPERIMENTAL VS ANALYTICAL SOLUTION (MODEL A21).

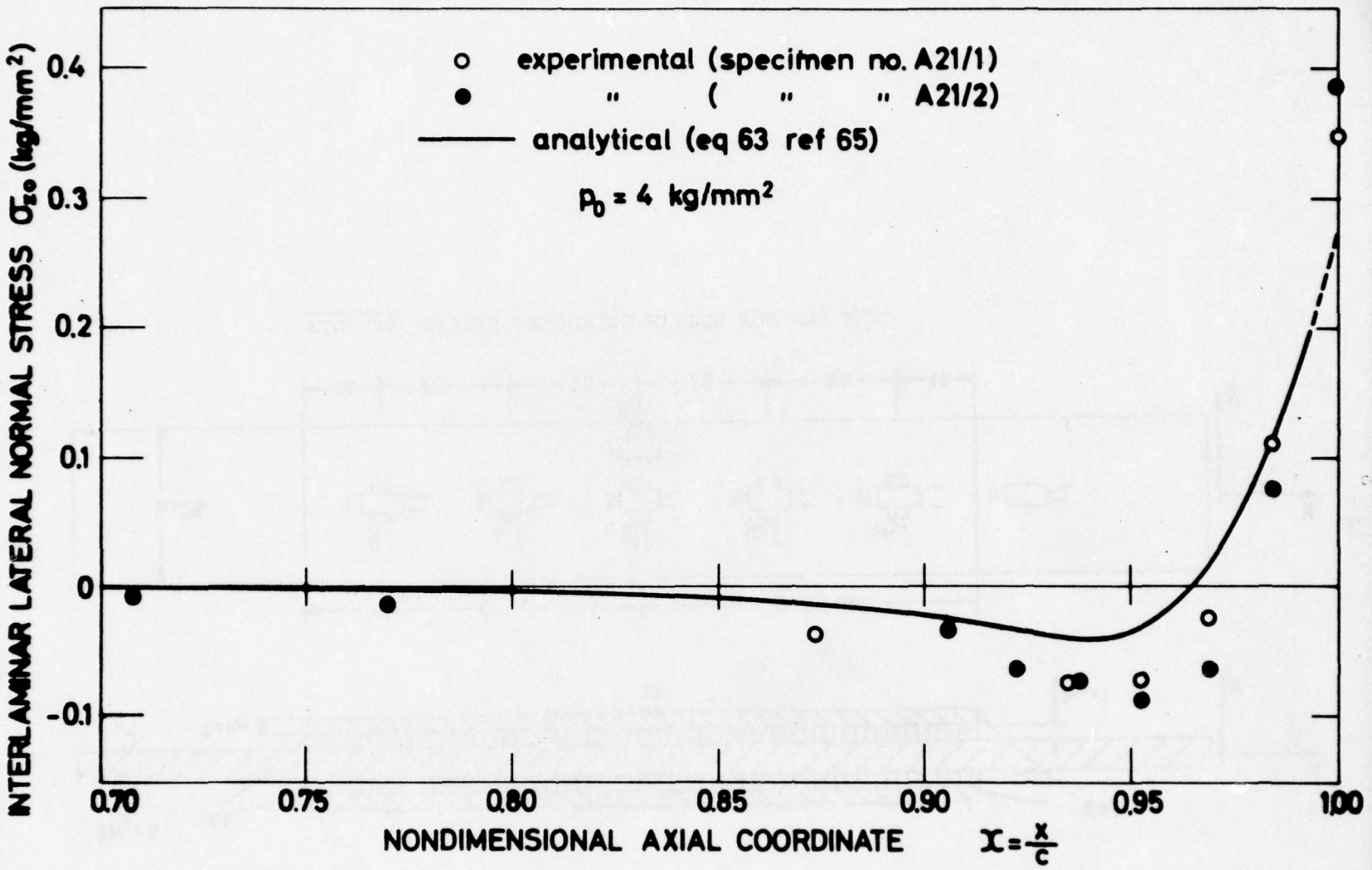


FIG. 24 INTERLAMINAR LATERAL NORMAL STRESS DISTRIBUTION (σ_{zo}).. EXPERIMENTAL VS ANALYTICAL SOLUTION (MODEL A21).

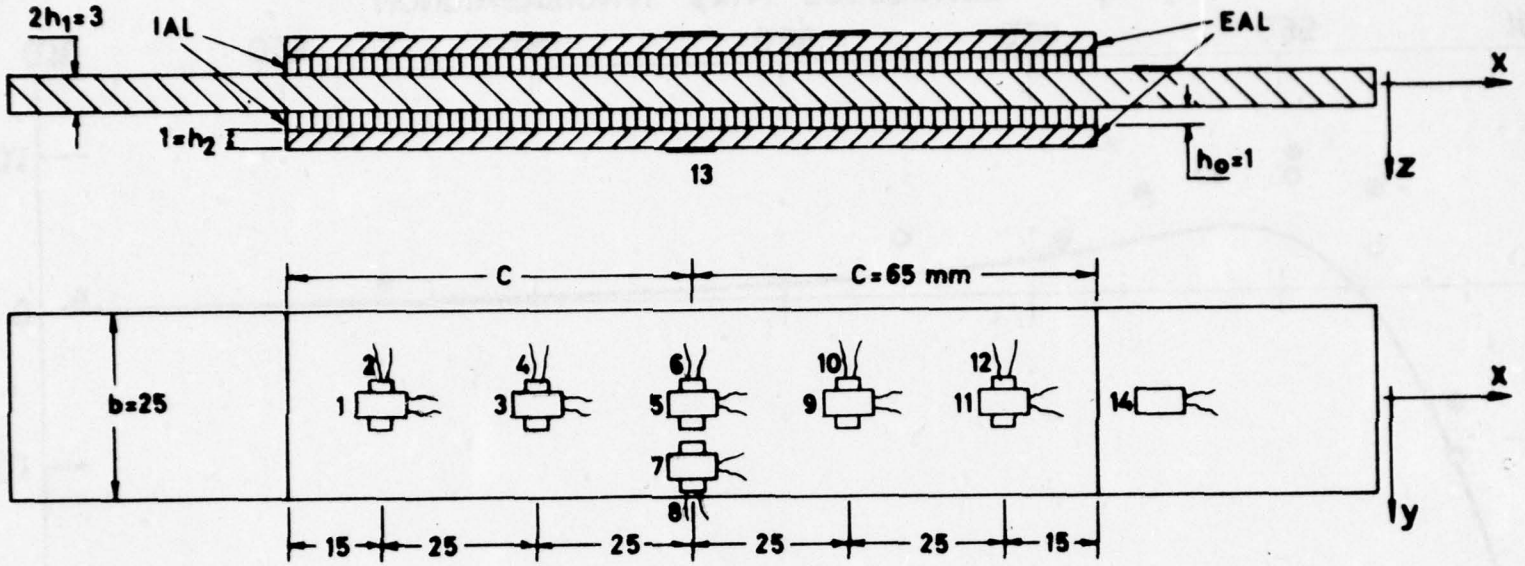


FIG. 25 STRAIN MEASURING SYSTEM FOR THE SMD.

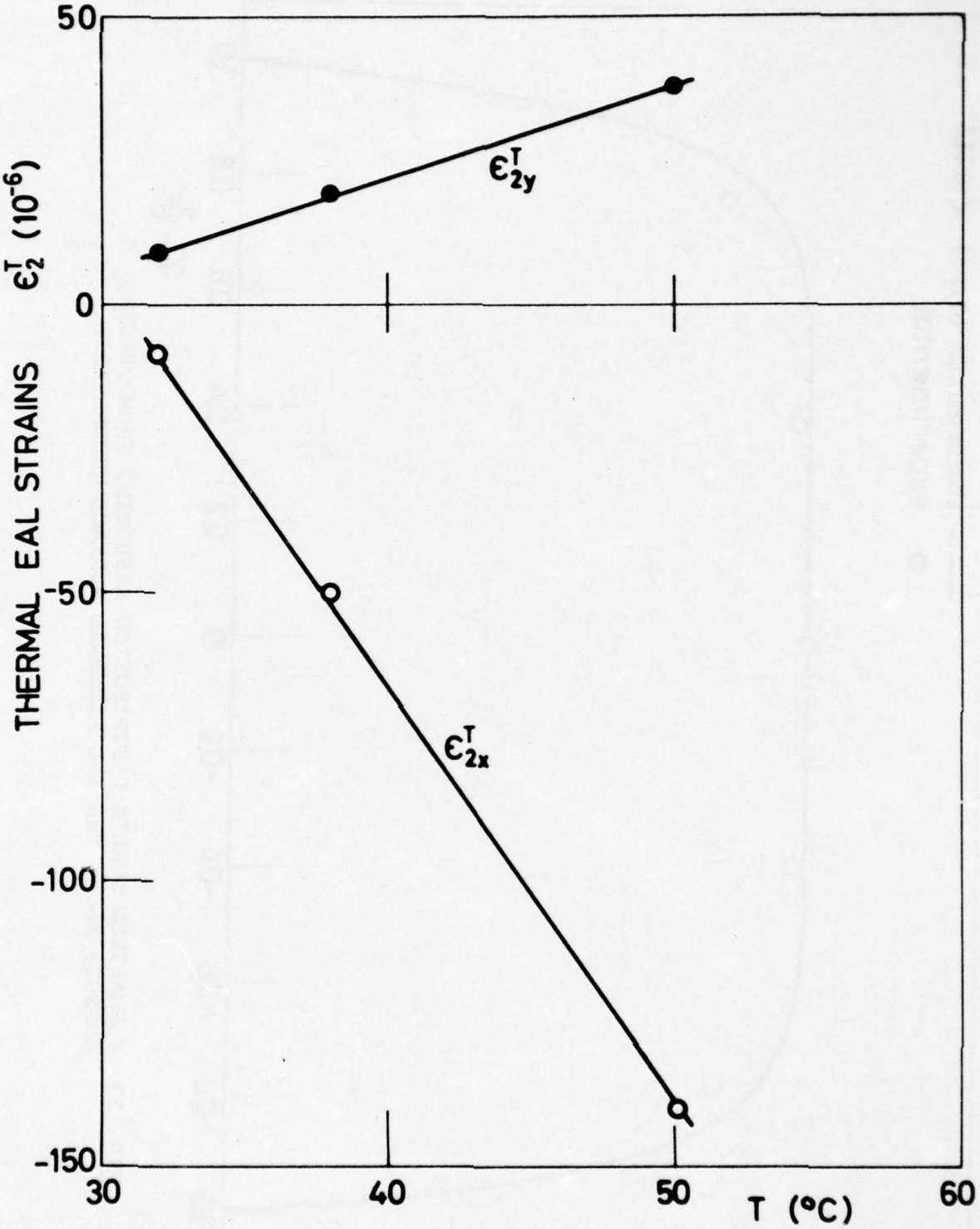


FIG. 26 EFFECT OF TEMPERATURE ON AXIAL STRAINS AT THE EAL SURFACE (MODEL A02).

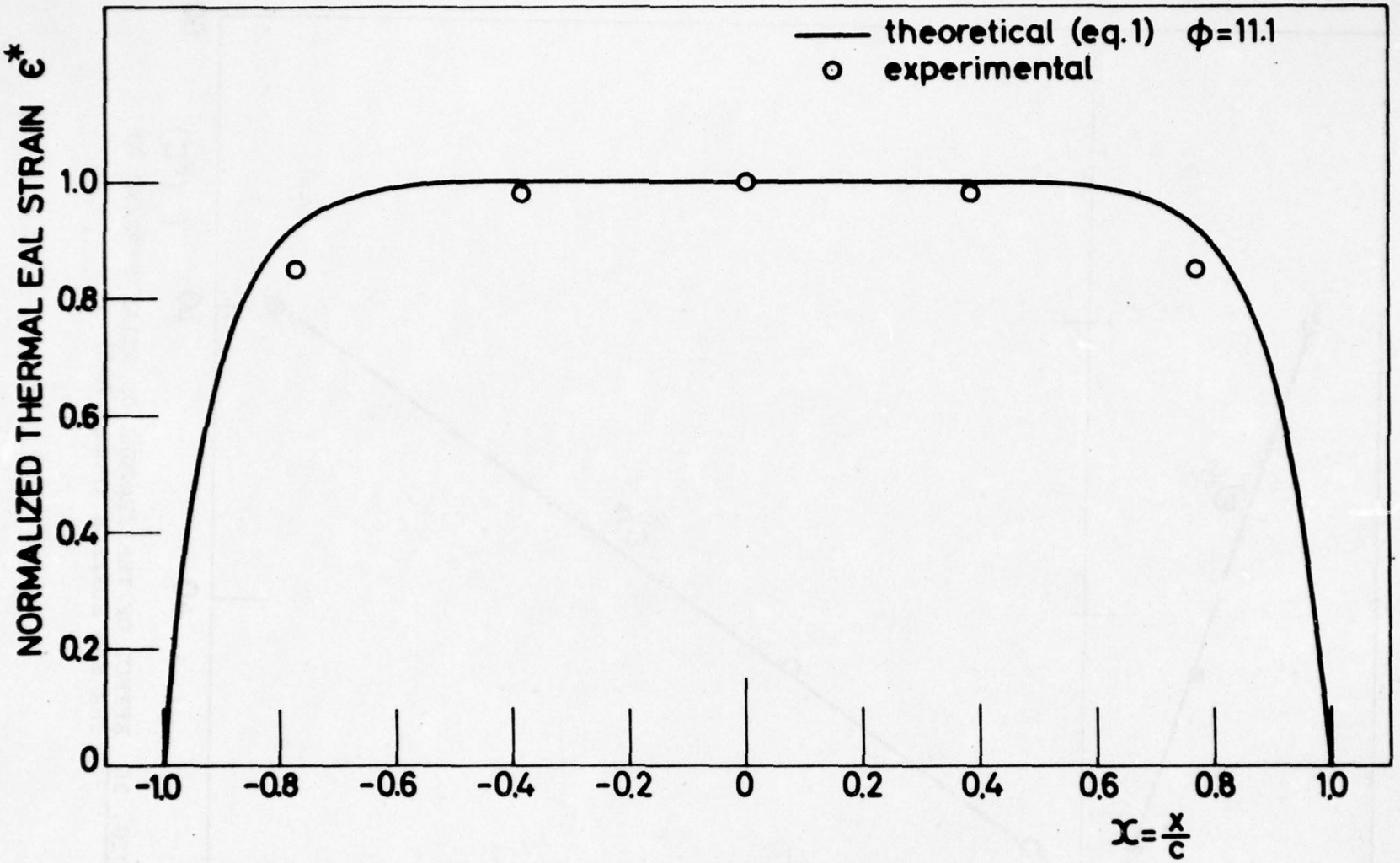


FIG. 27 NORMALIZED STRAIN DISTRIBUTION RESULTING FROM THERMAL CHANGES ALONG THE EAL EXTERNAL SURFACE (MODEL A02).

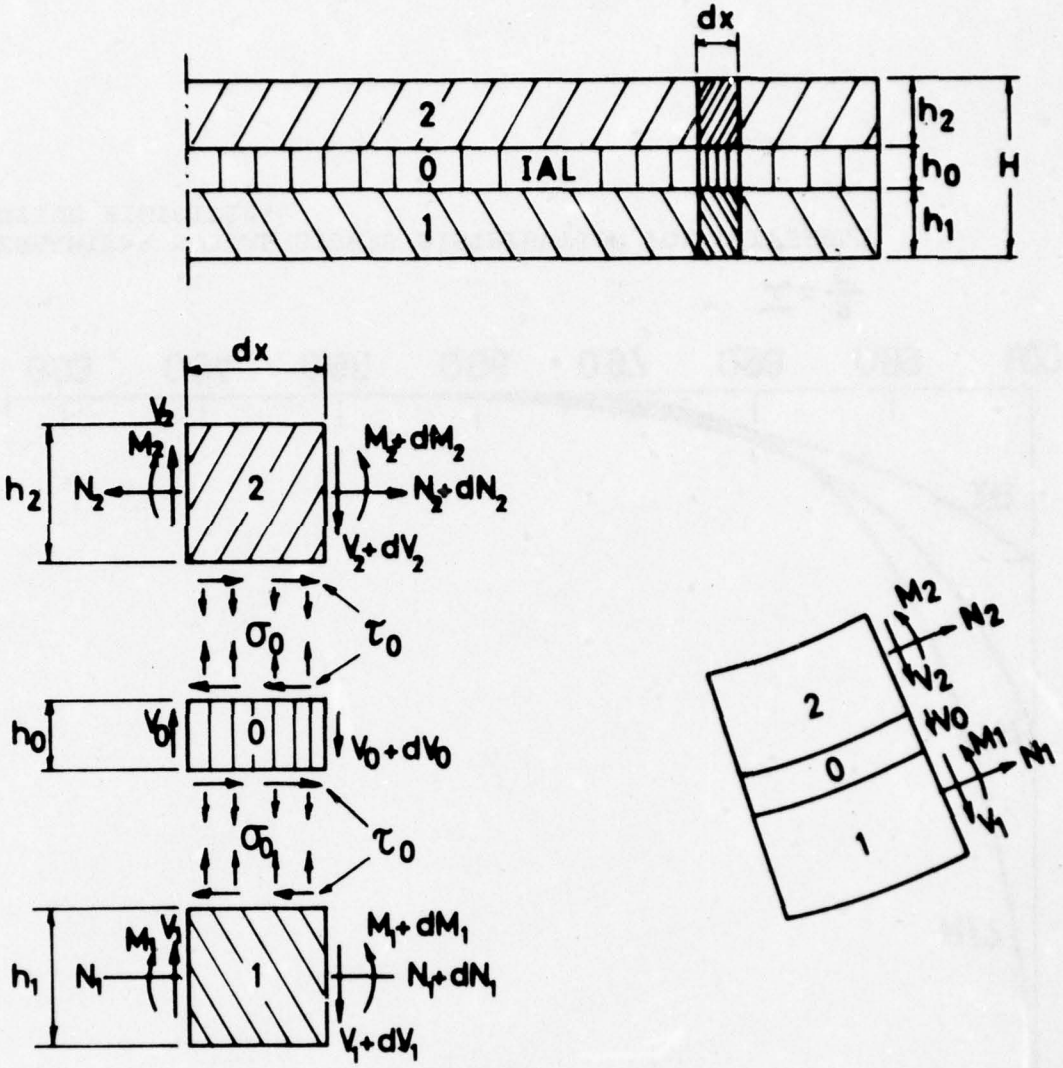


FIG. 28 STRESS ANALYSIS SCHEME OF A NONSYMMETRICAL DOUBLER MODEL (NMD).

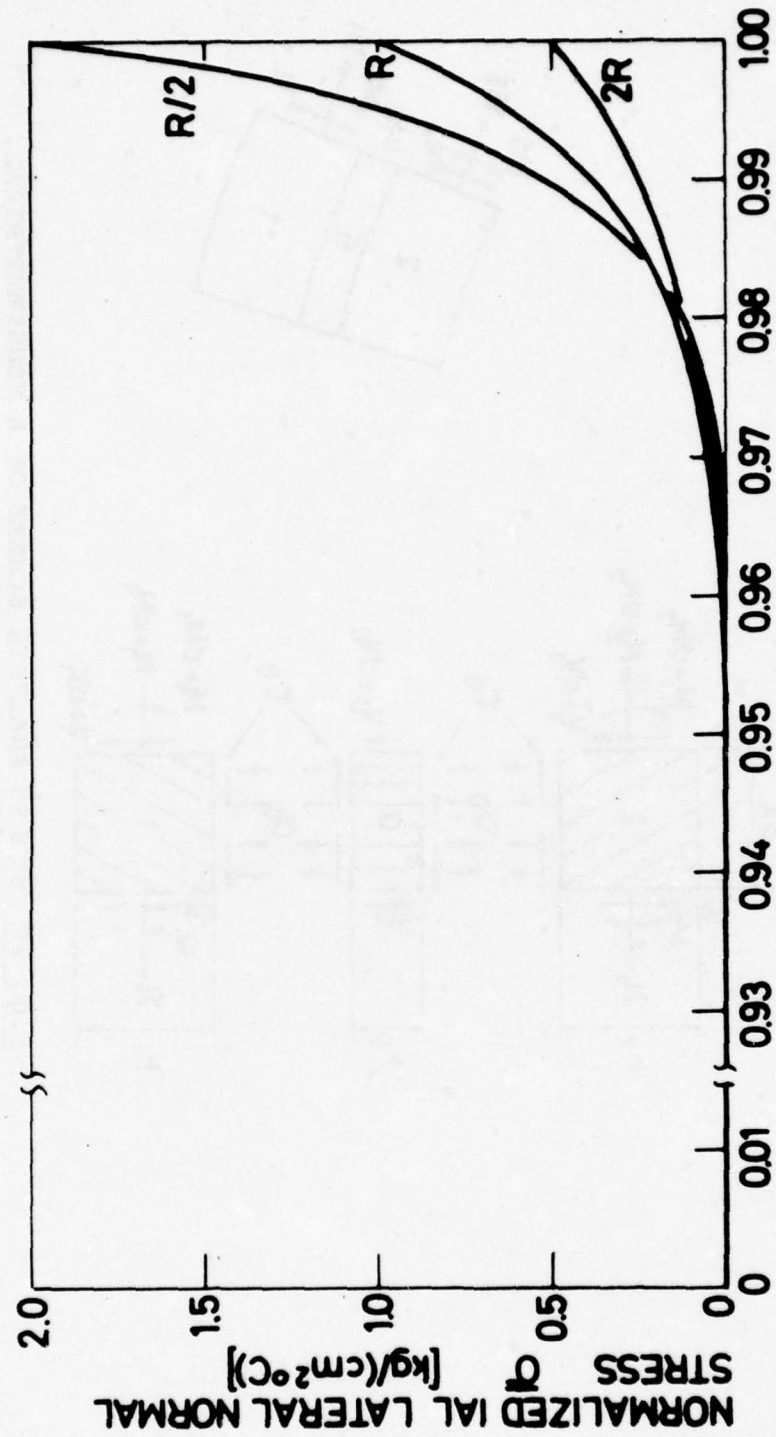


FIG. 29 INTERLAMINAR NORMAL STRESS DISTRIBUTION FOR DIFFERENT ADHESIVE RIGIDITIES.

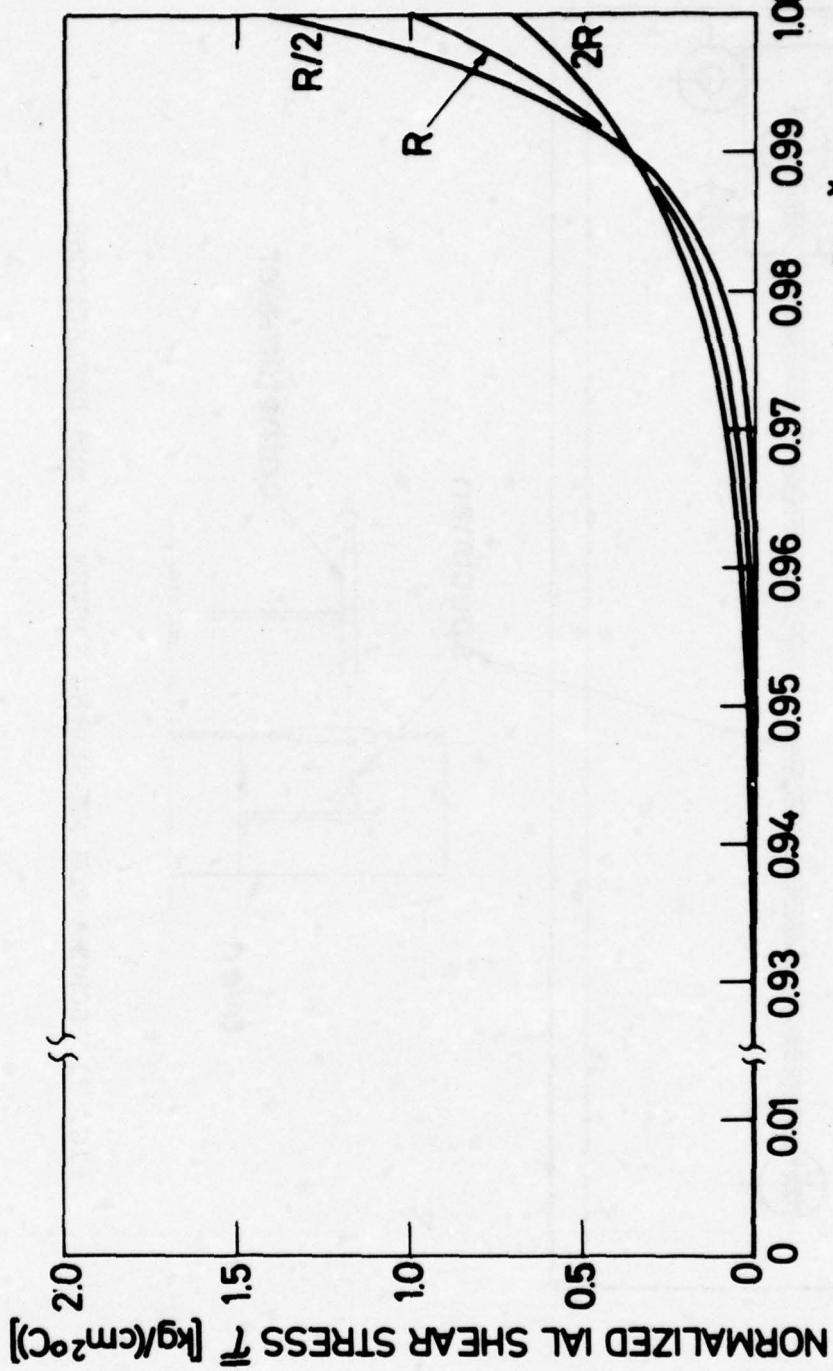


FIG. 30 INTERLAMINAR SHEAR STRESS DISTRIBUTION FOR DIFFERENT ADHESIVE RIGIDITIES.

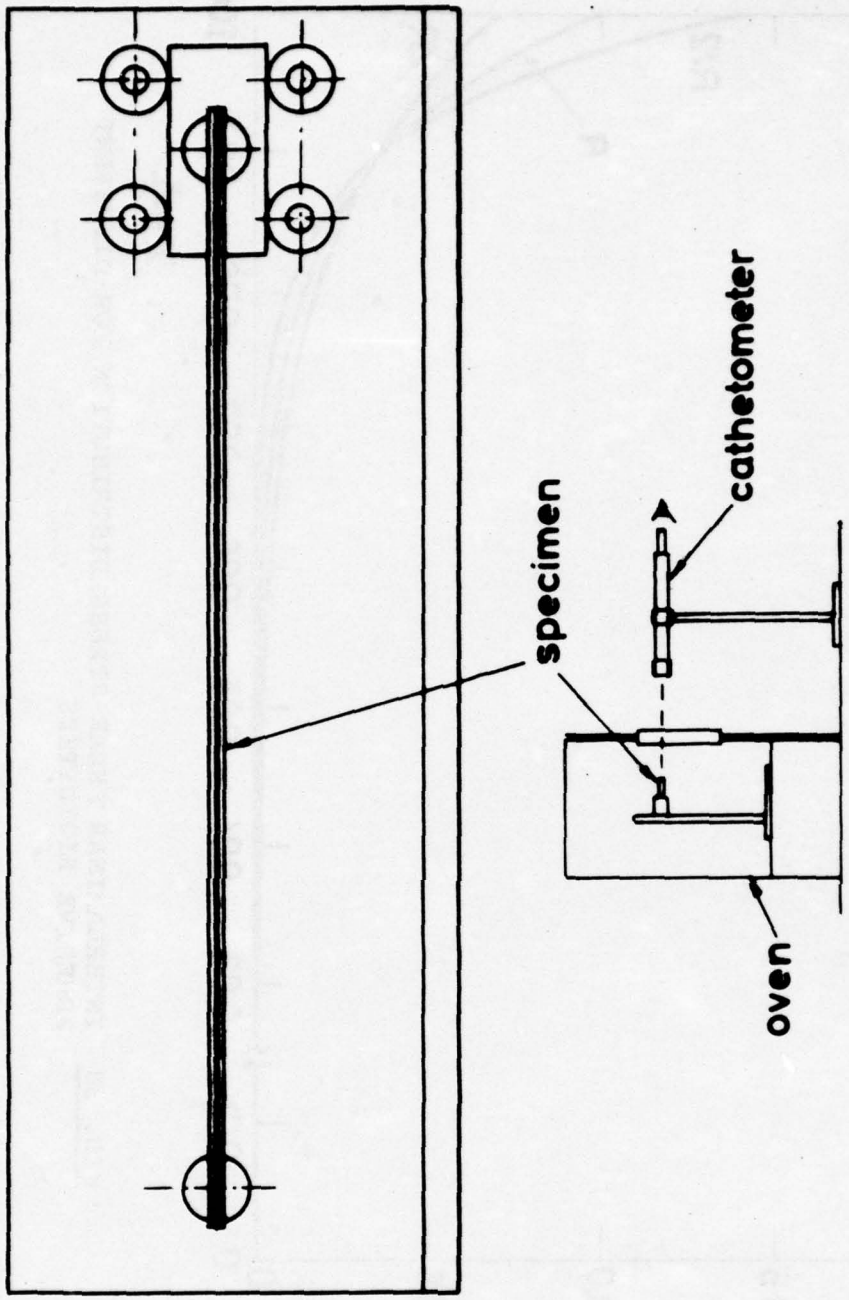


FIG. 31 SCHEMA FOR MEASURING SYSTEM OF NMD DEFLECTIONS.

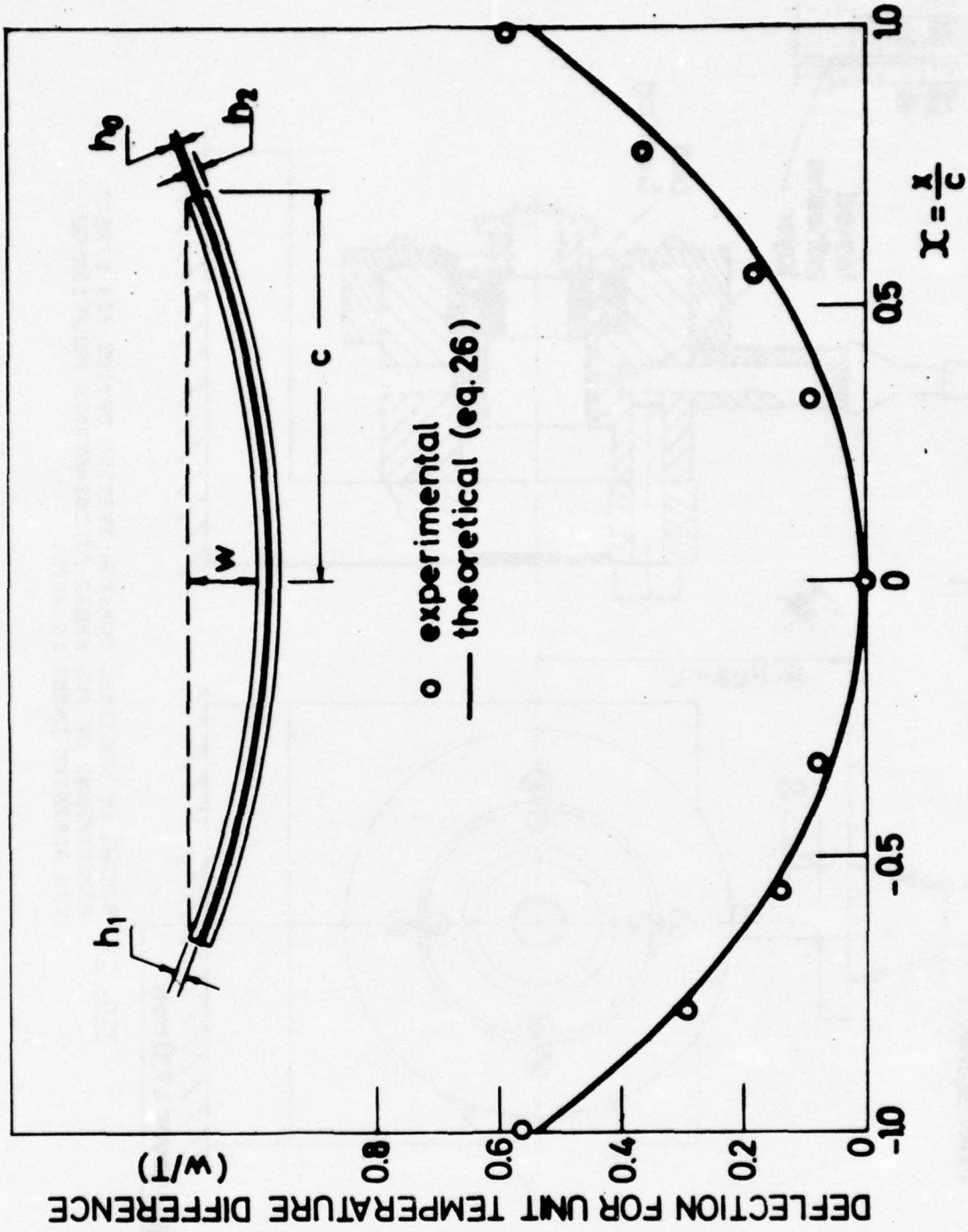


FIG. 32 THERMOELASTIC DEFLECTION CURVE OF NMD.

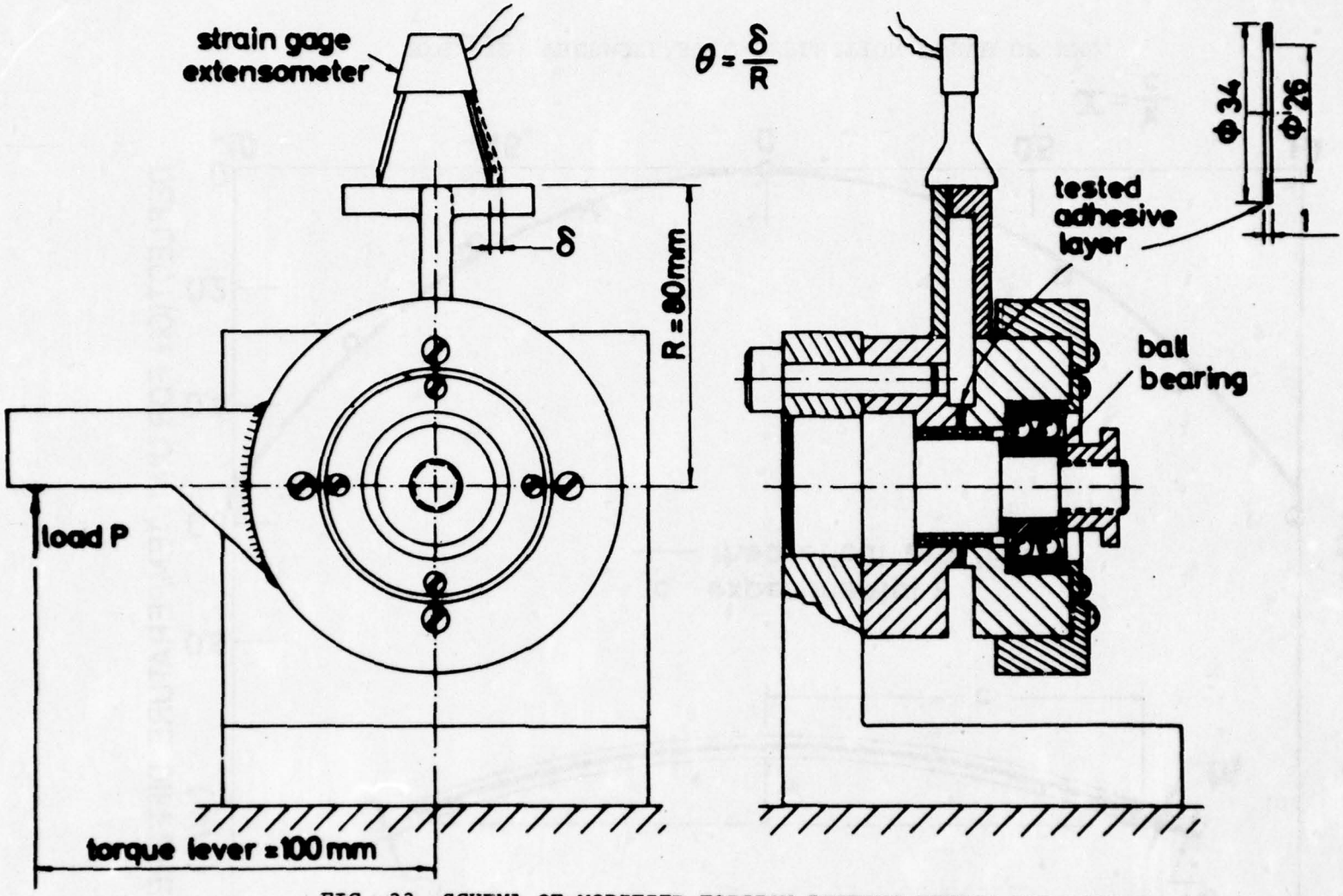


FIG. 33 SCHEMA OF MODIFIED TORSION TESTING DEVICE FOR DIRECT MEASUREMENT OF THE SHEAR STRESS-STRAIN BEHAVIOR OF THE ADHESIVE LAYER *IN SITU*.

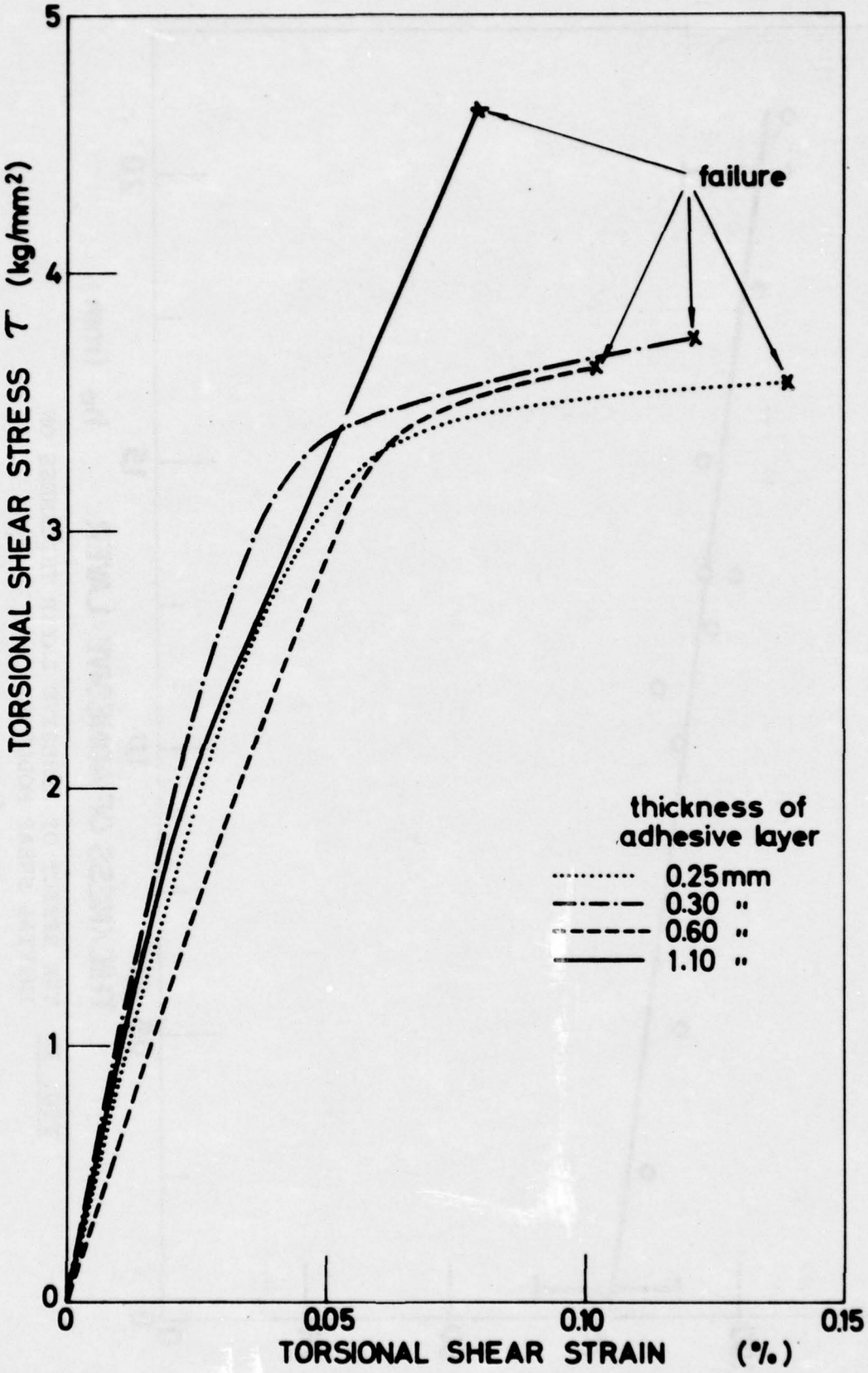


FIG. 34 TYPICAL SHEAR STRESS-STRAIN CURVES FOR THE ADHESIVE LAYER *IN SITU*.

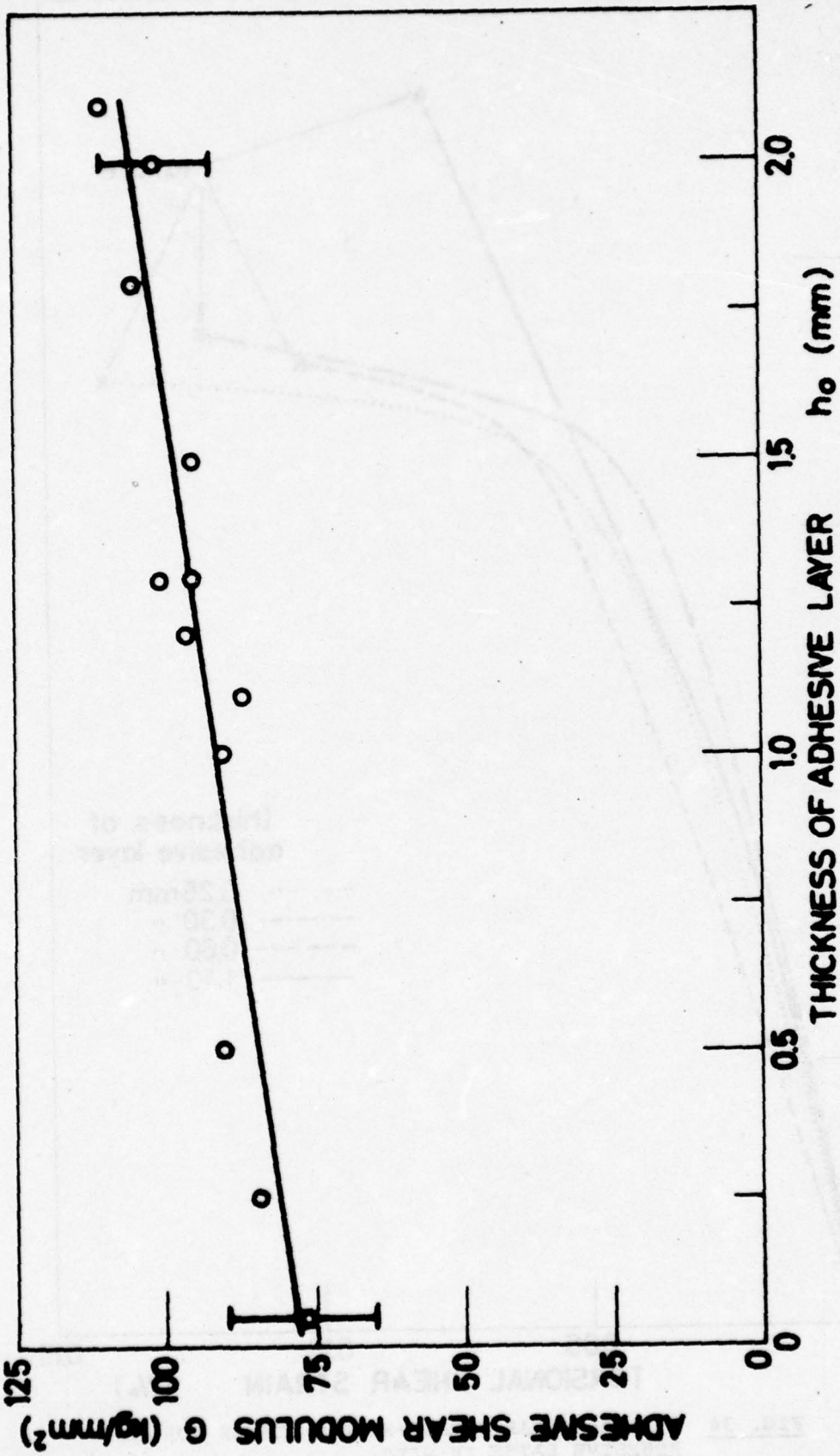


FIG. 35 THE EFFECT OF ADHESIVE LAYER THICKNESS ON INITIAL SHEAR MODULUS.

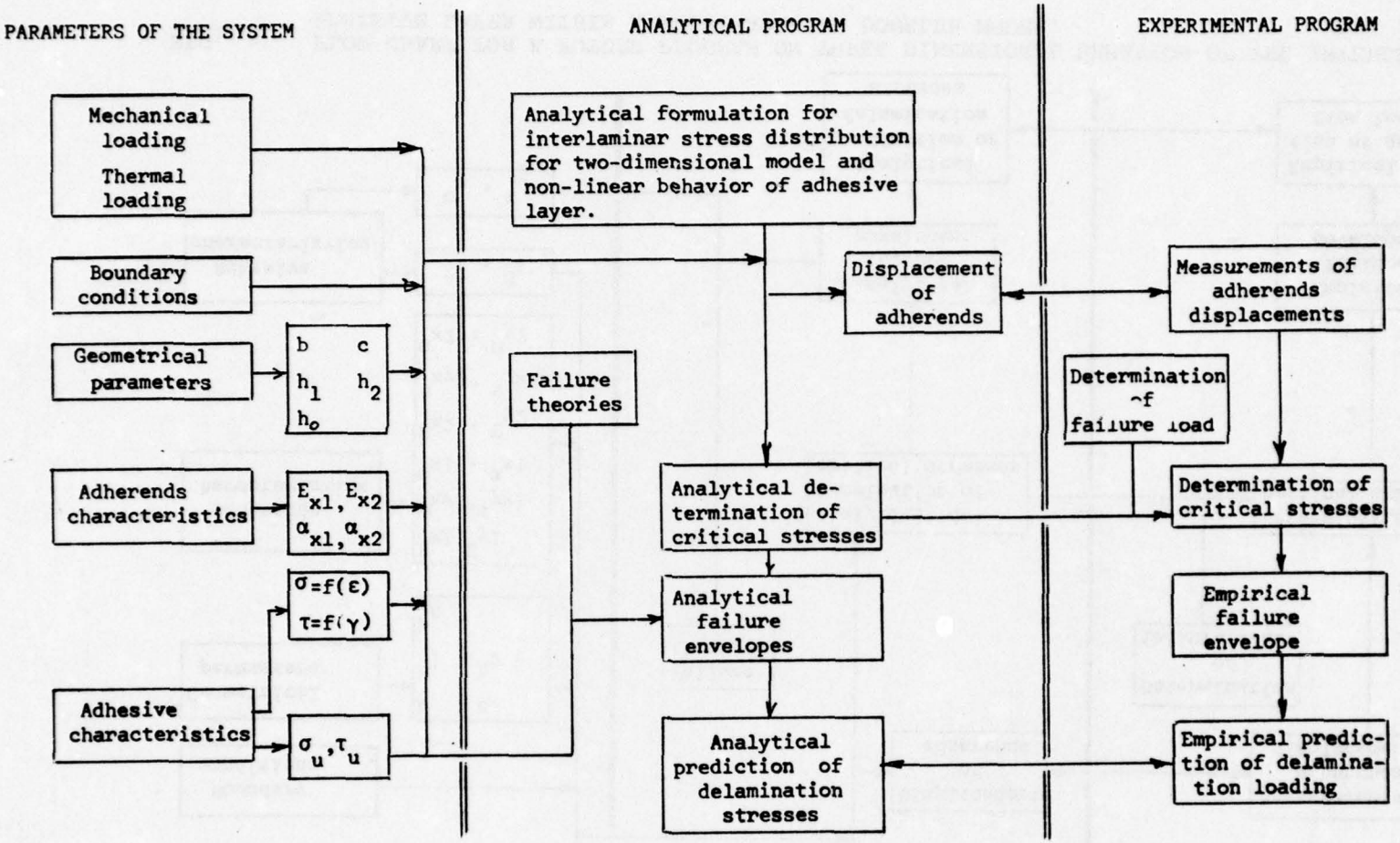


FIG. 36 FLOW CHART FOR A FUTURE PROGRAM ON NON-LINEAR BEHAVIOR OF THE INTERLAMINAR ADHESIVE LAYER WITHIN A MULTIMATERIAL DOUBLER MODEL.

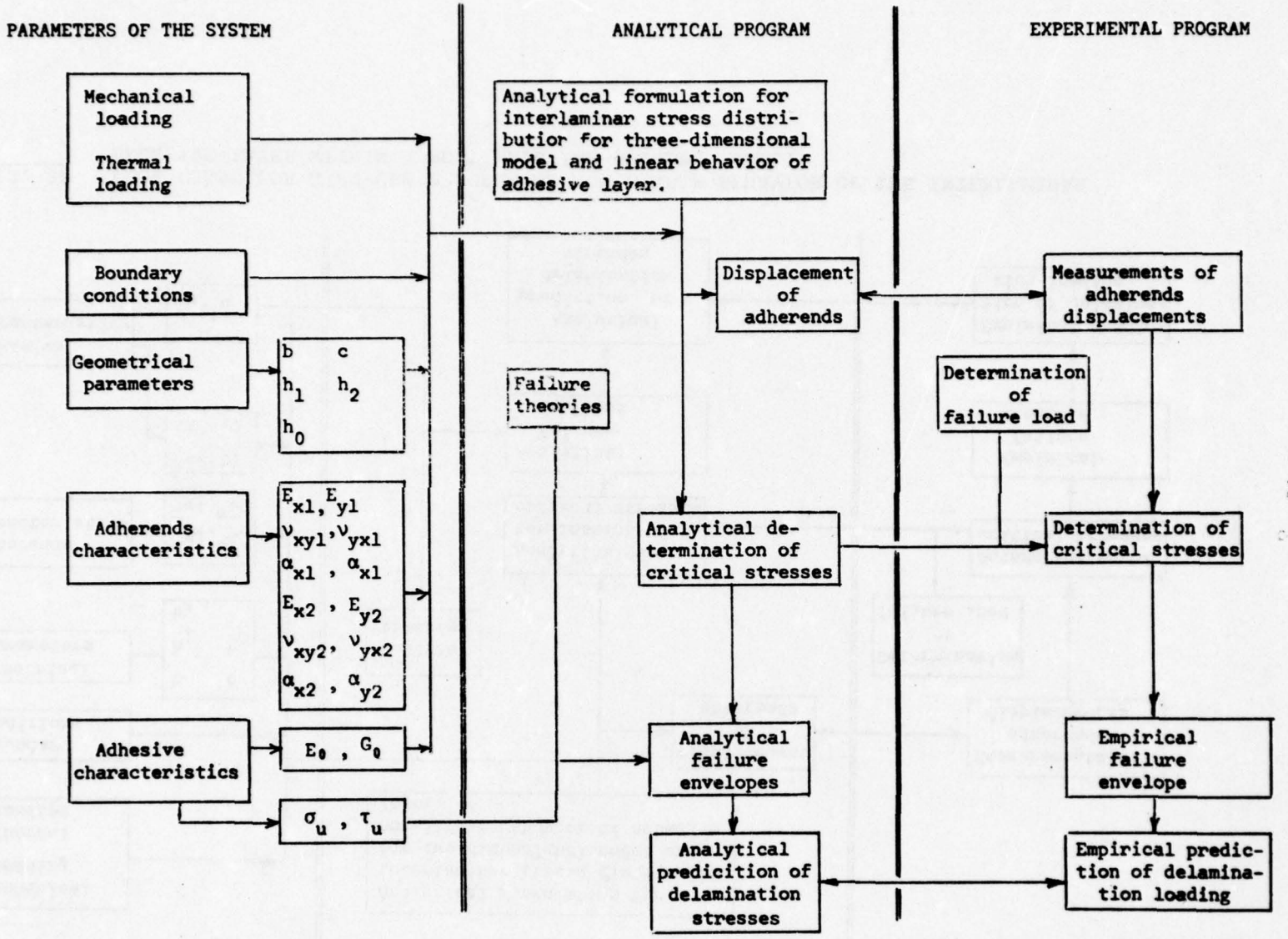


FIG. 37 FLOW CHART FOR A FUTURE PROGRAM ON THREE DIMENSIONAL BEHAVIOR OF THE INTERLAMINAR ADHESIVE LAYER WITHIN A MULTIMATERIAL DOUBLER MODEL.

TABLE 1: DIMENSIONS AND ELASTIC PARAMETERS OF TEST MODELS.

Model No.	Elastic Moduli [kg/mm^2]				Dimensions [mm]			
	G_0	E_0	E_1	E_2	h_0	h_1	h_2	c
A21	90	250	7500	7500	1.0	1.5	1.0	65
A02	90	250	3500	7500	1.0	1.5	1.0	65

TABLE 2: ELASTIC AND THERMOELASTIC PARAMETERS OF TEST MODEL A02.

Direction	kg/mm^2 Elastic Moduli			Poisson's Ratio		10^{-6}[c^{-1}] Coeff. of Thermal	
	E_1	E_2	G_0	ν_{xy1}	ν_{xy2}	α_1	α_2
x	3500	7500	90	0.28	0.33	$\sim$ 8.5	22
y	1000	7500	90	0.02	0.33	$\sim$22.0	22.0

COMPOSITION OF SMD (TABLES 1,2)

Model	Adherend 1	Adherend 2	Adhesive
A21	Aluminum 2024 T/3, nonclad	Aluminum 2024 T3, nonclad	2:1 mix of epon 828 and versamid 140
A02	E-glass fiber reinforced epoxy unidirectional laminate	"	"

TABLE 3: DIMENSIONS AND ELASTIC PARAMETERS OF NMD TEST MODEL.

Elastic Moduli kg/mm^2				Dimensions (mm)			
G_0	E_0	E_1	E_2	h_0	h_1	h_2	c
90	250	7500	3500	0.1	1	1	90

Composition:

Adherend 1: Aluminum 2024/T3 non-clad.

Adherend 2: E glass fiber reinforced unidirectional laminate.

Adhesive: 2:1 mix of Epon 828 resin and Versamid 140 hardener.

APPENDIX 1

ANALYSIS OF INFORMATION ON: "MECHANICAL BEHAVIOR OF ADHESIVE BONDED JOINTS".

No.	Model Geometry	Materials: Adhesive/ Adherend	Loading and Environment	Mechanical Behavior State of Stress	Analytical Methods	Experimental Techniques	Effect of Structural Parameters	Failure and Strength
2	SLJ	dissimilar adherends	axial tension neglecting bending	only shear adhesive strains; max. shear stress at edge	simplified differential eqs.		stress concentration increase with overlap length	
4	SLJ rectangular sheet adherends of equal thickness	very thin flexible adhesive compared with adherends	tensile axial force with eccentricity	beam theory or cylindrical bent-plate theory; plane strain at adhesive; shear and normal stress distribution	classical differential eqs. preassumption uniform stress distribution through thickness		relatively flexible and rigid adhesive cases	
7	SLJ adherend plates infinite springs adhesive		axial tension related to fatigue loading	beam theory and spring analogy applied to lab fatigue specimen shear and normal stress distribution	differential equation; spring beam analogy	photoelastic and brittle lacquer (stress coat) method	curved adhesive edges effect of thick adhesive	
9	SLJ sheets Butt joints	Araldite adhesive reinforced bakalite adherends metal adherends	uniaxial stress creep of adhesive	mainly plane strain		photoelastic measurements	effect of: overlap length; edge curvature; edge inclination length to thickness ratio in butt joint	
21	DLJ	Epoxy (Araldite)	fatigue tension temperature	shear stress behavior as function of overlap length	simplified solution of dif. eqs.	calculation of joint ultimate load as function of max. optimal lap length	effect of overlap length on strength	shear strength and failure strength

No.	Model Geometry	Materials: Adhesive/ Adherend	Loading and Environment	Mechanical Behavior State of Stress	Analytical Methods	Experimental Techniques	Effect of Structural Parameters	Failure and Strength
23	SLJ Scarfed joint DLJ	boron-epoxy adherend AF31, HT424 adhesives separate and mix	tension	stress concentration factor along joint axis		structural joint tests	effect of adhesive module(mixed rigidity) on joint efficiency	
24	torsion tube	Epon 828/ V40 Aluminum & stainless steel adherends metlbond 329	tension torsion temperature -100÷300°F	pure shear	calculation of shear modulus	measurement of adhesive, shear and tensile moduli in situ	effect of adhesive thickness on moduli	
25	SLJ DLJ different adherends supported & unsupported models scarf joint	adhesives: FM-1000 Metlbond 400 FM-47 (epoxy) adherends: GRP, Scotchply, Titanium GAl-4V Steel AISI 1025	static axial loading; fatigue loading	shear & normal stress distribution; elastic behavior plane stress or generalized plane strain	comparison of ref.4, numerical & finite element methods, shear lag analysis	static & fatigue data of DLJ; test of effect of edge tapering	effect of adhesive shear modulus, thickness overlap length, adherend width, thickness, modulus joint efficiency effect of adherend edge tapering	shear strength strength of adhesives fatigue strength
27	SLJ and DLJ	polyester sheet for photoelastic joint model steel adherend	static & fatigue loading	shear stress distribution along adhesive normal stresses along adherend tapered edges	simplified integration of shear stresses along IAL	photoelastic measurements of stress distribution in adhesive brittle lacquer technique	effect of angles of metal edges to reduce adhesive stress concentration; effect of lap length and adherend thickness	adhesive joint designed for metal failure
28	stringer bonded to elastic sheet of infinite size	flexible vs stiff adhesives metal adherends	line uniaxial loading	stringer in simple extension; pure shear in elastic adhesive bending neglected	integral equations method		uniform shear in flexible adhesive; high stress concentration in stiff adhesive	

No.	Model Geometry	Materials: Adhesive/ Adherend	Loading and Environment	Mechanical Behavior State of Stress	Analytical Methods	Experimental Techniques	Effect of Structural Parameters	Failure and Strength
29	SLJ Doubler	Flexible adhesive epoxy	tensile shear	nonlinear stress-strain adhesive shear stress distribution only	nonlinear differential eq. numerical solution finite element		effect of doubler stiffness and bond-line thickness	average shear stress at joint failure
30	Symmetric double lap joints	metal and FRC composite adherends (anisotropic) boron-epoxy-glass epoxy adhesive	axial tension	plane stress in adherends shear and normal stress distribution	differential equations		effect of adhesive thickness	
31	DLJ	plain metal adherends	static and fatigue loading	shear stress distribution only; elastic behavior of adhesive to failure approx. expression for normal stresses	semi-empirical approach and computer programming for optimum lap-length polynomials curve fitting		effect of overlap length on strength adhesive properties in thin film differs from bulk	joint strength optimization applying Hill failure criterion adherend & adhesive failure modes
32	DLJ	FM-123-2 modified nitrile e epoxy adhesive 2024-T3 clad adherends	static and fatigue loading		statistical analysis of fatigue data computer programming	Sontag fatigue machine with static load maintainer	effect of overlap length for optimization of fatigue endurance	S-N fatigue curves with 95% confidence limits

No.	Model Geometry	Materials: Adhesive/ Adherend	Loading and Environment	Mechanical Behavior State of Stress	Analytical Methods	Experimental Techniques	Effect of Structural Parameters	Failure and Strength
35	peel test model	adhesive tapes bakelite plates adherends	tensile peel test	viscoelastic behavior; relaxation weak boundary layer mechanism	rheological models and theories; rate-temperature super-position method	peeling test of adhesive tapes	effect of temperature on strength effect of strain-rate adhesive thickness effect	cohesion vs interfacial failure; failure criteria and envelopes peel strength
36	SLJ DLJ stepped joint	titanium aluminum and boron-epoxy adherends; epoxy adhesive Epon 9601	static and fatigue loadings thermal loading	linear and nonlinear adhesive stress-strain; transverse shear included; zero stresses at IAL edges plastic zone approach	finite element solution compared with closed form solutions computer program for numerical solution (Bonjo)	photostress and strain-gage strain measurements on adherend surfaces	effect of transverse shear in case of composite adherends	
37	SLJ step-J	Boron-Titanium	torsion tension temperature	elastic-linear nonlinear mainly shear stresses	finite element	torsion tube butt tension		shear and tensile adhesive strength
38	SLJ DLJ	$E=20,000 kg/mm^2$ $G_0=100 kg/mm^2$ linear viscoelastic adhesive	constant static tensile stress creep	time-dependent shear stress distribution pure shear assumption in adhesive	classical linear viscoelastic approach collocation method			
40	SLJ —— shear springs model	aluminum to steel adherends;high model epoxy adhesive	axial tension	adhesive,transverse & longitudinal shear distribution	approx. analytical closed form vs finite difference solutions	rubber model for measuring transverse adhesive strains	profiled adhesive layer to give uniform stress	

No.	Model Geometry	Materials: Adhesive/ Adherend	Loading and Environment	Mechanical Behavior State of Stress	Analytical Methods	Experimental Techniques	Effect of Structural Parameters	Failure and Strength
41	asymmetrical lap joints	anisotropic adherends: 1002-S GRP 45°/0° - 45°/0° U.S. film adhesive EA951	static and fatigue loading non-uniform fatigue loading	effect of transverse shear & normal stress strain distribution through adherend thickness linear plate theory; normal and shear stress distribution plane strain	comparison with close form solution (4) solution of 8 order linear differential eqs. + 6 boundary conditions	ultrasonic vs destructive tests for modulus shear & normal strength properties of adhesive in situ electro scanning microcopy for fracture	effect of ply orientation adhesive thickness overlap length adhesive shear proportional limit effect on fatigue	maximizing joint strength fatigue life adhesive & interlaminar failure modes
43	DLJ	ductile vs brittle adhesives	static axial load thermal effects	elasto-plastic solution shear and normal stress distribution	bound for nonlinear behavior simplified analytical approach	stress-strain curves for shear (torsion)	mix module adhesive effect of overlap adherend thickness	peel failure mode strength independent on large overlap length
44	SLJ	adherends: aluminum 7075-T6 CFRP, quasi-isotropic & U.D. adhesives: brittle & ductile epoxy	Axial tension	plane stress in adherend; adhesive linear elastic & elastic-plastic	differential eqs; closed form solution		load eccentricity lap/thickness ratio tapering adherend edges	interlaminar adherend failure; adhesive shear & transverse tension failure
45	Stepped & scarfed joints	ductile vs brittle adhesives: Hysol 951 vs Metlbond, 329 titanium & CFRP adherends	static and thermal loading	elastic-plastic shear stress distribution; shear and normal elastic stress distribution	explicit algebraic formulas for bounds of strength prediction	failure tests of adhesive (torsion) & joints	effect of adhesive plasticity on strength effect of overlap length	shear strength affected by ductility composite interlaminar failure mode

No.	Model Geometry	Materials: Adhesive/ Adherend	Loading and Environment	Mechanical Behavior State of Stress	Analytical Methods	Experimental Techniques	Effect of Structural Parameters	Failure and Strength
47	stepped & tapered lap joints	aluminum, steel adherend; orthotropic composite adherends epoxy adhesive	static in-plane loads	2-dimensional plane-stress plane-strain in plates shear stress distributions	finite element method		effect of adhesive thickness	
48	SLJ	$E=200kg/mm^2$ $G_0=0.2$ "	static axial tension	only shear stress distribution	classical differential equation approach		effect of varying shear moduli of adhesive (2 steps)	shear fracture strength (max.shear strain energy criterion)
49	SLJ, Doubler cleavage specimen	aluminum/ aluminum	uniaxial tension hostile environment	stress-corrosion analysis of shear stresses only	simplified analysis for max.shear stress	Extensometer for measuring shear displacment		crack propagation in hostile environment
50	double SLJ	adherend: Alum 2024 T3 adhesive: modified epoxy with anticorrosive primer (250°curing)	tensile loading in hot humid environment 120°F 100% R.H.	static stressing at constant level, creep rupture life measurements		constant load maintained by springs	effect of aging history load cycling effect on bond recovery	adhesive failure due to water penetration to interfaces in other cases, cohesive failure, fracture toughness

No.	Model Geometry	Materials: Adhesive/ Adherend	Loading and Environment	Mechanical Behavior State of Stress	Analytical Methods	Experimental Techniques	Effect of Structural Parameters	Failure and Strength
51	SLJ,DLJ Spew vs square edge	epoxy rigid AF-130 adhesives ($G=172kg/mm^2$) Aluminum adherends	tension shear	plane strain 2-d shear stress normal stress and principal adhesive stresses	finite element (triangle elements)		effects of adherend length, overlap length, spew size, adhesive thickness, adherend thickness	effect of adhesive thickness & edge geometry adherend improves strength
52	SLJ	flexible adhesive	uniaxial tension	plane stress plane strain stress distribution through adhesive adherend thickness	finite difference			
54	Doubler SLJ double notch tensile specimen	epoxy film adhesive AF 127; thick bond line	fatigue and environment 120°F 100% R.H.	flexural behavior of bonded structure design allowable data	design analysis; finite element method (NASTRAN)	flexural wing fatigue test. nondestructive inspection	effect of bond-line thickness	endurance test
55	SLJ	GRP adherends (1002 S-glass) Hysol EA951 nylon epoxy adhesive	fatigue and static loading	behavior at the linear elastic range up to proportional limit	use of analysis based on differential equations assumption of uniform adhesive stresses	fatigue life measurements micro observation of failure surfaces	effect of: overlap length, adhesive thickness, laminae orientation, adhesive proportional limit	adhesion-cohesion mode of failure composite interlaminar failure at 45° ply
56	SLJ	ductile adhesive: nylon-epoxy, anisotropic, GRP & Kevlar adherends	fatigue loading spectrum static loading	tensile & shear adhesive stress distribution zero shear at edges	fatigue life theory for two block loading spectrum	fatigue run-out tests	effects of: overlap length laminae orientation adhesive proportional limit	fatigue vs fracture toughness of ductile adhesives

No.	Model Geometry	Materials: Adhesive/ Adherend	Loading and Environment	Mechanical Behavior State of Stress	Analytical Methods	Experimental Techniques	Effect of Structural Parameters	Failure and Strength
59	stepped & tapered lap joints	metal & FRC composite adherends (anisotropic) boron-epoxy glass-epoxy epoxy adhesive	axial tension	plane stress in adherends shear & normal stress distribution	differential equations		effect of adhesive thickness	
60	double cantelever	elastomer-epoxy (CTBN) adhesive	tension, shear, off-axis loading	fracture toughness test interfacial behavior	fracture mechanics	mix failure mode test by inclined adhesive line cleavage test	bond thickness effect	crack propagation high toughness in matrix not reflected in joint
61	SLJ,SLJ step-joint plates	variation in adhesive moduli	uniaxial tension	strain displacement stress strain stress distribution along axial coordinate	polynomials differential equations		effect of edge tapering	
62	DLJ bonded layers		tensile shear	stress intensity factors, shear and normal stresses	singular integral eq. numerical solutions		effect of adherend thickness	
63	SLJ double notch specimen	adherend: S-glass adhesive: epoxy-nylon	fatigue & static tension loading	beyond the linear range interlaminar shear in composite shear and normal stress in adhesive	numerical analysis	double notch shear test	effect of fiber orientation and layer sequence in laminate	fatigue joint strength mainly affected by proportional limit in shear angly ply failed between layers

No.	Model Geometry	Materials: Adhesive/ Adherend	Loading and Environment	Mechanical Behavior State of Stress	Analytical Methods	Experimental Techniques	Effect of Structural Parameters	Failure and Strength
64	Double cantilever beam	adherends: 2024 T3 bare 7975 clad adhesives: modified epoxy and nitrile phenolic	sustained loading at high temperature and humidity, weathering exposure	time-temperature effects on strength & crack propagation		precracked cleavage model exposed to moist ambient	effect of surface preparation acid anodizing	residual shear strength; fracture toughness; delamination
71	multilayer laminate panel	orthotropic adherends, isotropic adhesive boron epoxy laminate	static & cycling loading; axial loading	elastic & plastic behavior of adhesive; plane stress in adherends interlaminar shear stress distribution	initial strain for inelastic behavior finite element solution; displacement method	stress-strain curves for Ramberg-Osgood parameters	effect of thickness to length ratio and layer number	

APPENDIX 2

FINITE ELEMENT COMPUTER PROGRAM FOR ELASTIC STRESS ANALYSIS IN ORTHOTROPIC BONDED STRUCTURAL SYSTEMS.

```
LEVEL 21.7 ( JAN 73 )                    OS/360  FORTRAN H                                    DATE

      COMPILER OPTIONS - NAME=  MAIN,OPT=02,LINECNT=60,SIZE=0000K,
                         SOURCE,EBCDIC,NOLIST,NODECK,LOAD,NOMAP,NOEDIT,ID,NOXREF
            C                                                                          C0001C00
            C TWO DIMENSION PLAN STRAIN/STRESS FINITE ELEMENT PROGRAM                  C0002000
            C FOR GENERAL MATERIAL                                                     C0003C00
            C                                                                          C0004000
ISN 0002          REAL*8 TITLE(9)                                                      C0005C00
ISN 0003          COMMON NNP,NEL,NMAT,NSLC,NOFT,NBODY,MTYP,IE(200,5),RO(10),TH(10),    C0006C00
                 1ET(10),LT(10),GGT(10),E1T(10),E2T(10),U12T(10),U21T(10),G12T(10),    C0007C00
                 2CQ(3,3),QM(3,3,10),E,U,GG,E1,E2,U12,U21,G12,QQT(3,3,10),             C0008C00
                 3X(200),Y(200),ULX(200),VLY(200),KODE(200),ISC(20),JSC(20),           C0009C00
                 4SURTRX(20,2),SURTRY(20,2),EP(10)                                     C0010C00
ISN 0004          COMMON/ONE/GK(10,10),Q(10),B(3,10),C(3,3),BT(3,6),XQ(5),YQ(5)        C0011C00
ISN 0005          COMMON /TWO/ IBAND,NEQ, R(400), AK(400,50)                           C0012000
ISN 0006          DATA MAXEL, MAXNP, MAXMAT, MAXEW, MAXSLC                             C0013C00
                 1     /  200,    200,       10,     50,     20/                      C0014C00
ISN 0007       5555 READ 100,NPROB, (TITLE(I),I=1,9)                                   C0015C00
ISN 0008          IF(NPROB.LE.0) GO TO 999                                             C0016000
ISN 0010       1020 PRINT 200,NPROB,(TITLE(I),I=1,9)                                   C0017000
ISN 0011          CALL DATAIN (MAXEL,MAXNP,MAXMAT,MAXSLC,ISTOP)                        C0018C00
ISN 0012               MAXDOF = 2*MAXNP                                                C0019000
ISN 0013               MAXDIF = 0                                                      C0020000
ISN 0014          DO 1 I=1,NEL                                                         C0021C00
ISN 0015          DO 1 J=1,4                                                           C0022C00
ISN 0016          DO 1 K=1,4                                                           C0023C00
ISN 0017               LL= IABS(IE(I,J)- IE(I,K))                                      C0024C00
ISN 0018          IF(LL.GT.MAXDIF) MAXDIF = LL                                         C0025C00
ISN 0020        1 CONTINUE                                                             C0026C00
ISN 0021               IBAND = 2*(MAXDIF + 1)                                          C0027000
ISN 0022               NEQ = 2*NNP                                                     C0028C00
ISN 0023          IF(IBAND.GT.MAXBW) GO TO 900                                         C0029000
ISN 0025          IF(ISTOP.GT.0) GO TO 999                                             C0030000
ISN 0027          CALL ASEMBL(ISTOP)                                                   C0031000
ISN 0028          IF(ISTOP.GT.0) GO TO 999                                             C0032C00
ISN 0030          CALL BANSOL(1,AK,R,NEQ,IBAND,MAXDOF,MAXEW)                           C0033C00
ISN 0031          CALL BANSOL(2,AK,R,NEQ,IBAND,MAXDOF,MAXEW)                           C0034000
ISN 0032        PRINT 300, (I,R(2*I-1),R(2*I),I=1,NNP)                                 C0035C00
ISN 0033          CALL STRESS                                                          C0036000
ISN 0034          GO TO 5555                                                           C0037C00
ISN 0035       900 PRINT 901, IBAND, MAXBW                                             C0038000
ISN 0036          GO TO 5555                                                           C0039C00
ISN 0037       100 FORMAT( I5,3X,9A8 )                                                 C0040C00
ISN 0038       200 FORMAT( /8H1PROBLEM,I5,3H.. ,9A8 )                                  C0041C00
ISN 0039       300 FORMAT(37H1OUTPUT TABLE 1.. NODAL DISPLACEMENTS //                  C0042C00
                 1       13X,4HNODE, 9X, 11HU = X-DISP.,9X, 11HV = Y-DISP./           C0043C00
                 2      (5X,I12,2E20.8))                                              C0044000
ISN 0040       901 FORMAT(///12H BANDWIDTH =,I4,25H EXCEEDS MAX. ALLOWABLE =,I4//      C0045C00
                 1 30H GO ON TO NEXT PROBLEM          )                                C0046C00
ISN 0041       555 STOP                                                                C0047C00
ISN 0042          END                                                                  C0048C00
```

```
        COMPILER OPTIONS - NAME=  MAIN,OPT=02,LINECNT=60,SIZE=0000K,
                           SOURCE,EBCDIC,NOLIST,NODECK,LOAD,NOMAP,NOEDIT,ID,NOXREF
ISN 0002              SUBROUTINE DATAIN(      MAXEL,MAXNP,MAXMAT,MAXSLC,ISTOP)                  CCCC1CCO
ISN 0003              COMMON NNP,NEL,NMAT,NSLC,NOPT,NECDY,MTYP, IE(200,6),RO(10),TH(10),        CCCC2CCO
                     1ET(10),UT(10),GGT(10),E1T(10),E2T(10),U12T(10),U21T(10),G12T(10),        CCCC3CCO
                     2QQ(3,3),GM(3,3,10),E,U,GG,E1,E2,U12,U21,G12,CQT(3,3,10),                 CCCC3500
                     3X(200),Y(200),ULX(200),VLY(200),KODE(200),ISC(20),JSC(20),               CCCC4CCO
                     4SURTRX(20,2),SURTRY(20,2),EP(10)                                         CCCC5CCO
                C                                                                              CCCC6CCO
ISN 0004              ISTOP = 0                                                                CCCC7CCO
ISN 0005              READ 1,NNP,NEL,NMAT,NSLC,NOPT,NECDY                                      CCCC8CCO
                C                                                                              CCCC9CCO
ISN 0006              PRINT 100,NNP,NEL,NMAT,NSLC,NOPT,NECDY                                   CCC10CCO
ISN 0007                   IF(NNP.LE.MAXNP) GO TO 201                                          CCC11CCO
ISN 0009                        ISTOP = ISTOP + 1                                              CCC12CCO
ISN 0010              PRINT 251, MAXNP                                                         CCC13CCO
ISN 0011         201       IF(NEL.LE.MAXEL) GO TO 202                                        CCC14CCO
ISN 0013                        ISTOP = ISTOP + 1                                              CCC15CCO
ISN 0014              PRINT 252, MAXEL                                                         CCC16CCO
ISN 0015         202       IF(NMAT.LE.MAXMAT) GO TO 203                                      CCC17CCO
ISN 0017                        ISTOP = ISTOP + 1                                              CCC18CCO
ISN 0018              PRINT 253, MAXMAT                                                        CCC19CCO
ISN 0019         203       IF(NSLC.LE.MAXSLC) GO TO 204                                      CCC20CCO
ISN 0021                        ISTOP = ISTOP + 1                                              CCC21CCO
ISN 0022              PRINT 254, MAXSLC                                                        CCC22000
ISN 0023         204       IF(ISTOP.EQ.0) GO TO 205                                          CCC23CCO
ISN 0025              PRINT 255, ISTOP                                                         CCC24CCO
ISN 0026              STOP                                                                     CCC25CCO
                C                                                                              CCC26CCO
ISN 0027         205 READ 2, (RO(I),TH(I),I=1,NMAT)                                            CCC27CCO
ISN 0028              PRINT 101                                                                CCC28CCO
ISN 0029              PRINT 51, (I,RO(I),TH(I),I=1,NMAT)                                       CCC29CCO
ISN 0030              READ 10,(ET(I),UT(I),GGT(I),E1T(I),E2T(I),U12T(I),U21T(I),               CCC30010
                     1G12T(I),I=1,NMAT)                                                        CCC30020
ISN 0031              PRINT 80, (I,ET(I),UT(I),GGT(I),E1T(I),E2T(I),U12T(I),U21T(I),           CCC31C40
                     1G12T(I),I=1,NMAT)                                                        CCC31050
ISN 0032              DO 150 IMAT=1,NMAT                                                       CCC31110
ISN 0033              DO 150 I=1,3                                                             CCC31120
ISN 0034              READ 11, (QQT(I,J,IMAT),J=1,3)                                           CCC31130
ISN 0035              PRINT 81, (QQT(I,J,IMAT),J=1,3)                                          CCC31140
ISN 0036         150 CONTINUE                                                                  CCC31150
ISN 0037              CALL MATSUB                                                              CCC31CCO
ISN 0038               DO 550 IMAT=1,NMAT                                                      CCC32510
ISN 0039              DO 550 I=1,3                                                             CCC32520
ISN 0040              PRINT 82, (GM(I,J,IMAT),J=1,3)                                           CCC32530
ISN 0041         550 CONTINUE                                                                  CCC32540
ISN 0042              PRINT 103                                                                CCC34CCO
ISN 0043                   N=1                                                                 CCC35CCO
ISN 0044               5 READ 3, M,KODE(M),X(M),Y(M),ULX(M),VLY(M)                            CCC36CCO
                            IF(M-N)4,6,7                                                       CCC37CCO
ISN 0046               4 PRINT 105, M                                                          CCC38CCO
ISN 0047                 PRINT 52,M,KODE(M), X(M),Y(M),ULX(M),VLY(M)                         CCC39CCO
ISN 0048                        ISTOP= ISTOP +1                                                CCC40CCO
ISN 0049                   GO TO 5                                                             CCC41CCO
ISN 0050               7           DF = M + 1 - N                                           CCC42CCO
ISN 0051                           RX=(X(M)-X(N-1))/DF                                      CCC43CCO
ISN 0052                           RY=(Y(M)-Y(N-1))/DF                                      CCC44CCO
ISN 0053               8           KODE(N)=0                                                CCC45CCO
```

```
ISN 0054                    X(N)=X(N-1)+RX                                                  C0C46CCO
ISN 0055                    Y(N)=Y(N-1)+RY                                                  C0C47CCO
ISN 0056                    ULX(N)=0.0                                                      C0C48CCO
ISN 0057                    VLY(N)=0.0                                                      C0C49CCO
ISN 0058                6 PRINT 52,N,KODE(N),X(N),Y(N),ULX(N),VLY(N)                        C0C5CCCO
ISN 0059                    N=N+1                                                           C0C51CCO
ISN 0060                  IF(M-N)9,6,8                                                      C0C52CCO
ISN 0061                9   IF(N.LE.NNP) GO TO 5                                          C0C53CCO
                          PRINT 106                                                       C0C54CCO
                       13                                                                 C0C55CCO
ISN 0064               14 READ 15, M,(IE(M,I),I=1,5)                                      C0C56CCO
ISN 0065                16          L=L+1                                                 C0C57CCO
ISN 0066                  IF(M-L)117,17,18                                                C0C58CCO
ISN 0067               117 PRINT 118,M                                                    C0C59CCO
ISN 0068                    PRINT 53,M, (IE(M,I), I=1,5)                                  C0C6CCCO
ISN 0069                    ISTOP=ISTOP+1                                                 C0C61CCO
ISN 0070                  GO TO 14                                                        C0C62CCO
ISN 0071                18          IE(L,1)= IE(L-1,1)+1                                  C0C63CCO
ISN 0072                            IE(L,2)= IE(L-1,2)+1                                  C0C64CCO
ISN 0073                            IE(L,3)=IE(L-1,3)+1                                   C0C65CCO
ISN 0074                            IE(L,4)=IE(L-1,4)+1                                   C0C66CCO
ISN 0075                            IE(L,5)=IE(L-1,5)                                     C0C67CCO
ISN 0076                17 PRINT 53, L,(IE(L,I),I=1,5)                                    C0C68CCO
ISN 0077                  IF(M-L)20,20,16                                                 C0C69CCO
ISN 0078                20  IF(NEL-L)21,21,14                                            C0C7CCCO
ISN 0079                21  CONTINUE                                                     C0C71CCO
ISN 0080                  IF(NSLC.EQ.0) GO TO 31                                          C0C72CCO
ISN 0081                30 PRINT 108                                                      C0C73CCO
ISN 0082                    DO  40 L=1,NSLC                                             C0C74CCO
ISN 0083                  READ 41,ISC(L),JSC(L),SURTRX(L,1),SURTRX(L,2),SURTRY(L,1),    C0C75CCO
                         1 SURTRY(L,2)                                                  C0C76CCO
ISN 0084                40 PRINT 42,ISC(L),JSC(L),SURTRX(L,1),SURTRX(L,2),SURTRY(L,1),  C0C77CCO
                         1 SURTRY(L,2)                                                  C0C78CCO
ISN 0085                31  IF(ISTOP.EQ.0) GO TO 999                                    C0C79CCO
ISN 0086                  PRINT 900, ISTOP                                              C0C8CCCO
                    C                                                                   C0C81CCO
ISN 0087                 1 FORMAT(6I5)                                                  C0C82CCO
ISN 0088               100 FORMAT(35H0INPUT TABLE 1.. BASIC PARAMETERS   //             C0C83CCO
                         1       5X, 40H NUMBER OF NODAL POINTS. . . . . ..I5/          C0C84CCO
                         2       5X, 40H NUMBER OF ELEMENTS. . . . . ..I5/              C0C85CCO
                         3       5X, 40H NUMBER OF DIFFERENT MATERIALS . . . . ..I5/    C0C86CCO
                         4       5X, 40H NUMBER OF SURFACE LOAD CARDS. . . . . ..I5/    C0C87CCO
                         5       5X, 40H 1 = PLANE STRAIN, 2 = PLANE STRESS. . ..I5/    C0C88CCO
                         6       5X, 40H BODY FORCES(1 = IN -Y DIREC., 0 = NONE),I5)    C0C89CCO
ISN 0089               251 FORMAT(////33H TOO MANY NODAL POINTS, MAXIMUM =, I5)          C0C9CCCO
ISN 0090               252 FORMAT(////30H TOO MANY ELEMENTS, MAXIMUM = ,I5)              C0C91CCO
ISN 0091               253 FORMAT(////30H TOO MANY MATERIALS, MAXIMUM =,I5)              C0C92CCO
ISN 0092               254 FORMAT(////40H TOO MANY SURFACE LOAD CARDS, MAXIMUM = ,I5)    C0C93CCO
ISN 0093               255 FORMAT(////28H EXECUTION HALTED BECAUSE OF,I5,13H FATAL ERRORS/)  C0C94CCO
ISN 0094                 2 FORMAT(8E10.3)                                               C0C95CCO
ISN 0095               101 FORMAT(36H0INPUT TABLE 2.. MATERIAL PROPERTIES //           C0C96CCO
                         1       10H  MATERIAL,5X,10HMODULUS OF,6X,9HPOISSON'S,7X,     C0C97CCO
                        28HMATERIAL,7X,  8HMATERIAL /                                   C0C98CCO
                        34X,6HNUMBER,5X,10HELASTICITY,8X,7H  RATIO,8X,7HDENSITY,6X,     C0C99CCO
                        49HTHICKNESS )                                                  C0D1CCCO
ISN 0096                51 FORMAT(I10,2E15.4)                                           C0D2CCCO
ISN 0097                10 FORMAT(8E10.3)                                               C0D3CC10
ISN 0098                80 FORMAT(I10,8E15.4)                                           C0D3CC20
```

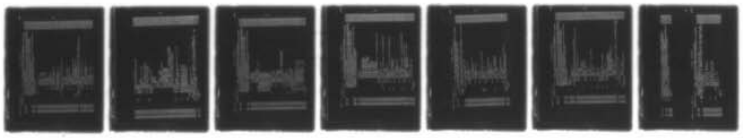
```
ISN 0102          11 FORMAT(3E10.3)                                                                C0105C30
ISN 0103          81 FORMAT(3E10.3)                                                                C0106C40
ISN 0104          82 FORMAT(3E10.3)                                                                C0107C50
ISN 0105         103 FORMAT(34H1INPUT TABLE 3.. NODAL POINT DATA //                                C0108CC0
                    1        5X,5HNODAL,48X,7HX-DISP.,8X,7HY-DISP./                               0010900
                   25X,5HPOINT,6X,4HTYPE,14X,1HX,14X,1HY,8X,7HCR LOAD,8X,7HOR LOAD)               C0110CC0
ISN 0106            3 FORMAT(2I5,4E10.3)                                                          C0111000
ISN 0107         109 FORMAT(5X,17HERROR IN CARD NO.,I5/)                                          C0112C00
ISN 0108          52 FORMAT(2I10,4E15.4)                                                          C0113C00
ISN 0109         106 FORMAT(34H1INPUT TABLE 4.. ELEMENT DATA      //                              C0114C00
                    1        11X,31HGLOBAL INDICES OF ELEMENT NODES/3X,7HELEMENT,                C0115C00
                   27X,1H1,7X,1H2,7X,1H3,7X,1H4,2X,8HMATERIAL )                                   C0116000
ISN 0110         118 FORMAT( 5X, 25HERROR IN ELEMENT CARD NO.. I5 )                               C0117000
ISN 0111          15 FORMAT(6I5)                                                                  C0118CC0
ISN 0112          53 FORMAT(I10,4I8,I10)                                                          C0119C00
ISN 0113         108 FORMAT(37H1INPUT TABLE 5.. SURFACE LOADING DATA  //                          C0120CC0
                   117X, 33HSURFACE LOAD INTENSITIES AT NODES/                                   C0121000
                   24X,6HNODE I,4X,6HNODE J,10X,2HXI,10X,2HXJ,10X,2HYI,10X,2HYJ)                 C0122CC0
ISN 0114          41 FORMAT(2I5,4E10.3)                                                           C0123CC0
ISN 0115          42 FORMAT(2I10,4E12.4)                                                          C0124C00
ISN 0116         900 FORMAT(///45H ASSEMBLY AND SOLUTION WILL NOT BE PERFORMED.,I5,               C0125C00
                   121H  FATAL CARD ERRORS     )                                               0012600
ISN 0117         999 RETURN                                                                      C0127C00
ISN 0118             END                                                                         C0128C00
```

```
      COMPILER OPTIONS - NAME= MAIN,OPT=02,LINECNT=60,SIZE=0000K,
                         SOURCE,EBCDIC,NOLIST,NODECK,LOAD,NOMAP,NOEDIT,ID,NOXREF
ISN 0002              SUBROUTINE MATERP                                          C0001000
ISN 0003              COMMON NNP,NEL,NMAT,NSLC,NCFT,NBODY,MTYP,IE(200,5),RO(10),TH(10),  C0002000
                     1ET(10),UT(10),GGT(10),E1T(10),E2T(10),U12T(10),U21T(10),G12T(10),  C0003000
                     2QQ(3,3),QM(3,3,10),E,U,GG,E1,E2,U12,U21,G12,QQT(3,3,10),          C0004000
                     3X(200),Y(200),ELX(200),ELY(200),KODE(200),ISC(20),JSC(20),        C0005000
                     4SURTRX(20,2),SURTRY(20,2),EP(10)                                  C0006000
ISN 0004              DO 350 IMAT=1,NMAT                                         C0007000
ISN 0005              E=ET(IMAT)                                                 C0008000
ISN 0006              U=UT(IMAT)                                                 C0009000
ISN 0007              GG=GGT(IMAT)                                               C0010000
ISN 0008              E1=E1T(IMAT)                                               C0011000
ISN 0009              E2=E2T(IMAT)                                               C0012000
ISN 0010              U12=U12T(IMAT)                                             C0013000
ISN 0011              U21=U21T(IMAT)                                             C0014000
ISN 0012              G12=G12T(IMAT)                                             C0015000
ISN 0013              DO 350 I=1,3                                               C0016000
ISN 0014              DO 350 J=1,3                                               C0017000
ISN 0015          350 QQ(I,J)=QQT(I,J,IMAT)                                      C0018000
ISN 0016              IF ( E .EQ. 0. .AND.GG .EQ. 0. ) GO TO 50                  C0019000
ISN 0018              IF ( E .EQ. 0. ) GO TO 300                                 C0020000
ISN 0020              IF ( U .EQ. 0. ) GO TO 200                                 C0021000
ISN 0022              IF (GG .EQ. 0. )GG = E*0.5/(1.+U)                          C0022000
ISN 0024              GO TO  400                                                 C0023000
ISN 0025          200 IF (GG .NE. 0. ) U = 1. - E*0.5/GG                         C0024000
ISN 0027              GO TO  400                                                 C0025000
ISN 0028          300 IF ( U .EQ. 0. ) GO TO 400                                 C0026000
ISN 0030              E = 2.*(1.+U)*GG                                           C0027000
ISN 0031          400 IF(NOPT.EQ.1)GO TO 450                                     C0028000
ISN 0033              QQ(1,1) = E/(1.-U*U)                                       C0029000
ISN 0034              QQ(2,1) = U*QQ(1,1)                                        C0030000
ISN 0035              QQ(2,2) = QQ(1,1)                                          C0031000
ISN 0036              QQ(3,3) = GG                                               C0032000
ISN 0037              GO  TO 1000                                                C0033000
ISN 0038          450 QQ(1,1)=E*(1-U)/((1+U)*(1-2*U))                            C0034000
ISN 0039              QQ(2,1)=E*U/((1+U)*(1-2*U))                                C0035000
ISN 0040              QQ(2,2)=QQ(1,1)                                            C0036000
ISN 0041              QQ(3,3)=GG                                                 C0037000
ISN 0042              GO TO 1000                                                 C0038000
ISN 0043          500 IF ( E1 .EQ. 0. .AND.  E2 .EQ. 0. ) GO TO 1000             C0039000
ISN 0045              IF ( U12 .EQ. 0. ) GO TO 700                               C0040000
ISN 0047              IF ( U21 .EQ. 0. ) U21 = U12*E2/E1                         C0041000
ISN 0049              GO TO 800                                                  C0042000
ISN 0050          700 U12 = U21*E1/E2                                            C0043000
ISN 0051          800 QQ(1,1) = E1/(1.-U12*U21)                                  C0044000
ISN 0052              QQ(2,1) = U21*QQ(1,1)                                      C0045000
ISN 0053              QQ(2,2) = E2/(1.-U12*U21)                                  C0046000
ISN 0054              QQ(3,3) = G12                                              C0047000
ISN 0055         1000 DO  1200 I=1,3                                             C0048000
ISN 0056              DO  1200 J=1,I                                             C0049000
ISN 0057              QM(I,J,IMAT)=QQ(I,J)                                       C0050000
ISN 0058              QM(J,I,IMAT)=QQ(I,J)                                       C0051000
ISN 0059         1200 CONTINUE                                                   C0052000
ISN 0060              DO  1300 I=1,3                                             C0053000
ISN 0061         1300 QM(I,3,IMAT)=2.*QM(I,3,IMAT)                               C0054000
ISN 0062          350 CONTINUE                                                   C0055000
ISN 0063              RETURN                                                     C0056000
ISN 0064              END                                                        C0057000
```

AD-A032 011 TECHNION RESEARCH AND DEVELOPMENT FOUNDATION LTD HAI--ETC F/G 11/1
MECHANICAL BEHAVIOR OF MULTIMATERIAL COMPOSITE SYSTEMS, INTERLA--ETC(U)
APR 76 O ISHAI, D PERETZ, S GALI DAJA37-75-C-1890

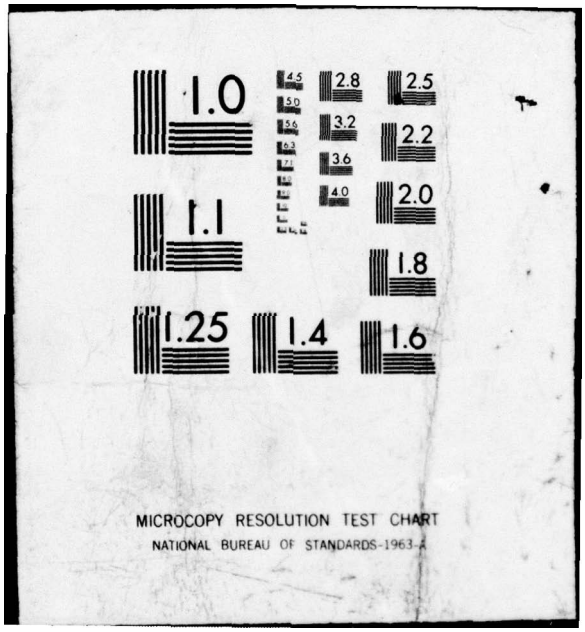
UNCLASSIFIED NL

2 OF 2
AD
A032011



END

DATE
FILMED
1-77


1.0
1.1
1.25
1.4
1.6
1.8
2.0
2.2
2.5
2.8
3.2
3.6
4.0
4.5
5.0
5.6
6.3
MICROCOPY RESOLUTION TEST CHART
NATIONAL BUREAU OF STANDARDS-1963-A

```
        COMPILER OPTIONS - NAME=  MAIN,OPT=02,LINECNT=60,SIZE=0000K,
                           SOURCE,EBCDIC,NOLIST,NODECK,LOAD,NOMAP,NOEDIT,ID,NOXREF
ISN 0002              SUBROUTINE  ASEMBL(ISTOP)                                  C0001000
ISN 0003              COMMON NAP,NEL,NMAT,NSLC,NOPT,NPODY,MTYP,IE(200,5),RO(10),TH(10),  C0002000
                     1ET(10),LT(10),GGT(10),E1T(10),E2T(10),U12T(10),U21T(10),G12T(10),  C0003000
                     2QQ(3,3),QM(3,3,10),E,U,GG,E1,E2,U12,U21,U12,GQT(3,3,10),          C0003500
                     3X(200),Y(200),ULX(200),VLY(200),KODE(200),ISC(20),JSC(20),        C0004000
                     4SURTRX(20,2),SURTRY(20,2),EP(10)                                  C0005000
ISN 0004              COMMON/ONE/ QK(10,10),Q(10),B(3,10),C(3,3),BT(3,6),XQ(5),YQ(5)     C0006000
ISN 0005              COMMON/TWO/ IBAND,NEQ,R(400), AK(400,80)                           C0007000
ISN 0006              DIMENSION LP(6)                                                    C0008000
                    C                                                                    C0009000
ISN 0007              REWIND 1                                                           C0010000
ISN 0008                    ISTOP = 0                                                    C0012000
ISN 0009                    BT(1,4) = 0.0                                                C0014000
ISN 0010                    BT(1,5) = 0.0                                                C0015000
ISN 0011                    BT(1,6) = 0.0                                                C0016000
ISN 0012                    BT(2,1) = 0.0                                                C0017000
ISN 0013                    BT(2,2) = 0.0                                                C0018000
ISN 0014                    BT(2,3) = 0.0                                                C0019000
ISN 0015                 DO  2 I=1,NEQ                                                   C0020000
ISN 0016                    R(I)=0.0                                                     C0021000
ISN 0017                 DO  2 J =1,IBAND                                                C0022000
ISN 0018               2    AK(I,J) = 0.0                                               C0023000
ISN 0019                 DO 10 M=1,NEL                                                   C0030000
ISN 0020                 IF(IE(M,5).GT.0) GO TO 11                                       C0034000
ISN 0022                    ISTOP = ISTOP + 1                                            C0035000
ISN 0023                 GO TO 10                                                        C0036000
ISN 0024              11 CALL QUAD(M,AREA)                                               C0037000
ISN 0025                 IF(AREA.GT.0.0) GO TO 16                                        C0038000
ISN 0027                    ISTOP = ISTOP + 1                                            C0039000
ISN 0028              PRINT 20,M                                                         C0040000
ISN 0029              16 IF(IE(M,3).EQ.IE(M,4)) GO TO 26                                 C0044000
ISN 0031                 DO 31 J = 1,2                                                   C0045000
ISN 0032                    IJ= 10-J                                                     C0046000
ISN 0033                    IK= IJ+1                                                     C0047000
ISN 0034                    PIVOT = QK(IK,Ik)                                            C0048000
ISN 0035                 DO 33 K= 1,IJ                                                   C0049000
ISN 0036                    F = QK(IK,K)/PIVOT                                           C0050000
ISN 0037                    QK(IK,K)=F                                                   C0051000
ISN 0038                 DO 33 I=K,IJ                                                    C0052000
ISN 0039                    QK(I,K)=QK(I,K)- F*QK(I,IK)                                  C0053000
ISN 0040              33    QK(K,I) = QK(I,K)                                            C0054000
ISN 0041              32    Q(K) =Q(K)-QK(IK,K)*Q(IK)                                    C0055000
ISN 0042              31    Q(IK) =Q(IK)/PIVOT                                           C0056000
ISN 0043              26 WRITE (1) ((QK(I,J),J=1,10),I=9,10), Q(9), Q(10),             C0061000
                     1((B(I,J),J=1,10),I=1,3),(((C(I,J),J=1,3),I=1,3),XQ(5),YQ(5)       C0062000
ISN 0044                    LIM=8                                                        C0066000
ISN 0045                 IF(IE(M,3).EQ.IE(M,4)) LIM = 6                                  C0067000
ISN 0047                 DO 40 I=2,LIM,2                                                 C0068000
ISN 0048                    IJ = I/2                                                     C0069000
ISN 0049                    LP(I-1) = 2*IE(M,IJ) - 1                                     C0070000
ISN 0050              40    LP(I) = 2*IE(M,IJ)                                           C0071000
ISN 0051                 DO 50 LL=1,LIM                                                  C0072000
ISN 0052                    I = LP(LL)                                                   C0073000
ISN 0053                    R(I) = R(I) + Q(LL)                                          C0074000
ISN 0054                 DO 50 MM=1,LIM                                                  C0075000
ISN 0055                    J = LP(MM) - I + 1                                           C0076000
```

```
ISN 0056                    IF (J.LE. 0 ) GO TO 50                                  C0C77C00
ISN 0058                        AK(I,J)= AK(I,J)+ GK(LL,MM)                         C0C78C00
ISN 0059          50        CONTINUE                                                C0C79C00
ISN 0060          10        CONTINUE                                                C0C80C00
ISN 0061                    DO 55 N=1,NNP                                           C0C81C00
ISN 0062                    IF(KODE(N).EQ.3) GO TO 55                               C0C82C00
ISN 0064                        K=2*N                                               C0C83C00
ISN 0065                    IF( KODE(N).EQ.1) GO TO 57                              C0C84C00
ISN 0067                        R(K-1) = R(K-1) + ULX(N)                            C0C85C00
ISN 0068                    IF(KODE(N).NE.0) GO TO 55                               C0C86C00
ISN 0070          57            R(K) = R(K) + VLY(N)                                C0C87C00
ISN 0071          55        CONTINUE                                                C0C88C00
ISN 0072                    IF(NSLC.EQ.0) GO TO 60                                  C0C89C00
ISN 0074                    DO 61 L = 1,NSLC                                        C0C90C00
ISN 0075                        I = ISC(L)                                          C0C91C00
ISN 0076                        J = JSC(L)                                          C0C92C00
ISN 0077                        II=2*I                                              C0C93C00
ISN 0078                        JJ=2*J                                              C0C94C00
ISN 0079                        DX = X(J) - X(I)                                    C01C0C00
ISN 0080                        DY = Y(J) - Y(I)                                    C01C1C00
ISN 0081                        EL = SQRT(DX*DX + DY*DY)                            C01C2C00
ISN 0082                        PXI=SURTRX(L,1)*EL                                  C01C3C00
ISN 0083                        PXJ=SURTRX(L,2)*EL                                  C01C4C00
ISN 0084                        PYI=SURTRY(L,1)*EL                                  C01C5C00
ISN 0085                        PYJ=SURTRY(L,2)*EL                                  C01C6C00
ISN 0086                        R(II-1) = R(II-1) + PXI/3.0 + PXJ/6.0               C01C7C00
ISN 0087                        R(JJ-1) = R(JJ-1) + PXI/6.0 + PXJ/6.0               C01C8C00
ISN 0088                        R(II)=R(II)+ PYI/3.0 + PYJ/6.0                      C01C9C00
ISN 0089                        R(JJ)= R(JJ) + PYI/6.0 + PYJ/3.0                    C01CCC0
ISN 0090          61        CONTINUE                                                C01C1C00
ISN 0091          60        DO 70 M=1,NNP                                           C01C2C00
ISN 0092                    IF(KODE(M).GE.0.AND.KODE(M).LE.3) GO TO 72              C01C3C00
ISN 0094                        ISTOP = ISTOP + 1                                   C01C4C00
ISN 0095                    GO TO 70                                                C01C5000
ISN 0096          72        IF(KODE(M).EQ.0) GO TO 70                               C01C6C00
ISN 0098                    IF(KODE(M).EQ.2) GO TO 71                               C01C7C00
ISN 0100                    CALL GECMBC(ULX(M),2*M-1)                               C01C8C00
ISN 0101                    IF(KODE(M).EQ.1) GO TO 70                               C01C9C00
ISN 0103          71        CALL GECMBC(VLY(M),2*M)                                 C01D0000
ISN 0104          70        CONTINUE                                                C01D1C00
ISN 0105                  ENDFILE 1                                                 C01D2C00
ISN 0106                    IF(ISTOP.EQ.0) GO TO 81                                 C01D3C00
ISN 0108                  PRINT 100, ISTOP                                          C01D4C00
ISN 0109          20 FORMAT(/5X,17H AREA OF ELEMENT ,I5,14H  IS NEGATIVE  /)        C01D5000
ISN 0110         100 FORMAT(////42H SOLUTION WILL NOT BE PERFORMED BECAUSE OF  ,I5,  C01D6C00
                   1 15H   DATA ERRORS      /)                                    C01D7C00
ISN 0111          81 RETURN                                                       C01D8C00
ISN 0112                  END                                                     C01D9000
```

```
        COMPILER OPTIONS - NAME=  MAIN,OPT=02,LINECNT=60,SIZE=0000K,
                           SOURCE,EBCDIC,NOLIST,NODECK,LOAD,NOMAP,NOEDIT,ID,NOXREF
ISN 0002            SUBROUTINE QUAD(M,TOTALA)                                    C0001C00
ISN 0003            COMMON NNP,NEL,NMAT,NSLC,NOPT,NECDY,MTYP,IE(200,5),RD(10),TH(10),  00002C00
                   1ET(10),LT(10),GGT(10),E1T(10),E2T(10),U12T(10),U21T(10),G12T(10),  C0003C00
                   2GO(3,3),GM(3,3,10),E,U,GG,E1,E2,U12,U21,G12,GGT(3,3,10),          C0003E00
                   3X(200),Y(200),ULX(200),VLY(200),KODE(200),ISC(20),JSC(20),        C0004C00
                   4SURTRX(20,2),SURTRY(20,2),EP(10)                                  C0005C00
ISN 0004            COMMON/ONE/ QK(10,10),G(10),B(3,10),C(3,3),ET(3,6),XQ(5),YQ(5)   C0006C00
ISN 0005            COMMON/TWO/ IBAND,NEQ,R(400), AK(400,50)                         C0007C00
                  C                                                                  C0008C00
ISN 0006                    I= IE(M,1)                                               C0009C00
ISN 0007                    J= IE(M,2)                                               C0010C00
ISN 0008                    K= IE(M,3)                                               C0011C00
ISN 0009                    L= IE(M,4)                                               C0012C00
ISN 0010                    MTYP = IE(M,5)                                           C0013C00
ISN 0011                    TOTALA = 0.0                                             C0014C00
ISN 0012            IF(NMAT.EQ.1.AND.M.GT.1) GO TO 5                                 C0015C00
ISN 0014            C(1,1)=GM(1,1,MTYP)                                              C0020C00
ISN 0015            C(1,2)=GM(1,2,MTYP)                                              C0021C00
ISN 0016            C(1,3)=GM(1,3,MTYP)                                              C0022C00
ISN 0017            C(2,1)=GM(2,1,MTYP)                                              C0023C00
ISN 0018            C(2,2)=GM(2,2,MTYP)                                              C0024C00
ISN 0019            C(2,3)=GM(2,3,MTYP)                                              C0025C00
ISN 0020            C(3,1)=GM(3,1,MTYP)                                              C0026C00
ISN 0021            C(3,2)=GM(3,2,MTYP)                                              C0027C00
ISN 0022            C(3,3)=GM(3,3,MTYP)                                              C0028C00
ISN 0023          5             LIM = 4                                              C0033C00
ISN 0024                  IF(K.EQ.L) LIM = 3                                         C0034C00
ISN 0026                    XQ(5) = 0.0                                              C0035C00
ISN 0027                    YQ(5) = 0.0                                              C0036C00
ISN 0028                  DO 10 N=1,LIM                                              C0037C00
ISN 0029                    NN = IE(M,N)                                             C0038C00
ISN 0030                    XQ(N) = X(NN)                                            C0039C00
ISN 0031                    YQ(N) = Y(NN)                                            C0040C00
ISN 0032                    XQ(5) = XQ(5) + X(NN)/FLOAT(LIM)                         C0041C00
ISN 0033         10         YQ(5) = YQ(5) + Y(NN)/FLOAT(LIM)                         C0042C00
ISN 0034                  DO 13 II =1,10                                             C0045C00
ISN 0035                    G(II)=0.0                                                C0046C00
ISN 0036                  DO 12 JJ = 1,10                                            C0047C00
ISN 0037         12         QK(II,JJ)=0.0                                            C0048C00
ISN 0038                  DO 13 JJ=1,3                                               C0049C00
ISN 0039         13         B(JJ,II) = 0.0                                           C0050C00
ISN 0040                  IF(K.NE.L) GO TO 15                                        C0051C00
ISN 0042              CALL CST(1,2,3,TOTALA)                                       C0052C00
ISN 0043                  GO TO 999                                                C0053C00
ISN 0044         15   CALL CST(1,2,5,AREA)                                         C0054C00
ISN 0045                    TOTALA = TOTALA + AREA                                 C0055C00
ISN 0046              CALL CST(2,3,5,AREA)                                         C0056C00
ISN 0047                    TOTALA = TOTALA + AREA                                 C0057C00
ISN 0048              CALL CST(3,4,5,AREA)                                         C0058C00
ISN 0049                    TOTALA = TOTALA + AREA                                 C0059C00
ISN 0050              CALL CST(4,1,5,AREA)                                         C0060C00
ISN 0051                    TOTALA = TOTALA + AREA                                 C0061C00
ISN 0052        999   RETURN                                                       C0062C00
ISN 0053              END                                                          C0063C00
```

```
LEVEL 21.7 ( JAN 73 )                    OS/360  FORTRAN H                                    DATE

      COMPILER OPTIONS - NAME=  MAIN,OPT=02,LINECNT=60,SIZE=0000K,
                         SOURCE,EBCDIC,NOLIST,NODECK,LOAD,NOMAP,NOEDIT,ID,NOXREF
ISN 0002            SUBROUTINE  CST(I,J,K,AREA)                                    C0CC1000
ISN 0003            COMMON NNP,NEL,NMAT,NSLC,NCPT,NECDY,MTYP,IE(200,9),RO(10),TH(10),  C0CC2CC0
                   1ET(10),LT(10),GGT(10),E1T(10),E2T(10),U12T(10),U21T(10),G12T(10),  C0CC3CC0
                   2QQ(3,3),CM(3,3,10),E,U,GG,E1,E2,U12,U21,G12,CGT(3,3,10),           C0CC3SC0
                   3X(200),Y(200),LLX(200),VLY(200),KCDE(200),ISC(20),JSC(20),         C0CC4CC0
                   4SURTRX(20,2),SURTRY(20,2),EP(10)                                  C0CC5CC0
ISN 0004            COMMON/CNE/ GK(10,10),G(10),B(3,10),C(3,3),ET(3,6),XQ(5),YQ(5)     C0CC6CC0
ISN 0005            COMMON/TWO/ IBAND,NEG,R(400), AK(400,50)                           C0CC7C00
ISN 0006            DIMENSION CB(3,6),LC(6),LT(3),TK(6,6)                              C0CC8C00
                  C                                                                    C0CC9C00
ISN 0007                  LT(1)= I                                                     C0C10CC0
ISN 0008                  LT(2)= J                                                     C0C11CC0
ISN 0009                  LT(3)= K                                                     C0C12000
ISN 0010                  BT(1,1)= YQ(J)-YQ(K)                                         C0C13C00
ISN 0011                  BT(1,2)= YQ(K)-YQ(I)                                         C0C14C00
ISN 0012                  BT(1,3) = YQ(I)-YQ(J)                                        C0C15C00
ISN 0013                  BT(2,4)=XQ(K)-XQ(J)                                          C0C16000
ISN 0014                  BT(2,5) = XQ (I)-XQ(K)                                       C0C17CC0
ISN 0015                  BT(2,6) = XQ(J) -XQ(I)                                       C0C18CC0
ISN 0016                  BT(3,1)=BT(2,4)                                              C0021000
ISN 0017                  BT(3,2) = BT(2,5)                                            C0022C00
ISN 0018                  BT(3,3) = BT(2,6)                                            C0023000
ISN 0019                  BT(3,4) = BT(1,1)                                            C0024000
ISN 0020                  BT(3,5)= BT(1,2)                                             C0025C00
ISN 0021                  BT(3,6)= BT(1,3)                                             C0026C00
ISN 0022                  AREA =(BT(2,4)*BT(1,3) - BT(2,6)*BT(1,1))/2.0                C0027C00
ISN 0023            DO 10 II=1,3                                                       C0028CC0
ISN 0024            DO 10JJ = 1,6                                                      C0031CC0
ISN 0025                  CB(II,JJ) = 0.0                                              C0032000
ISN 0026            DO 10 KK = 1,3                                                     C0033000
ISN 0027      10          CB(II,JJ) = CB(II,JJ) + C (II,KK)*BT(KK,JJ)                  C0034CC0
ISN 0028            DO 12 II = 1,6                                                     C0037CC0
ISN 0029            DO 12 JJ = 1,6                                                     C0038CC0
ISN 0030                  TK(II,JJ)=0.0                                                C0039CC0
ISN 0031            DO 12 KK=1,3                                                       C0040CC0
ISN 0032      12          TK(II,JJ)=   TK(II,JJ)+BT(KK,II)*CB(KK,JJ)                   C0041CC0
ISN 0033            DO 15 II=1,3                                                       C0042CC0
ISN 0034                  LC(II) = 2*LT(II) - 1                                        C0043C00
ISN 0035      15          LC(II+3) = 2*LT(II)                                          C0044CC0
ISN 0036            DO 30 II=1,6                                                       C0045CC0
ISN 0037                  LL = LC(II)                                                  C0046CC0
ISN 0038                  FK = 1.0/(4.0*AREA)                                          C0047C00
ISN 0039                  FB = 2.0*FK                                                  C0048000
ISN 0040            DO 20 JJ=1,6                                                       C0049CC0
ISN 0041                  MM = LC(JJ)                                                  C0050CC0
ISN 0042      20          GK(LL,MM) = GK(LL,MM) + TK(II,JJ)*TH(MTYP)*FK                C0051CC0
ISN 0043            DO 30 JJ = 1,3                                                     C0052000
ISN 0044      30          B(JJ,LL) = B(JJ,LL) + BT(JJ,II)*FB                           C0053CC0
ISN 0045            IF(NBODY.EQ.0) GO TO 999                                           C0054C00
ISN 0047                  TBODYF =  AREA* RO(MTYP)*  TH(MTYP)                          C0055CC0
ISN 0048                  BODYF  = -TBODYF/3.0                                         C0056CC0
ISN 0049            DO 35 II=1,3                                                       C0057C00
ISN 0050                  JJ= 2* LT(II)                                                C0058C00
ISN 0051      35          Q(JJ)= Q(JJ)+ BODYF                                          C0059CC0
ISN 0052          999 RETURN                                                         C0060CC0
ISN 0053            END                                                              C0061C00
```

```
        COMPILER OPTIONS - NAME=  MAIN,OPT=02,LINECNT=60,SIZE=0000K,
                           SOURCE,EBCDIC,NOLIST,NODECK,LOAD,NOMAP,NOEDIT,ID,NOXREF
ISN 0002              SUBROUTINE BANSOL(KKK,AK,R,NEQ,IBAND,NDIM,MDIM)                  C0001C00
                C SYMMETRIC BAND MATRIX EQUATION SOLVER.  (REF. 2)                     C0002C00
                C                                                                      C0003C00
                C KKK = 1 TRIANGULARIZES THE BAND MATRIX AK, EQ. (2-2)                 C0004C00
                C KKK = 2 SOLVES FOR RIGHT HAND SIDE R, SOLUTION RETURNS IN R, EQ.(2-3) C0005C00
                C                                                                      C0006C00
ISN 0003              DIMENSION AK(NDIM,MDIM), R(1)                                    C0007C00
ISN 0004                    NRS = NEQ - 1                                              C0008C00
ISN 0005                    NR = NEQ                                                   C0009C00
ISN 0006                  IF(KKK.EQ.2) GO TO 200                                       C0010C00
ISN 0008                  DO 120 N= 1,NRS                                              C0011C00
ISN 0009                    M= N-1                                                     C0012C00
ISN 0010                    MR = MIN0(IBAND,NR-M)                                      C0013C00
ISN 0011                    PIVOT = AK(N,1)                                            C0014C00
ISN 0012                  DO 120 L=2,MR                                                C0015C00
ISN 0013                    CR= AK(N,L)/PIVOT                                          C0016C00
ISN 0014                    I = M+L                                                    C0017C00
ISN 0015                    J = 0                                                      C0018C00
ISN 0016                  DO 110 K=L,MR                                                C0019C00
ISN 0017                    J = J + 1                                                  C0020C00
ISN 0018       110          AK(I,J)= AK(I,J) -CR*AK(N,K)                               C0021C00
ISN 0019       120          AK(N,L) = CR                                               C0022C00
ISN 0020                  GO TO 400                                                    C0023C00
ISN 0021       200        DO 220 N=1,NRS                                               C0024C00
ISN 0022                    M= N-1                                                     C0025C00
ISN 0023                    MR = MIN0(IBAND,NR-M)                                      C0026C00
ISN 0024                    CR= R(N)                                                   C0027C00
ISN 0025                    R(N)=CR/AK(N,1)                                            C0028C00
ISN 0026                  DO 220  L=2,MR                                               C0029C00
ISN 0027                    I = M + L                                                  C0030C00
ISN 0028       220          R(I)= R(I) - AK(N,L)*CR                                    C0031C00
ISN 0029                    R(NR) = R(NR)/AK(NR,1)                                     C0032C00
ISN 0030                  DO 320 I = 1,NRS                                             C0033C00
ISN 0031                    N= NR- I                                                   C0034C00
ISN 0032                    M= N-1                                                     C0035C00
ISN 0033                    MR = MIN0(IBAND,NR-M)                                      C0036C00
ISN 0034                  DO 320 K = 2,MR                                              C0037C00
ISN 0035                    L = M+K                                                    C0038C00
                C  STORE COMPLETED DISPLACEMENTS IN LOAD VECTOR R                      C0039C00
ISN 0036       320          R(N)= R(N)- AK(N,K)*R(L)                                   C0040C00
ISN 0037       400 RETURN                                                            C0041C00
ISN 0038           END                                                               C0042C00
```

```
        COMPILER OPTIONS - NAME=  MAIN,OPT=02,LINECNT=60,SIZE=0000K,
                           SOURCE,EBCDIC,NOLIST,NODECK,LOAD,NOMAP,NOEDIT,ID,NOXREF
ISN 0002              SUBROUTINE STRESS                                                 CCCC1CCO
ISN 0003              COMMON NAE,NEL,NMAT,NSLC,NOPT,NECDY,MTYP,IE(200,5),RO(10),TH(10), CCCC2CCO
                     1ET(10),GT(10),GGT(10),E1T(10),E2T(10),U12T(10),U21T(10),G12T(10), CCCC3CCO
                     2QQ(3,3),QM(3,3,10),E,U,GG,E1,E2,U12,U21,G12,GQT(3,3,10),         CCCC3CCO
                     3X(200),Y(200),ULX(200),VLY(200),KODE(200),ISC(20),JSC(20),       CCCC4CCO
                     4SURTRX(20,2),SURTRY(20,2),EP(10)                                 CCCC5CCO
ISN 0004              COMMON/ONE/ QK(10,10),G(10),B(3,10),C(3,3),BT(3,6),XQ(5),YQ(5)    CCCC6CCO
ISN 0005              COMMON/TWO/ IBAND,NEG,R(400), AK(400,50)                          CCCC7CCO
ISN 0006              DIMENSION SIG(6)                                                  CCCC8CCO
                    C                                                                   CCCC9CCO
ISN 0007              REWIND 1                                                          CCC10CCO
ISN 0008              PRINT 300                                                         CCC11CCO
ISN 0009                    NOLINE = 47                                                 CCC12CCO
ISN 0010              DO 5 M=1,NEL                                                      CCC13CCO
ISN 0011              READ(1) ((QK(I,J),J=1,10),I=1,2),  G(9), Q(10),                   CCC14CCO
                     1      ((B(I,J),J=1,10),I=1,3), ((C(I,J),J=1,3),I=1,3), XC,YC     CCC15CCO
ISN 0012                    LIM = 4                                                     CCC21CCO
ISN 0013              IF(IE(M,3).EQ.IE(M,4)) LIM = 3                                    CCC22CCO
ISN 0014              DO 10 I=1,LIM                                                     CCC23CCO
ISN 0015                    II = 2*I                                                    CCC24CCO
ISN 0016                    JJ = 2*IE(M,I)                                              CCC25CCO
ISN 0017                    Q(II-1) = R(JJ-1)                                           CCC26CCO
ISN 0018              10    Q(II) = R(JJ)                                               CCC27CCO
ISN 0019              IF(LIM.EQ.3) GO TO 16                                             CCC30CCO
ISN 0020              DO 15 K=1,2                                                       CCC31CCO
ISN 0021                    JK = K + 8                                                  CCC32CCO
ISN 0022                    IK = JK - 1                                                 CCC33CCO
ISN 0023              DO 15 L=1,IK                                                      CCC34CCO
ISN 0024              15    Q(JK) = Q(JK) - QK(K,L)*G(L)                                CCC35CCO
ISN 0025                    LIM = 10                                                    CCC36CCO
ISN 0026                    FAC = 0.25                                                  CCC37CCO
ISN 0027              GO TO 17                                                          CCC40CCO
ISN 0028              16    LIM = 6                                                     CCC41CCO
ISN 0029                    FAC = 1.0                                                   CCC42CCO
ISN 0030              17    DO 20 I=1,3                                                 CCC43CCO
ISN 0031              EP(I)=0.0                                                         CCC44CCO
ISN 0032              DO 20 J=1, LIM                                                    CCC45CCO
ISN 0033              20     EP(I)=EP(I)+B(I,J)*G(J)*FAC                              CCC46CCO
ISN 0034              DO 30 I=1,3                                                       CCC47CCO
ISN 0035                    SIG(I) = 0.0                                                CCC50CCO
ISN 0036              DO 30 J=1,3                                                       CCC51CCO
ISN 0037              30     SIG(I)=SIG(I)+C(I,J)*EP(J)                               CCC52CCO
ISN 0038                    SP = (SIG(1)+SIG(2))/2.0                                    CCC53CCO
ISN 0039                    SM = (SIG(1)-SIG(2))/2.0                                    CCC54CCO
ISN 0040                    DS = SQRT(SM*SM+SIG(3)*SIG(3))                              CCC55CCO
ISN 0041                    SIG(4) = SP + DS                                            CCC56CCO
ISN 0042                    SIG(5) = SP - DS                                            CCC57CCO
ISN 0043                    SIG(6) = 0.0                                                CCC60CCO
ISN 0044              IF(SIG(3).NE.0.0.AND.SM.NE.0.0) SIG(6) = 28.648*ATAN2(SIG(3),     CCC61CCO
                     1                                                          SM)     CCC62CCO
ISN 0045              IF(NOLINE.GT.0) GO TO 54                                          CCC63CCO
ISN 0046              PRINT 1000                                                        CCC64CCO
ISN 0047                    NOLINE = 49                                                 CCC65CCO
ISN 0048              54    NOLINE = NOLINE - 1                                         CCC66CCO
ISN 0049              5 PRINT 1010, M,XC,YC,(SIG(I),I=1,6)                              CCC67CCO
ISN 0050              ENDFILE 1                                                         CCC68CCO
```

```
ISN 0055        300 FORMAT(47H1OUTPUT TABLE 2.. STRESSES AT ELEMENT CENTROIDS //      C0C65C00
                   11X,7HELEMENT,9X,1HX,9X,1HY,4X,8HSIGMA(X),4X,8HSIGMA(Y),4X,      C0C66C00
                   28HTAU(X,Y),4X,8HSIGMA(1),4X,8HSIGMA(2), 7X,5HANGLE )            C0C67C00
ISN 0056       1000 FORMAT(1H1,   7HELEMENT,9X,1HX,9X,1HY,4X,8HSIGMA(X),4X,8HSIGMA(Y),  C0C68C00
                   14X,3HTAU(X,Y),4X,8HSIGMA(1),4X,8HSIGMA(2), 7X,5HANGLE )         C0C69C00
ISN 0057       1010 FORMAT(I8, 2F10.2,1P6E12.4)                                     C0C70C00
ISN 0058            RETURN                                                          C0C71C00
ISN 0059            END                                                             C0C72C00
```



```
      COMPILER OPTIONS - NAME=  MAIN,OPT=02,LINECNT=60,SIZE=0000K,
                         SOURCE,EBCDIC,NOLIST,NODECK,LOAD,NOMAP,NOEDIT,ID,NOXREF
ISN 0002            SUBROUTINE GEOMBC(L,N)                                       C0C01C00
ISN 0003            COMMON/TWO/ IBAND,NEQ,R(400), AK(400,50)                     C0C02C00
                  C  THIS SUBROUTINE MODIFIES THE ASSEMBLAGE STIFFNESS AND LOADS FOR THE  C0C03C00
                  C  PRESCRIBED DISPLACEMENT U AT DEGREE OF FREEDOM N, EQ.(6-18B). (REF.1)C0C04C00
ISN 0004                  DO 100 M=2,IBAND                                       C0C05C00
ISN 0005                  K = N - M + 1                                          C0C06C00
ISN 0006                  IF(K.LE.0) GO TO 50                                    C0C07C00
ISN 0008                  R(K) = R(K) - AK(K,M)*U                                C0C08C00
ISN 0009                  AK(K,M) = 0.0                                          C0C09C00
ISN 0010            50    K = N + M - 1                                          C0C10C00
ISN 0011                  IF(K.GT.NEQ) GO TO 100                                 C0C11C00
ISN 0013                  R(K) = R(K) - AK(N,M)*U                                C0C12C00
ISN 0014                  AK(N,M) = 0.0                                          C0C13C00
ISN 0015            100   CONTINUE                                               C0C14C00
ISN 0016                  AK(N,1) = 1.0                                          C0C15C00
ISN 0017                  R(N) = U                                               C0C16C00
ISN 0018            RETURN                                                       C0C17C00
ISN 0019            END                                                          C0C18C00
```